FUNCTIONAL *IN VITRO* ANALYSIS OF THE HIV-1 *NEF* H40Y MUTATION ON ENDOTHELIAL FUNCTION

Tanani Sayimane

A Dissertation submitted to the Faculty of Health Sciences, University of the Witwatersrand, Johannesburg, in fulfilment of the requirements for the degree ofMaster of Science in Medicine (Chemical Pathology)

Johannesburg, September 2022.

Supervisor: Dr Genevieve Mezoh

Co-supervisor: Dr Adriaan E. Basson

Declaration

I, Tanani Sayimane declare that this dissertation submitted to the University of the Witwatersrand for the degree of Master of Science in Medicine (Chemical Pathology) has not been submitted before for any degree or examination at this or any other University. This is my work with exception of the referenced material which has been cited in text and acknowledge

Student name	Signature	Date
Tanani Sayimane	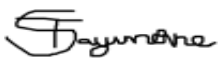	26-09-2022

Dedication

This dissertation is dedicated to my late father. Thank you for making this possible.

To my family, my mother, sister, and brothers. Thank you for your unwavering support and belief in me.

ABSTRACT

There is an increase in cardiovascular disease in people living with HIV (PLWH). Literature suggests the observed increased risk in this population is due to the HIV-1 Nef protein which causes endothelial dysfunction. Nef is a polymorphic accessory protein of which mutations in Nef have been associated with disease outcome. In a previous study, H40Y was associated with increased plasma concentration of markers of endothelial activation. This project therefore sought to confirm the reported effects of the H40Y polymorphism on endothelial cells. HIV-Nef expressing clones were constructed using an HIV-1 *nef* gene isolated from a clinical sample and the pMJ4 plasmid. The Nef-40Y variant was generated by site-directed mutagenesis. Human pulmonary microvascular endothelial cells (HPMECs) were transfected with the Nef-expressing constructs to determine the expression of the adhesion molecules ICAM-1 and VCAM-1 using RT-qPCR and ELISA analyses. The HIV-1 Nef-40H and Nef-MJ4 variants significantly increased ICAM-1 and VCAM-1 mRNA expression compared to HIV-1 Nef-40Y. Additionally, HIV-1 Nef-40H and Nef-MJ4 were seen to work in synergy with TNF-α to significantly increase VCAM-1 mRNA expression. However, a multiple comparisons test revealed that no variant significantly outperformed the other when measuring the concentration of soluble VCAM-1 proteins. No synergistic relationship was observed between the HIV-1 Nef variants and TNF-α at the protein level. This suggests a weak correlation between VCAM-1 mRNA and protein expression following Nef-induced endothelial activation. This study demonstrated that the HIV-1 Nef-40H variant had a greater negative effect on endothelial function compared to the Nef-40Y variant.

ACKNOWLEDGMENTS

I would like to thank my supervisors, Dr Genevieve Mezoh and Dr Adriaan E. Basson for the opportunity to do this project with them and for their guidance, patience, and support throughout the study.

I would like to extend my gratitude to Dr Marketa Toman for being generous with her time, expertise, and assistance with the ELISA experiments.

To the staff and fellow students at the Department of Chemical Pathology at the University of Witwatersrand, thank you for your words of encouragement and willingness to provide any assistance during my studies.

I would like to extend a special thank you to Alice Nndwammbi for her support and encouragement.

I would like to thank the members of FullStop club for their support.

My gratitude goes to South African National Health Laboratory Service (NHLS), the South African National Research Foundation (NRF) and the Poliomyelitis Research Foundation (PRF) for providing funding for support this project.

Table of Content

List of Figures

List of Tables

List of abbreviations

AIDS - Acquired immunodeficiency syndromeAng - Angiopoietin

ART - Antiretroviral therapyARV - Antiretroviral drug

CA — Capsid

CAM – Cellular adhesion molecules

CVD - Cardiovascular disease

ELISA - Enzyme-linked immunosorbent assay

eNOS - Endothelial nitric oxide synthetase Env - Envelope

HAART - Highly active antiretroviral therapy

HPMEC - Human pulmonary microvascular endothelial cells

HIV-1 - Human immunodeficiency virus type-1

HIV-2 - Human immunodeficiency virus type-2

ICAM-1 - Intercellular adhesion molecule-l

IL - InterleukinIN - Integrase

INSTIs - Integrase strand transfer inhibitors

kDa - kilo Dalton

LTNP – Long-term non-progressors

LTR - Long terminal repeats

MA - Matrix

NC - Nucleocapsid

Nef - Negative regulator factor

NF-kB - Nuclear factor kappa-light-chain-enhancer of activated B cells

NNRTIs - Non-nucleoside reverse transcriptase inhibitors

NO - Nitric oxide

NRTIs – Nucleos(t)ide reverse transcriptase inhibitors

PCR - Polymerase chain reaction

PLWH – People living with HIV

Pol - PolymerasePR – Protease

PrEP – Pre-exposure prophylaxis

Rev - Regulator of virion gene expression

ROS - Reactive oxygen species

SDS-PAGE - Sodium dodecyl sulphate polyacrylamide gel electrophoresis

Tat - Transcriptional trans activator protein

TM - Transmembrane glycoprotein

TNF-α- Tumour necrosis factor alpha

VCAM-1 - Vascular cell adhesion molecule-1

Vif - Viral infectivity factor

Vpr - Viral protein r

Vpu - Viral protein u

vWF - von-Willebrand factor

Chapter 1: Introduction

1.1. The HIV/AIDS epidemic

Acquired immunodeficiency syndrome (AIDS) is a communicable disease characterized by a severe reduction of CD4+ T cells, rapid weight loss, recurring fever and contracting of opportunistic diseases like candidiasis, pneumonia, and tuberculosis (Jeevani, 2011). AIDS is caused by Human Immunodeficiency Virus-1 and -2 (HIV-1 and HIV-2), viruses classified under the *Lentivirus* genus within the family of *Retroviridae* (Fanales-Belasio *et al*., 2010). Phylogenetic analysis revealed that the HIV-1 closest relatives are the Simian Immunodeficiency Viruses (SIV) from chimpanzees found in west central Africa. HIV-1 crossed over to humans from the primate's from central African chimpanzees (Gurtler *et al*., 2016). The *Pan troglodyte* chimpanzees are considered as the source of HIV-1 (Sharp & Hahn, 2010). HIV-2 is related to SIVs found in monkeys living in the wild in west Africa (Gurtler *et al*., 2016). *The Cercocebus atys* monkey is regarded as the source of HIV-2 (Sharp & Hahn, 2010). HIV-1 is divided into four groups: Major (M), Outlier (O), non-M or non-O (N), and non-O or non-N (P) (Hemelaar, 2012). The HIV-1 group M is further divided into 9 genetically distinct subtypes (A- D, F-H, J and K) along with several recombinant viruses known as circulating recombinant forms (CRFs) (Lau and Wong, 2013). HIV-2 has nine subtypes (A-I), with subtype A and B being endemic to West Africa (Visseaux *et al*., 2016). HIV-2 is also found in Portugal, France, Spain, Belgium, and other countries with historical ties with West Africa (Mendoza, *et al*., 2020). It is estimated that 1-2 million people are infected with HIV-2 worldwide (Berzow, *et al*., 2021).

HIV-1 occurs worldwide with subtype C being the most common type of strain at 47%, followed by subtype B and A which accounts for 12% and 10% of infections, respectively

(Figure 1.1; Hemelaar *et al*., 2019). HIV-2 is predominately found in western Africa, where it infects up to 2 million people and in European countries with socioeconomic ties to western Africa like Portugal and France (Nyamweya *et al*., 2013). HIV-2 infections have also been identified in Brazil, India, and the United States of America (Visseaux *et al*., 2016). HIV-1 and HIV-2 share similar intracellular replication pathways, transmission modes and clinical effects leading to AIDS. However, HIV-2 is less likely to progress to AIDS due to its lower transmissibility, longer asymptomatic stage, and slower decline in CD4+ T-cell count (Esbjörnsson *et al*., 2012). Development of immune dysfunction and AIDS is observed in most people who have untreated HIV-1 infection, as compared to 20-30% of persons affected with HIV-2 (Esbjörnsson *et al*., 2012).

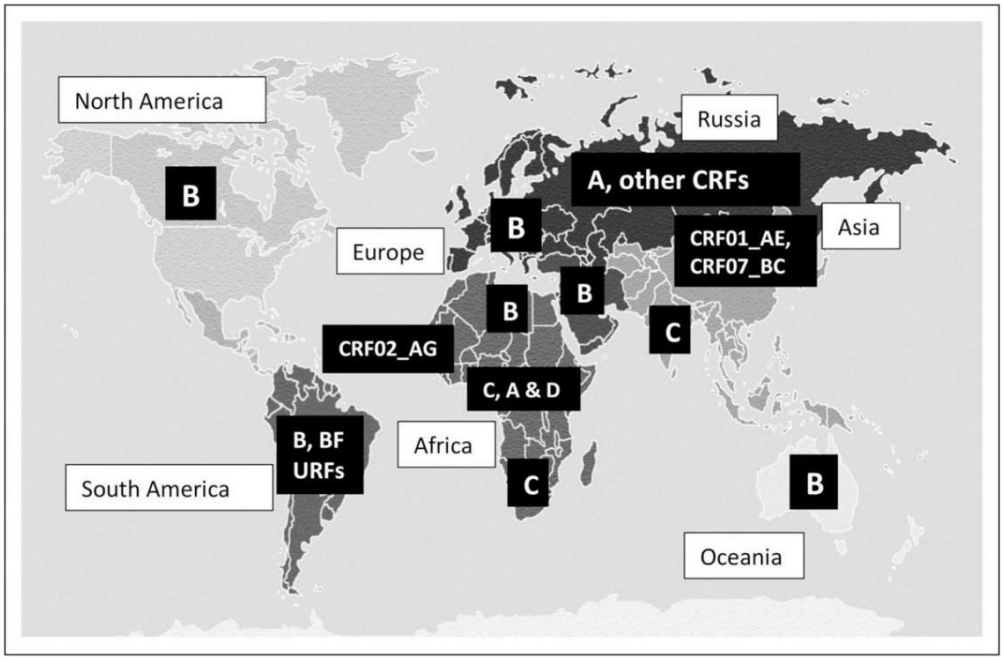

Figure 1.1: Worldwide prevalence of HIV-1 group M subtypes.
Map showing the global distribution of group M strains and circulating recombinant forms. Subtype B is widely distributed worldwide, however, it only accounts for 12% of all HIV-1 infections. Subtype C is prevalent in Southern Africa and India but is responsible for over 47% of total infections. Eastern Africa and Europe is dominated by subtype A while circulating recombinant forms are prevalent in East Asia and Southeast Asia at 5.3% of total HIV-1 infections. Figure sourced from Bbosa *et al*., (2019).

HIV-1 is a severe health problem worldwide of which it is most prevalent in sub-

Saharan Africa (Figure 1.2; Dwyer-Lindgren *et al*., 2019). Southern Africa accounts for 43% of all AIDS-related deaths, with most deaths being of adults between the ages of 15-49 years old (UNAIDS, 2019). In 2019, it was estimated that over 1.8 million children and 36.2 million adults were living with HIV worldwide, with many infections being amongst females (UNAIDS, 2019). HIV-1 places a heavy burden on health care systems around the world. It is estimated that 26.2 billion USD is needed annually from 2020 to 2030 in low- and middle-income countries for the AIDS response in these regions (UNAIDS, 2019). The AIDS response includes providing HIV education, national distribution of male and female condoms, providing pre-exposure prophylaxis (PrEP) and antiretroviral therapies (ARVs) in both public and private facilities (UNAIDS, 2019). In Southern and Eastern Africa, only 20% of the AIDS response resources are domestically sourced. An additional 800 million USD is required in additional resources (UNAIDS, 2019). The burden on individual countries starts from the reallocation of funds from essential services, and to reductions in productivity due to loss of workers, which further translates to reduced economic growth and development.

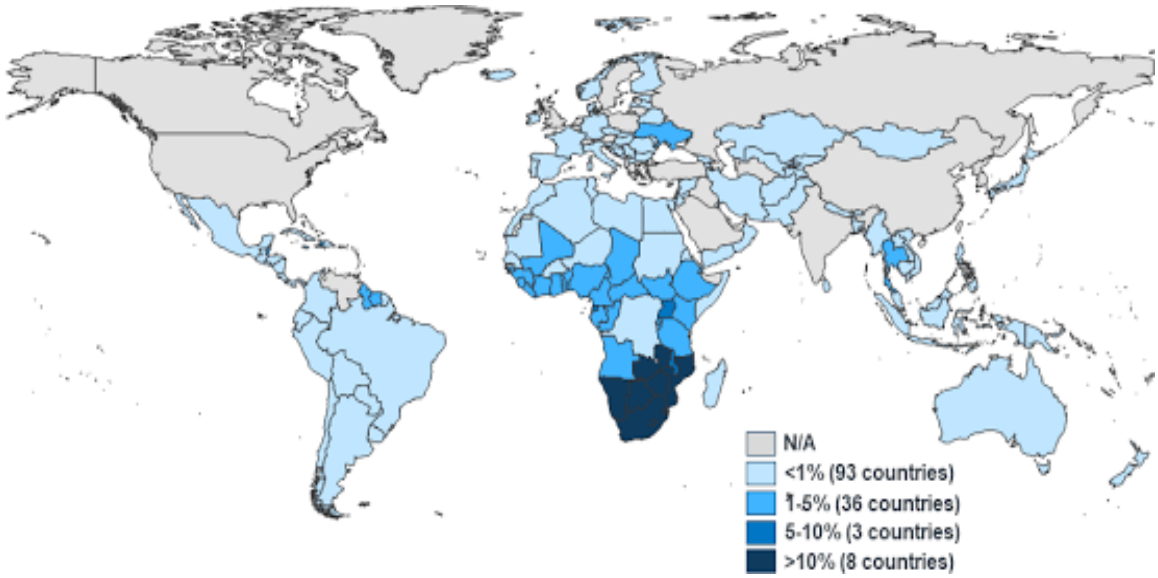

Figure 1.2: The global incidence of HIV-1 infection.
The highest prevalence rates of HIV-1 infections are found in sub-Saharan Africa, where over 10% of the adult population aged 15-49 years old is infected. High rates of

occurrence in infections are observed in South America and Central Asia. Figure sourced from UNAIDS 2019 Report on the global AIDS epidemic UNAIDS, (2019).

1.2. HIV-1 genome, structure, and replication pathway

1.2.1.1. HIV-1 genome

The HIV-1 genome is 9719 bases in length, composed of two copies of 9.2 kb single stranded RNA that codes for 9 viral genes (Figure 1.3; Frankel and Young, 1998). The HIV-1 genome is composed of three groups of genes: the major structural genes (*gag, pol* and *env*), regulatory genes (*tat* and *rev*) and accessory genes (*vpu, vpr, vif and nef*) (Table 1.1; Frankel and Young, 1998). The *gag* gene encodes for structural proteins p17 (Matrix), p24 (Capsid), p7 (Nucleocapsid) and p6, while the *env* gene encodes for the envelope glycoproteins gp120 and gp41. The *pol* gene encodes for the viral enzymes p10 (Protease), p51/p66 (Reverse Transcriptase) and p32 (Integrase), while the regulatory genes are encoded by *rev* and *tat*. The accessory genes encode for Vif, Vpr, Vpu and Nef proteins (Musumeci *et al*, 2015). Two long terminal repeats (LTR) are located at both ends of the HIV genome. The 5‘ LTR mediates the transcription of all 9 HIV genes and the 3‘ LTR is required for cleavage and polyadenylation of the viral mRNA (Frankel and Young, 1998).

Table 1.1: Synopsis of the HIV-1 genome and protein functions.

Gene	Protein	Function	Reference
gag	Pr55Gag	Unprocessed precursor of inner structural proteins	Bryant and Ratner, (1990); Göttlinger *et al.,* (1989); Turner and Summers, (1998)
	Capsid (CA)	Proteins that encapsulate HIV genome and enzymes	
	Matrix (MA)	Layer of proteins forming a ring beneath the lipid membrane	
	Nucleoprotein(NC)	Proteins coating the HIV-1 genome	
	P6	Involved in virion formation and release during maturation	
pol	Pr160GagPol	Unprocessed Precursor of the viral enzymes	Ashorn *et al*., (1990); Zack *et al*., (1990); Bushman *et al.,* (1990); Muller and Varmus,(1994)
	Protease (PR)	Peptide bond hydrolysis of viral enzymes precursor protein to form functional viral enzymes	
	Reverse transcriptase (RT)	Synthesizes complementary DNA strands from RNA	
	RNase H	Breaks down RNA strands within DNA/RNA complex during replication in the viral RNA/DNA	
	Integrase (IN)	Integrates newly synthesized viral DNA into host genome	
env	PrGp160	Precursor of the envelope proteins	Turner and Summers, 1998; Capon and Ward, (1991); Feng *et al*., (1996)
	Surface glycoprotein (SU)	Attachment site of virus to host cells	
	Transmembraneprotein (TM)	Anchors of SU to the lipid membrane	
tat	transactivator protein	Up regulates viral transcription	Asamitsu and Okamoto, (2017)
rev	RNA splicing regulator	Binds to unprocessed viral RNA for transportation to the cytoplasm	Blissenbach *et al*., (2010)
vif	viral infectivity protein	Disrupts antiviral mechanisms of infected host cells	Andrew and Strebel, (2014)
vpr	virus protein r	Transport preintegrated viral DNA into the host cell's nucleus	Kogan and Rappaport, (2011)
vpu	virus protein unique	Down regulates CD4 production	Andrew and Strebel, (2014)
nef	negative regulating factor	Influence on HIV replication, essential to infectivity of viral particles and downregulation of MHC-I molecules	Geyer *et al*., (2001); Fackler and Baur, (2002); Landi *et al.,* (2011)

* Numbers correspond to the size of the protein (p) or glycoprotein (gp) in kilodaltons (kDa)

The LTR is composed of three sub-regions: U3, R and U5 (Damgaard *et al*., 2004). The U3 region is ~450 bp in length and is located at the 5‘ end of the LTR. The U3 region contains most of the cis-acting DNA elements, which are the binding sites for various

cellular transcription factors. The R region is located at the centre of each LTR and is 100 bp long. Transcription of the HIV transcript starts at the first base of this region, and polyadenylation occurs immediately after the last base of the R region (Roebuck and Saifuddin, 1999). The U5 region is 180 bp long and contains the Tat binding site and packaging sequences of HIV-1. The3‘ end of the U5 region is defined by the location of the AAUAAA polyadenylation signal and a lysis tRNA binding site (Fanales-Belasio *et al*., 2010).

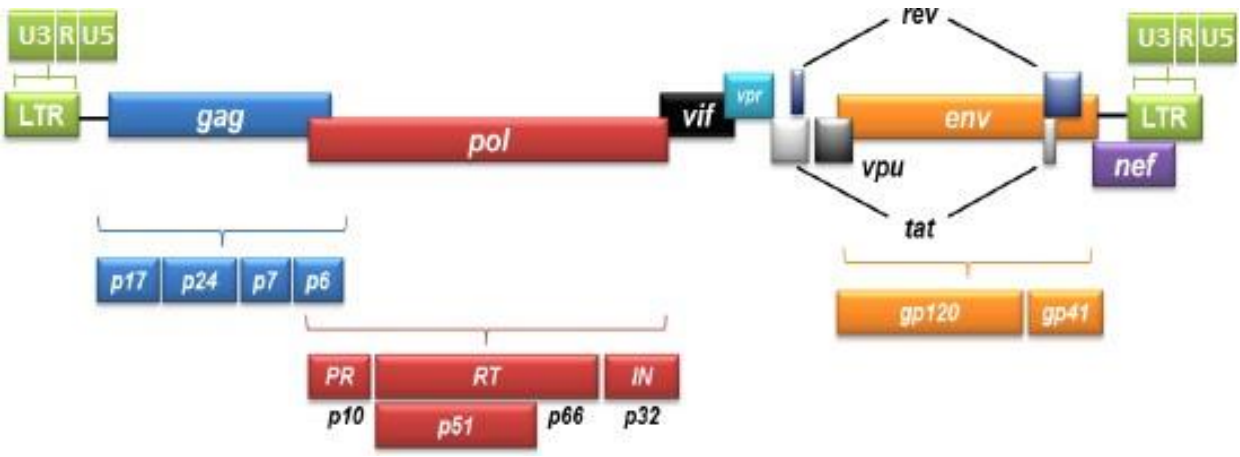

Figure 1.3: Genomic organization of the HIV-1 genome.
The HIV-1 genome contains nine open reading frames that produce 15 proteins. The gag gene produces the structural proteins p17 (Matrix), p24 (Capsid), p7 (Nucleocapsid) and p6 while the *env* gene encodes for the envelope glycoproteins gp120 and gp41. The viral enzymes p10 (Protease), p51/p66 (Reverse Transcriptase) and p32 (Integrase) are produced by the *pol* gene. The regulatory proteins are encoded by the *rev* and *tat* genes. The accessory proteins are encoded by the *vif, vpr, vpu* and *nef* genes of the HIV-1 genome. Figure adapted from Watts *et al., (*2009).

1.2.2. HIV-1 proteins

1.2.2.1. HIV-1 major structural proteins

The *gag* gene expresses the 55 kilo Dalton (kDa) Gag precursor protein, p55. The N-terminal glycine residue of p55 is modified by the covalently attached myristoyl group, a process called myristylation during translation, allowing for its association with the cytoplasmic portion of the cell membrane (Bryant and Ratner, 1990). The viral protease

cleaves the p55 protein into four smaller proteins, which are known as the Matrix (p17), Capsid (p24), Nucleocapsid (p9) and the p6 protein (Göttlinger *et al*., 1989). In the early phase of HIV-1 replication, the Matrix protein forms a protective shell attached to the inner surface of the virion lipid bilayer, thus stabilizing the particle, and facilitates the nuclear transport of pre-integrated viral genome to the nucleus due to its karyophilic signal (Gallay *et al*., 1995). This allows HIV-1 to infect non- dividing cells which is usual amongst retroviruses (Fiorentini *et al.,* 2006). The Capsid protein forms the conical core of mature viral particles and acts to shield the viral genome from host factors in the cytoplasm during early replication, which detect viral RNA and initiate an antiviral response capable of inhibiting infection (Campbell and Hope, 2015). During the early phase of the HIV-1 replication cycle, the genomic RNA is coated by dimeric forms of Nucleocapsid molecules acting as a chaperoning partner of the viral RNA and the reverse transcriptase during the process of reverse transcription (Darlix *et al.,* 2011). Nucleocapsid binds to the packaging signal through its interaction with two zinc-finger motifs, facilitating reverse transcription (Turner and Summers, 1998). During the late phase of viral replication, Nucleocapsid is responsible for recognizing the packaging signal of HIV-1 and mediates incorporation of a heterologous RNA into HIV virions (Darlix *et al*., 2011). In the late phase of HIV-1 replication, the C-terminal p6 domain of p55 mediates the interaction between Gag and Vpr, which leads to the incorporation of Vpr into assembling virions (Dubois *et al.,* 2018). The late domain in the p6 region is required for the release of budding virions from an infected cell (Paxton *et al*., 1993).

Products of the *pol* gene are essential for the synthesis and integration of proviral DNA into the host genome and the generation of capsid proteins. The Pol enzymatic proteins include HIV-1 reverse transcriptase (RT, p50), integrase (IN, p31), protease (PR, p10) and RNase

H (p15) (Ashorn *et al*., 1990; Zack *et al*., 1990). The RT and RNase H form a heterodimeric 66 kDa enzyme that has both DNA polymerase and ribonucleic activities (Gorshkova *et al.,* 2001). During the early stage of HIV replication, the RT uses the viral RNA as a template to generate a pre-integrated double stranded DNA molecule (Preston *et al*., 1988). The RT (p50) enzyme does not possess proofreading properties, resulting in errors during the replication process, which leads to the introduction of point mutations in each copy of the viral genome during reverse transcription in the early phase of replication (Turner and Summers, 1998). RNase H removes the original viral RNA from the newly synthesized DNA strand, allowing the RT to facilitate synthesis of a new complementary DNA strand (Kohlstaedt *et al*., 1992). In the host‘s nucleus, the IN (p31) enzyme facilitates insertion of viral DNA into the infected cell‘s genomic DNA, which involves three main steps; firstly, the exonuclease activity of the IN trims two nucleotides from each 3‘ end of the linear viral DNA; secondly, the endonuclease activity of IN cleaves the host DNA at the integration site within the nucleus located chromosomal DNA; and finally, the ligase activity of IN covalently links each end of the viral DNA to the host‘s genomic DNA, resulting in an integrated provirus within the host genome (Bushman *et al*., 1990; Muller and Varmus, 1994).

The PR enzyme is responsible for processing the Gag and Gag-Pol polyproteins during the late phase of HIV-1 replication, producing individual Gag and Pol proteins (Gulnik *et al.,* 2000). Protease is only functional as a dimer and its enzymatic activity is required for mature virions capable of infecting other cells (Zhang *et al.*, 2009)

The viral envelope (Env) is a 160 kDa protein (gp160) that undergoes glycosylation with the addition of carbohydrate side chains to asparagine residues, required for infectivity (Turner and Summers, 1998). The addition of ~90 N-linked oligosaccharides on Env in the endoplasmic reticulum restricts the binding of neutralizing antibodies on the gp120

subunits, improving the infectivity of the virions as they are free to bind to host cellular receptors (Go *et al*., 2017). A cellular furin protease cleaves gp160, producing mature gp41 and gp120 proteins that remain associated by noncovalent interactions (Schneck *et al*., 2020). Three proteins each of gp41 and gp120 form a heterotrimeric mature HIV-1 glycoprotein spike (Checkley *et al*., 2011). The gp120 is located on the exoplasmic surface of the virion while the transmembrane protein, gp41, anchors the gp120 to the lipid bilayer of the virion (Capon and Ward, 1991). The interactions between the virion, CD4 and secondary receptors (CXCR4 and CCR5) are mediated by the domains within gp120 to initiate the infection cycle (Feng *et al*., 1996).

1.2.2.2. HIV-1 regulatory proteins

The HIV-1 genome encodes for two regulatory genes (*tat* and *rev*) which play an essential role within the virus life cycle. The Tat protein is a transcriptional trans-activator, which is expressed early within the HIV-1 life cycle (Ruben *et al*., 1989). Tat is an RNA binding protein that binds the short-stem loop structure called the transactivation response element (TAR), located on the 5‘ end terminal of the HIV-1 genome (Das *et al*., 2011). Binding of Tat to TAR leads to increased processivity of cellular RNA-Polymerase II, enhancing the efficiency of the elongation polymerase (Asamitsu and Okamoto, 2017). Rev is a 16 kDa, RNA binding protein that binds to a 240 bp region of complex RNA secondary structure known as the rev response element (RRE), located within the *env*-coding region of the viral RNA (Zapp and Green, 1989). The Rev-RRE complex then associates with the chromosome region maintenance 1 (Crm1) protein, also known as exportin 1 (Xpo1), and ran loaded with guanosine triphosphate (RanGTP) to form a host export complex enabling translocationthrough the nuclear pore (Fang *et al*., 2013). The Rev-RRE complex facilitates the export of unspliced and singly spliced transcripts to the cytoplasm, where the transcripts

serve as templates for translation, and are encapsulated during assembling into new viral particles during the late phrase of viral replication (Blissenbach *et al*., 2010).

1.2.2.3. HIV accessory proteins

The HIV-1 genome has the prototypical retrovirus genes *gag, pol, tat, rev* and *env*, but also contains four additional accessory genes, designated *vif, vpr, vpu and nef* (Aylinde *et al*., 2010). The HIV-1 accessory proteins target different cellular regions but do not possess any enzymatic activity. However, they function as molecular adapters to the host cell, resulting in the proteolytic degradation of the cellular target (Strebel, 2013). The viral infectivity factor (*vif*) gene encodes for a 23 kDa protein that is essential for the replication of HIV-1 *in vivo* (Andrew and Strebel, 2014). Vif targets apolipoprotein B mRNA editing enzyme, catalytic polypeptide- like 3 G (APOBEC3G), a cellular cytidine deaminase that in the absence of Vif is packaged into virions causing critical damage to the viral genome (Strebel, 2013). Deamination of the cytosine residues of the viral genome, during reverse transcription, produces deoxyuridine. This is misread by reverse transcriptase as thymidine during cDNA synthesis, resulting in the insertion of alanine in place of guanine (Harris and Liddament, 2004; Strebel, 2013). The G-to- A hypermutation contributes to genetic variation in HIV-1 populations resulting in immune escape and drug resistant HIV-1 variants (Russell *et al.,* 2009). Vif binds to APOBEC3G and redirects it to degradation by ubiquitination in the proteasome, thus preventing viral DNA mutation (Manen *et al*., 2012).

The viral protein R (Vpr) is incorporated into viral particles through direct interaction with the Gag precursor, making it readily available upon cell entry (Guenzel *et al*., 2014). Vpr is a 14kDa protein that mediates the nuclear transport of the HIV-1 pre-integration complex (PIC) into the nucleus of non-dividing cells (Kogan and Rappaport, 2011). During infection of dividing cells, Vpr is known to arrest the cell cycle in G2, a phase where the LTR

promoter is more active, thus increasing viral expression (Gonzalez, 2017). The Vpr polypeptide has the capacity to trigger permeabilization of mitochondrial membrane in CD4+ T cell, resulting in the collapse of the mitochondrial membrane potential, which induces apoptosis, by releasing pro- apoptotic proteins like cytochrome C (Guenzel *et al*., 2014).

The viral protein U (*vpu*) gene encodes a 16 kDa membrane associated protein translated from a Rev-dependent viral mRNA which encodes the viral envelope glycoprotein (Dube *et al.,* 2010). Vpu has a N-terminal domain, a single transmembrane domain and a charged hydrophilic C-terminal domain that extends into the cytoplasm (Strebel, 2014). The Vpu protein has two main functions which include the down-modulation of CD4 and enhancement of virion release (Andrew and Strebel, 2014). Phosphorylated Vpu interacts with beta-transducin repeats containing proteins (β-TrCP) and newly synthesized endoplasmic reticulum localized CD4, to form a CD4-Vpu-β-TrCP complex, leading to CD4 ubiquitination (Dube *et al*., 2010; Andrew and Strebel, 2014). Vpu also interacts with bone marrow stromal antigen 2 (BST-2), a host restriction factor that blocks the release of enveloped viruses by directly tethering virions to the membrane of infected cells, leading to lysosomal degradation of BST-2 (Douglas *et al*., 2009; Andrew and Strebel, 2014). This leads to the enhancement of virion release from infected cells.

The negative factor (*nef)* gene encodes for a 27 kDa myristoylated protein of great importance for the pathogenesis of HIV-1 (Geyer *et al*., 2001). Kestler and colleagues (1991) demonstrated the requirement of an intact *nef* allele in the maintenance of high viral load and development of immunodeficiency by infecting Rhesus macaques with a mutated strain of cloned $SIVmac_{239}$ absent the *nef* open reading frame (Kestler *et al*.,

1991). A study on a cohort of haemophiliacs, with either progressive or non-progressive HIV-1 infection, revealed the presence of defective *nef* variants resulted in non-progressors (Bramilla *et al*., 1999). Nef is expressed early within the HIV-1 replication cycle and is characterized by a globular core domain flanked by a flexible N-terminal arm and a disordered C-terminal loop (Basmciogullari and Pizzato, 2014). *In vivo* studies have shown Nef to have numerous activities in the cell, which includes shielding HIV-infected cells from the host ‘s immune system (Geyer *et al*., 2001), enhancing the infectivity of the HIV-1 virion (Rosa *et al*., 2015) and optimizing viral replication (Basmciogullari and Pizzato, 2014). Nef actions require tethering to intracellular and plasma membranes, which is dependent on the post-translational modification where a myristic acid is covalently attached to the alpha-amino group on the N-terminal glycine residue (Fackler *et al*., 2006). Immune evasion activities of Nef include the down regulation of plasma membrane localized CD4 receptors. This is achieved by Nef binding to CD4 and the clathrin adaptor protein (AP-2), which accelerates the endocytosis of CD4 through clathrin-coated vesicles (Jin *et al*., 2005; Lenassi *et al*., 2010). A study by Schaefer and colleagues (2008) observed that Nef interacts with the coatomer subunit beta protein (β-COP) to direct the endocytosed CD4 receptor to the endosomal pathway for degradation (Schaefer *et al*., 2008). HIV-1 infected cells evade lysis by cytotoxic T lymphocytes (CTLs), responsible for neutralizing virally infected cells, by down-regulation the major histocompatibility complex class I (MHC-I) from the cell surface (Landi *et al*., 2011). Nef binds to the cytoplasmic tail of MHC-1 to recruit the AP-1 protein, which diverts MHC-1 to lysosomes for degradation instead of the cell surface (Singh *et al*., 2009; Landi *et al*., 2011). Downregulation of the cell surface receptors MHC-II on Antigen- Presenting Cells (APCs) by Nef leads to a defective T-helper lymphocyte-mediated immune response (Abraham and Fackler, 2012). Studies on HIV-infected APCs demonstrated lowered maturity of MHC-II on the cell surface compared to uninfected APCs,

and immature MHC-II inside the cell in the presence of Nef (Landi *et al*., 2011). Promotion of virion infectivity by Nef is achieved by redirecting transmembrane serine incorporator 5 (SERINC5) and 3 (SERINC3), potent inhibitors that impair virion penetration of susceptible cells, to an endosomal compartment, thereby excluding them from budding HIV-1 virions (Rosa *et al*., 2015; Usami *et al*., 2015). HIV-1 Nef mediates the activation of T cells, which is essential for HIV-1 replication and infection to start since quiescent T cells do not support efficient transcription, integration, and expression of the HIV-1 genome (Abbas and Herbein, 2013).

1.2.3. HIV-1 structure

The mature HIV-1 particles are round in morphology and measure approximately 100-120 nm in diameter. The outermost layer of the virion is a host-derived lipid bilayer embedded with 72 knobs, composed of trimers of the gp120 surface proteins associated to gp41 transmembrane proteins (Fig. 1.4; Checkley *et al*., 2011). The envelope covers a symmetrical capsid membrane formed by the Matrix protein (p17). The inner conical capsid composed of Capsid protein (p24) lays beneath the capsid membrane. Located within the capsid are two identical copies of single-stranded RNA, viral enzymes (RT, IN and PR) and accessory proteins (Musumeci *et al*., 2015).

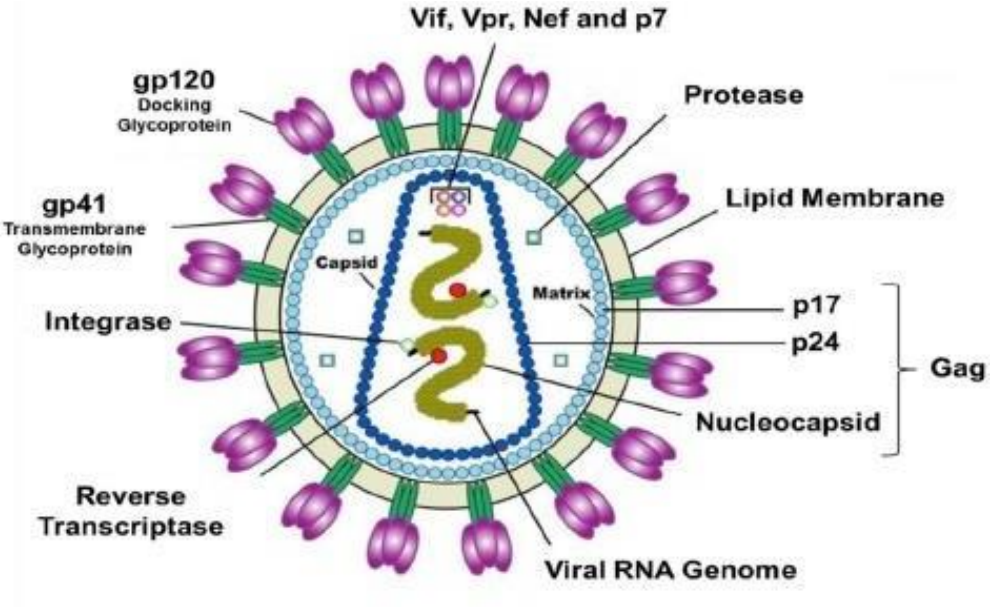

Figure 1.4: Schematic illustration of the HIV-1 structure.
The structure of a mature HIV virion is characterized by a lipid bilayer envelope with glycoproteins knobs gp120 and gp41 anchored into the envelope. Two identical RNA molecules, accessory proteins and viral enzymes Integrase, Reverse transcriptase and Protease are found within the conical capsid. Figure sourced from Musumeci *et al*., (2015).

1.2.4. HIV life cycle

The initial step of HIV replication within the CD4+ T cells requires binding of viral surface proteins to the host cell surface receptors (Figure 1.5). The viral surface gp120 protein recognizes the binding site on the CD4 receptors and binds, which leads to a conformational change in the virus envelope protein that exposes a specific domain in gp120 that binds the β- chemokine receptor (CCR5 or CXCR4) on the cell membrane (Fanales-Belasi *et al*., 2010). The co-receptor, CCR5, is expressed on the surface of macrophages and CD4+ T- lymphocytes. The strains of HIV-1 that bind to this receptor are known as macrophage-tropic (M-tropic) or R5-tropic viruses (Chen, 2019). The CXCR4 co-receptor is used by T-lymphocyte tropic (T-tropic) or X4-tropic strains of HIV-1 for entry into primary CD4+ T-cells. CXCR4 is expressed on the surface of T-lymphocytes whereas CCR5 is present on APCs such as macrophages, dendritic cells and activated T-

lymphocytes (Alkhatib, 2009; Wilen *et al.,* 2012). Some viral strains can utilize both co-receptors and are termed dual-tropic or X4/R5- tropic viruses (Fanales-Belasio *et al.*, 2010).

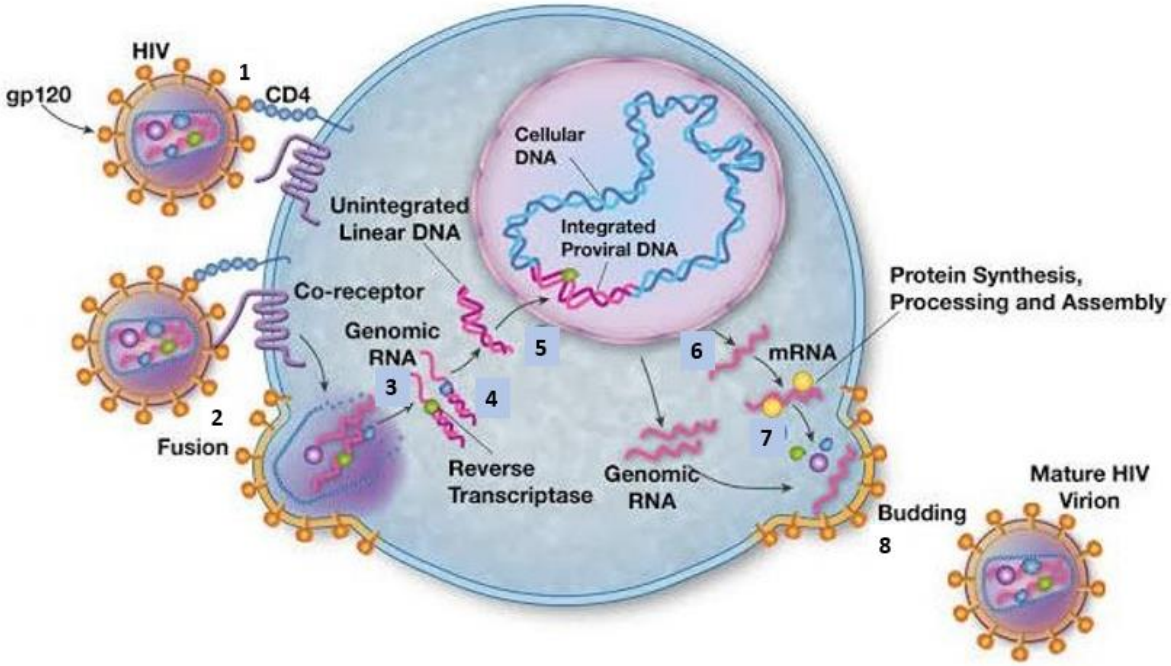

Figure 1.5: The life cycle of HIV-1 replication.
The main stages of HIV-1 replication are numbered from 1 to 8. (**1**) Binding of the virus to CD4 receptor and co-receptor on the target cell is mediated by the viral surface envelope proteins (gp41/gp120). (**2**) Binding of the receptors allows for the fusion of viral envelope and cellular membrane to release the viral core (**3**) into the cytoplasm. (**4**) This is followed by the generation of viral DNA from genomic RNA by the reverse transcriptase. (**5**) Viral DNA enters the nucleus where it integrates into the host‘s genome, facilitated by the Integrase enzyme. (**6**) The integrated provirus is transcribed by cellular RNA polymerase II. (**7**) Viral transcripts are translated into proteins in the cytoplasm and transported to the cell membrane for assembly of new virions. (**8**) New virions bud from the cell inheriting the lipid bilayer from the cell and mature into infectious viral particles. Figure sourced from The National Institute of Allergy and Infectious Diseases, (2018).

After binding, the N-terminal of gp41 penetrates the cell membrane bringing the viral envelope membrane in close proximity to the cell membrane, allowing them to merge together. Post successful membrane fusion, the virus is released into the cytoplasm of the target cell (Chen, 2019). The CA protein helps protect the viral genome against host

defence mechanisms in the cytoplasm as the viral core migrates towards the susceptible cell nucleus (Achuthan *et al.,* 2019). Partial shedding of the viral capsid and binding of cleavage and polyadenylation specificity factor 6 (CPSF6) is required during the migration towards the nucleus, allowing the competent viral core passage into the nucleus through the nuclear pores (Blanco-Rodriguez *et al.*, 2020). Within the partially shed viral core, also known as the reverse transcription complex (RTC), reverse transcription of the viral genome takes place (Achuthan *et al.*, 2019).

The single stranded RNA is used as a template by RT to generate a complementary single stranded DNA molecule. The RNA-DNA complex formed is a substrate for RNase H, which degrades the viral RNA strand within the RNA-DNA complex exposing the newly synthesized minus-stranded DNA. The RT uses the single stranded DNA to generate the plus-stranded DNA, thus, producing a double-stranded HIV proviral DNA (Hu and Hughes, 2012). Upon completion of reverse transcription, the viral core uncoats within 180 minutes before integration and approximately 1.5 µm from the chromosomal integration site (Burdick *et al.,* 2020).

The newly synthesized viral DNA associates with IN, cellular proteins Lens Epithelium-derived Growth Factor (LEDGF) and CPSF6 as a high-molecular-weight nucleoprotein complex, thus transforming the RTC into the Pre-integration Complex (PIC) (Achuthan *et al.,* 2018; Burdick *et al.,* 2020). Within the PIC, the IN multimerizes on the newly formed viral DNA to form a functional integrase-viral complex known as the intasome (Lusic and Siliciano, 2017). The intasome is a tetramer of IN subunits, with one subunit of each IN dimer binding to the ends of the viral DNA strand (Krishnan *et al.*, 2010). The HIV IN catalyses processing of the 3‘ end and formation of the integration intermediate by

removing two nucleotides from each 3‘ end of the viral DNA (Craigie and Bushaman, 2012). This involves attacking a pair of phosphodiester bonds in the linear viral DNA, generating reactive CAOH-3‘-hydroxyl ends (Lusic and Siliciano, 2017). The IN makes a staggered cleavage in the host‘s cellular DNA, allowing the 3‘ end of the viral DNA to join the 5‘ end of the target DNA at the site of cellular DNA cleavage. This activity of IN is known as strand transfer (Freed, 2001). To complete integration of the DNA recombination intermediate, cellular repair machinery is required to fill in the single stranded gaps. This results in a 5 bp duplication site that flanks the integrated provirus (Lusic and Siliciano, 2017). Integration in the host genome is not random as HIV-1 integration prefers the interior regions of genes that reside in gene-dense, transcriptionally active regions of the chromatin to ensure the presence of HIV-1 viral DNA in daughter cells after cell division (Engelman and Singh, 2018)

Upon antigen or cytokine activation during the late phase of HIV-1 replication, post-integrated host cells can begin replication of HIV-1. Activation of host cells results in the recruitment of cellular transcription factors such as Transcription factor IID (TFIID), TATA-box Binding Protein (TBP), specificity protein 1 (Sp1) and nuclear factor kappa B (NF-kB) to the HIV-1 transcription initiation site LTR (Freed, 2001). The binding of transcription factors to the TATA element within the HIV-1 LTR directs the binding of RNA polymerase II to the HIV-1 DNA (Tjitro *et al.,* 2019). Transcription of the proviral DNA results in over 30 viral RNA transcripts divided into three classes; 1st multi spliced mRNA (~1.8 kb), 2nd partially spliced mRNA (~4 kb) and 3rd unspliced RNA (~9 kb) (Esquiaqui *et al.*, 2020). Firstly, the multi spliced mRNA are synthesized, of which they encode for the nucleus located regulatory proteins Rev and Tat, as well as Nef, which control HIV-1 gene expression (Esquiaqui *et al.,* 2020). Basal transcription of HIV-1 genome is very low; however,

synthesis of RNA is increased exponentially by the binding of Tat to TAR on HIV-1 LTR (Freed, 2001).

Rev binds to RRE to facilitate exportation of the unspliced and partially spliced transcripts to the cytoplasm using the cellular chromosome maintenance factor 1 (CRM1) export pathway (Fernandes *et al*., 2016). Once the partially spliced mRNA transcripts reach the cytoplasm, they will be translated by ribosome into Env and accessory proteins Vif, Vpr and Vpu (Esquiaqui *et al.,* 2020). The Env glycoproteins are translated by the fixed ribosomes and trafficked via the secretory pathway, starting at the endoplasmic reticulum to the Golgi, and then in vesicles to the plasma membrane (Freed, 2015). The unspliced HIV-1 RNA has a dual role as a mRNA that encodes Gag and Gag/Pol proteins, and as genomic RNA (gRNA) that will be encapsidated in the formation of new virions (Ohlmann *et al.*, 2014). The HIV-1 mRNA is translated by free ribosomes in the cytoplasm using the Programmed-1 ribosomal frameshifting (-1 PRF) mechanism to produce Gag and Gag-Pol precursors (Karn and Stoltzfus, 2012; Korniy *et al.,* 2019). The -1 PRF mechanism allows for maintaining of the 20:1 Gag to Gag-Pol ratio as it is essential for virus propagation (Korniy *et al.,* 2019). Dysregulation of -1 PRF negatively effects HIV-1 replication, virion formation and infectivity (Korniy *et al.,* 2019). The MA domain in the $Pr55^{Gag}$ targets Gag to the plasma membrane and promotes incorporation of the viral Env glycoproteins into forming virions; the CA domain promotes Gag multimerization during assembly (Li *et al.*, 2007; Freed, 2015). The viral RNA genome is recruited by NC for the virion assembly process (Kempf *et al.,* 2015). Following arrival of the Gag protein, the Gag-Pol precursor, and the viral genomic RNA at the plasma membrane, they assemble into a nascent immature virus particle ready for the budding off process (Freed, 2015). The p6 domain within Gag facilitates budding by recruiting and binding the Endosomal Sorting

Complex Required for Transport (ESCRT) apparatus, which catalyses release of the immature virion from the host plasma membrane and membrane fusion reaction after release (Sundquist and Kräusslich, 2012). After release of the virus particle, maturation is needed to turn the virion into a mature virus. The viral PR, encoded within the Gag-Pol polyprotein precursor, cleaves the Gag precursor into mature NC, CA, MA and p6 proteins and triggers the morphological transformation that forms the conical capsid core (Freed, 2015).

1.3. HIV pathology

Infection with HIV-1 occurs via several ways such as sexual contact across mucosal surfaces, maternal-infant exposure, by percutaneous inoculation with contaminated needles and blood transfusion (Shaw and Hunter, 2012). Penetrative sex accounts for most new infections, with the risk of transmission through anal sex being 10 times higher than vaginal sex (UNAIDS, 2019). Although epithelial cells do not express HIV-1 CD4 receptors, alternate receptors such as gp340 have been shown to facilitate attachment of HIV-1 to vaginal epithelial cells (Kinlock *et al.,* 2014). Free HIV-1 virions attach to epithelial cells and traverse the epithelial cells by transcytosis or endocytosis, where they gain access to dendritic cells, Langerhans and CD4 T cells in the epithelium (Gurtler *et al.*, 2016). The immune cells harbouring virions migrate from the epithelium into the lymphatic and venous micro vessels to be transported to local lymph nodes and into the blood circulation, respectively, initiating systemic infection (Hladik and McElrath, 2008). During early infection, target cells expressing the CCR5 chemokine receptors are strongly preferred by HIV-1 virions. This is confirmed by reports which show that humans with homozygous defective expression of CCR5 are protected from HIV-1 infection (Berger *et al.*, 1999; Shaw and Hunter, 2012). CXCR4 viruses are rarely transmitted, which favours the R5-tropic virus as founder viruses. This was confirmed by a phenotypical analysis

study by Keele *et al.* (2008) which observed 98 Env from 102 HIV-1-infected subjects were dependent on CCR5 for cell entry. Genetic and phenotypic analysis conducted by Derdeyn, and colleagues (2004) observed a bottleneck effect, suggesting that one or few virus variants initiated infection in a new host from the bulk ofthe virus from the donor host. Using a single genome amplification technique, Keele and colleagues (2008) were able to confirm the genome population bottleneck to HIV-1 transmission. The bottleneck effect on HIV-1 transmission is as a result of many factors, including viral compartmentalization as viral migration between some anatomical sites or tissues is restricted, especially in the central nervous system and genital tract (Blackard, 2012). Neutralization of Env spikes by antibodies block the attachment of viral glycoproteins to CD4 receptors, thereby stopping viral entry (Klasse, 2014). The development of the vaginal mucosa results in a flat and keratinized basal layer that restricts the passive diffusion of HIV-1 through it (Kariuki *et al.,* 2017).

During the initial stages of HIV-1 infection, the virus will encounter a high density of primary target cells in the intraepithelial pocket, which support viral replication and amplification, with subsequent migration of the virus and infected cells to the lymph nodes (Lackner *et al.*, 2012). Within the latter, HIV-1 RNA plasma viremia levels rapidly increase (Figure 1.6, page 20), reaching peak levels at which point HIV-1 RNA may be detected in plasma by a polymerase chain reaction (PCR). However, serum antibodies to HIV-1 are not sufficiently elevated for detection by an enzyme-linked immunosorbent assay (ELISA). This is known as the window period (Marlink *et al.*, 1986). This period is associated with the development of seroconversion,which takes 3-6 weeks after infection, often mistaken for as a flu infection (Weston and Marett, 2009). Fiebig and colleagues were the first to identify distinct laboratory stages of HIV infection to clarify the time course of detection of viremia

and antibody seroconversion following acute HIV infection (Fiebig *et al.,* 2003). The 51 participants involved in the study were seen to follow a systematic transition where no markers of HIV-1 were detected, to stage I were only HIVRNA was detected after 5 days of HIV-1 infection. Stage II allowed the identification of HIVRNA and p24 antigen within 10 days and stage III showed the positive identification of antibodies and negative western blot identification within 14 days of primary HIV-1 infection (Fiebig *et al.*, 2003; Stekler *et al.*, 2018). After 19 days of HIV-1 infection, stage IV was established when positive antibodies identification was observed but western blot identification was indeterminate, and stage V produced positive western blot identification but as missing the p31 protein band after 88 days with the HIV infection (Fiebig *et al.*, 2003; Cohen *et al.*, 2010). Post 88 days of the HIV infection, all tests produced positive identification of HIV RNA, p24 antigen, antibodies, and western blot, including the p31 band (Fiebig *et al.*, 2003). The CDC later validated this work to establish the window period for all HIV screening and tests (Stekler *et al.*, 2018).

Decline of CD4+ lymphocytes are halted as the host generates a humoral and cellular immune response that controls viral replication, ensuring high levels of HIV-1 viremia is brief (Fanales- Belasio *et al.*, 2010; Swanstrom and Coffin, 2012). This control is a result of the virus-specific cell mediated immune response of the CD8+ T-cell cytotoxic activities, before theestablishment of anti-HIV binding antibodies (Fanales-Belasio *et al.*, 2010).

Over the following weeks, a dynamic equilibrium between viral replication and destruction is achieved where the population of viremia declines to a lower steady level known as the viral setpoint (Weston and Marett, 2009). Activation of both the innate and adaptive immune systems does not eradicate the infection. This is as a result of the virus integrating into the lymphatic tissues (reservoirs) where low expression of virus antigen and high viral mutation

is observed, shielding it from the immune system (Ford *et al.*, 2009). HIV-1 forms stable reservoirs of latent HIV-1 in multiple cell types and anatomical sites that prevent the total eradication of HIV-1 even when replication and transmission is suppressed by Highly Active Antiretroviral Therapy (HAART) (Ait-Ammar *et al.,* 2020). HIV-1 infected memory CD4+ T cells are the best characterized cellular reservoirs (Kandathil *et al.,* 2016), however, non-CD4+ T cells like mast cells (Sundstrom *et al.,* 2007), macrophages (Honeycutt *et al.,* 2017) and hematopoietic stem and progenitor cells have shown potential to be cellular reservoirs (Araínga *et al.*, 2017; Zaikos *et al.*, 2018). The well-established anatomical HIV-1 reservoirs include lymph nodes, gut-associated lymphoid tissue (GALT), central nervous system and genital tract (Ait-Ammar *et al.,* 2020). The respiratory tract, liver, kidney and adipose tissue are other anatomical sites gaining recognition as HIV-1 reservoirs (Couturier *et al.*, 2015; Cribbs *et al.*, 2015; Chaillon *et al.*, 2020). Following establishment of the viral setpoint, a long asymptotic period (8 years or longer) of HIV clinical latency is achieved, characterized by continuous viral replication and steady loss of CD4+ lymphocytes. However, when low CD4+ cells (below 200 cells/µl) levels are reached, it facilitates the onset of AIDS defining life-threating opportunistic infections by bacteria, viruses, fungi, and tumours, due to dismantling of the immune system (Figure 1.6; Lackner *et al.*, 2012; Weston and Marett, 2009). Once a patient is diagnosed with AIDS, the survival rate is typically three years, however, a dangerous opportunistic infection can lower the life expectancy to one year (Lackner *et al.,* 2012). This is considerably less when compared to the survival rate of people living with HIV (PLWH) receiving constant treatment. If treatment is received before CD4 count drops below 500 cell/µl, life expectancy in PLWH is similar to people not living with HIV (Marcus, *et al*., 2020). Additionally, individuals receiving HAART survive >10 years after the development of AIDS (Poorolajal *et al*., 2016).

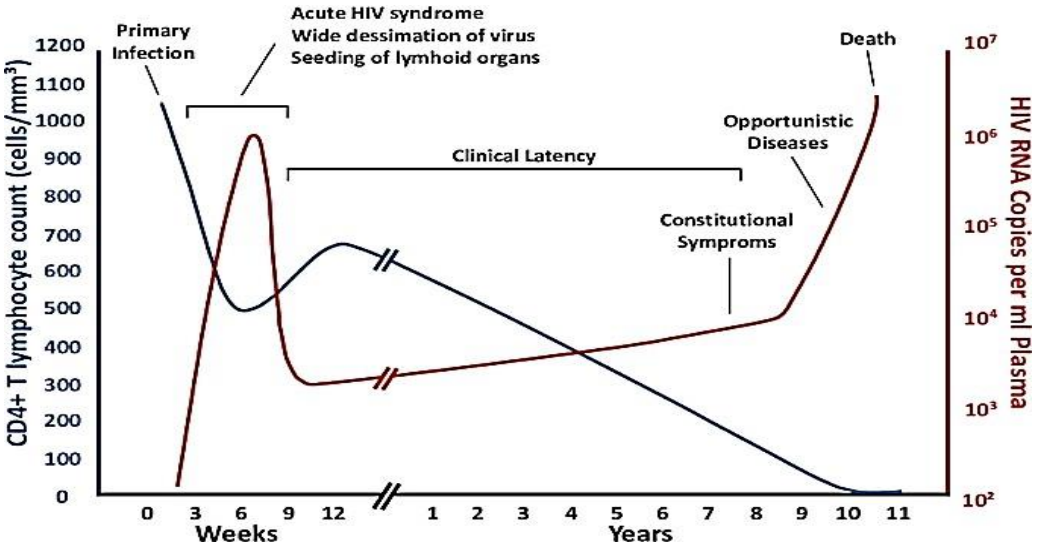

Figure 1.6: The general course of HIV-1 infection.
The acute stage of HIV infection is characterized by the exponential amplification of HIV RNA (red) copies in the host, peaking at 3-6 weeks, while experiencing a rapid decline in CD4+ T lymphocyte population (blue) in the host's lymphatic tissues and bloodstream. Post dramatic replication of HIV RNA, a decline is observed due to an immune response producing new CD4+ lymphocytes. Clinical latency is established where persistent viral replication occurs as a gradual loss of CD4+ lymphocytes is witnessed. Loss of immunity results in the development of AIDS-defining opportunistic diseases which are life threating. Figure sourced from Fauci *et al.*, (1996).

1.4. HIV antiviral therapy

While no cure for HIV/AIDS exists, multiple drugs have been developed to suppress HIV replication to undetectable levels (<50 RNA copies/ml[3]) and stop the transmission of HIV to uninfected individuals (Arts and Hazuda, 2012). The first class of HIV antiviral drugs developed were inhibitors against the HIV viral enzymes IN, RT and PR, as they were exclusively expressed by the virus and are absent in the human genome (Sierra-Aragón and Walter, 2012). The first line of HIV-specific treatments administered as a monotherapy were RT inhibitors in the form of non-nucleoside RT inhibitors (NNRTI) and nucleoside analogs (Sierra- Aragón and Walter, 2012). These drugs had limited success as the therapy was challenged by rapid drug resistance by the virus within months of treatment (Sierra-Aragón and Walter, 2012). This brought about the evolution of HIV-1 treatment from

monotherapies to cocktails of antiretroviral agents (ARVs), also known as HAART, to treat HIV-1 infections as these new therapies were more potent and the drugs more stable, thus preventing drug resistance (Kuritzkes, 2011). The combination therapy consists of two nucleoside analogs with a PR inhibitor or NNRTI, or IN inhibitor (Sierra-Aragón and Walter, 2012).

The effectiveness of drug combinations in HAART is as a result of the development of new classes of drugs that target different stages within the HIV replication cycle. There are five classes of antiretroviral drugs produced, namely, (1) nucleoside/nucleotide reverse transcriptase inhibitors (NRTIs), (2) non-nucleoside reverse transcriptase inhibitors (NNRTIs), (3) IN inhibitors, (4) Viral entry inhibitors, and (5) Protease inhibitors (PI) (Table 1.2; Greenea *et al.,* 2008; Pebody, 2021). The antiretroviral drugs are developed to target and disrupt a specific stage in the HIV-1 replication cycle, thereby halting viral replication, ultimatelycontrolling HIV infection (Sierra-Aragón and Walter, 2012).

Table 1.2: Classes of HIV-1 antiretroviral drugs and their targets

Class	Mechanism of action	HIV replication stage target	Names of antiretroviral drug	References
NRTIs	Incorporates into viral DNA in RT reactions to terminate further viral DNA synthesis	Reverse transcription	Abacavir, Lamivudine, Tenofovir disoproxil, Zidoovudine	Sluis-Cremer *et al.*, (2000); Arts and Hazuda; 2012. Pebody, (2021)
NNRTIs	Allosterically binds to RT domains to restrict flexibility, thus reducing enzyme efficiency	Reverse transcription	Doravirine, Efavirenz, Etravirine, Neviraoine, Rilpivirine	Pauwels, (2004). Sierra-Aragón and Walter, (2012)
Integrase inhibitors	Prevents the formation of covalent bonds with host DNA and prevents provirus development	Integration	Bictegravir, Dolutegravir, Elvitegrravir, Raltegravir, Cabotegravir	Mouscadet and Tchertanov, (2009); Dow and Bartlett, (2014). Pebody, (2021)
Viral entry inhbitors	Binds to viral envelope protein gp120, host membrane co-receptor CCR5 to block viral Entry	Entry	Maraviroc, Enfuvirtide Fostermsavir, Ibalizumab	Qian *et al.*,(2009). Haqqani and Tilton, (2013)
Protease inhibitors	Binds and blocks the active site of HIV protease to stop development of mature virions	Assembly and Maturation	Atazanavir, Darunavir, Lopinavir, Saquinavir	Lv *et al.*, (2015). Pebody, (2021)

1.5. Trends in HIV mortality

The HIV/AIDS epidemic has seen a significant shift since it was first described in the early 1980s. Initially regarded as a death sentence, it is now fast becoming a manageable chronic illness due to the development of Highly Active Antiretroviral Therapies (HAART) (Danforth *et al.*, 2017). HIV/AIDS related deaths were on the rise since 1980, reaching its peak between 2004 and 2005 with over 2 million deaths, and has since then been on a steady decline (UNAIDS, 2019). The decline in deaths is because of the early initiation of ART, improved access to health care and improved prevention measures (Danforth *et al.*, 2017; Ebne *et al.*, 2020). The United Nation Fast-Track Targets for 2030 proposed challenging, yet achievable 95-95-95 goals, which aim to reduce the number of deaths by 200 000 per year (UNAIDS, 2019). The Fast-Track targets set are that 95% of the PLWH know their status, 95% of this population are receiving treatment and 95% of HIV-treated patients have a suppressed HIV viral load so the likelihood of their infection being passed is reduced (UNAIDS, 2019). The sub-Saharan Africa region remains the epicentre of the HIV/AIDS pandemic with the biggest challenge of achieving the 95-95-95 target (Gona *et al.*, 2020).

Widespread administering of ART has improved the life expectancy of PLWH to levels comparable to their HIV-1 negative counterparts (Erlandson and Karris, 2019). The increased longevity of PLWH bears the burden of increased non-AIDS-related comorbidities, usually associated with advancing age (Guaraldi *et al.*, 2011). A study by Schouten *et al.*, (2014) observed an increased risk of age-associated non-communicable comorbidities such as hypertension, diabetes mellitus, impaired renal function and cardiovascular diseases in PLWH compared to HIV-uninfected control groups. Cardiovascular diseases (CVDs) have emerged as one of the major causes of death among PLWH (Table 1.3; Wang *et al.*, 2015).

Table 1.3: Studies on cardiovascular mortality among HIV-infected people

Study	Number of HIV-infected participants	Participants characteristics	Number of HIV deaths due to CVD	Study outcomes
Feinstein *et al.*, (2016)	189 703 (HIV-infected dying from any cause)	25 years or older; 74% male; 54% black	5313	The number of HIV deaths due to CVD had increased from 307 (1.95%) to 400 (4.62%) from 1999 and 2013 in the United State of America HIV-infected population. However, total HIV mortality was decreasing during the same period.
Hanna *et al.*, (2016)	145 845	13 years or older; 72.5% males; 45,5% black and 32.6% Hispanic; 68,8% had HIV-1 viral suppression (<400 copies/mL)	2971	10% of deaths among people infected with HIV in New York, USA between 2001-2012 were a result of CVDs. CVD mortality rates were lower among those on HIV treatment (3.99 per 1000 PY) vs HIV treatment-naïve (8.02 per 1000 PY), however, bothCVD mortality were higher than those of the general population (3.22 per 1000 PY)
D: A; D Group, (2010)	33 308	74,1% males; 53,6% white; median age of 39; 24374 (73,2%) had received HIV-treatment at study entry and 48,6% had HIV RNA less than 400 copies/mL	289	11,6% of all HIV deaths were a result of CVD among HIV-positive individual at 212 clinics in 21 countries in Europe, the United States and Australia from 1999 to 2008.
Antiretroviral Therapy Cohort Collaboration, (2010)	39 272	16 years or older; 73% males; all on HIV treatment; 87% had HIV-1 RNA levels 4 log copies/mL	103	CVDs were the definitive cause of death, accounting for 6.5% of total deaths among HIV-infected patients a on ART in Europe and North America from 1996 to 2006

1.6. Cardiovascular diseases in the HIV-infected population

Cardiovascular diseases (CVDs) refer to medical conditions that involve the narrowing or blockage of blood vessels, which may lead to hypertension, heartattack, angina, or stroke (Shiel, 2018). CVDs are the leading cause of deathaccounting for 17 million deaths globally, with over three quarter of deaths occurring in low- and middle-income countries (WHO, 2017). CVDs are acknowledged as complications of HIV-1 infection, compounding on already recognized traditional riskfactors (Mathebul *et al.*, 2020). Multiple studies have attributed the cause of CVD in the people with HIV-1 to long-term HIV exposure (Danforth *et al.*, 2017), chronic inflammation (Subramanian *et al.*, 2012; Tawakol *et al.*, 2014), dyslipidaemia (Grunfeld *et al.*, 1992), microbial translocation (Pedersen *et al.*, 2013) and insulinresistance (Hruz, 2011; Shah *et al.*, 2018).

The elevated risk of CVDs among PLWH has been associated with the use of HAART and protease inhibitors (Nsagha *et al.*, 2015). However, recent studies have also observed an increased risk of CVDs amongst treatment-naïve patients infected with HIV-1 (Stein *et al.*, 2013; Guo *et al.*, 2017; Martínez-Ayala *et al.*, 2020). While studies may attribute higher risk of developing CVD to either HIV-1 treatment-naïve or medicated patients, all agree that PLWH have a higher risk of CVD than their HIV-negative counterparts (Rethy *et al.*, 2020). A clinical study conducted in 33 countries in Australia, Europe, and the Americas by the SMART study group (2006) involving 5,472 (27% female and 56% white) participants infected with HIV-1 over the age of 13, who had a CD4+ cell count of more than 350 cells/ml^3 were used in investigating the adverse health risks associated with continuous antiviral therapy compared to intermittent therapy (El-Sadr *et al.*, 2006). Therapy was stopped for 2,720 participants until their CD4+ cell count dropped below 250 cells/ml^3 and then re-administered until CD4+ cell count reached 350 cells/ml^3 (i.e., intermitted therapy

group), while the other 2,752 participants continued to receive therapy (i.e., viral suppression group). Among the intermittent therapy group, 65 (2.4%) people had at least one episode of major cardiovascular, renal, or hepatic disease, as did 39 (1.4%) participants in the viral suppression group (hazard ratio, 1.7; 95% CI, 1.1 to 2.5; P = 0.009). These findings showed that stopping therapy was associated with higher risk of cardiovascular events, thus suggesting that viral replication, immunodeficiency, or inflammation may be the cause of premature CVD (SMART study Group, 2006). A study by Triant *et al.* (2007) with 3,851 people with HIV-1 (1,578 participants were on antiretroviral therapy medicine) and 1,044,589 non-HIV patients receiving longitudinal care between 1996 and 2004 observed an increased in acute myocardial infraction (AMI) and cardiovascular risk factors in patients with HIV-1 compared with uninfected patients, particularly among women (Volpe *et al.*, 2017). The AMI rates per 1000 person-years were increased in HIV *vs*. non-HIV patients [11.13 (95% confidence interval [CI] 9.58–12.68) *vs*. 6.98 (95% CI 6.89–7.06)] (Triant *et al.*, 2007). These findings were later confirmed by a meta-analysis study by Islam *et al.* (2012) in which they observed a relative increased CVD risk of 1.61 [95% CI] among PLWH who were not on HAART compared with people without HIV. In the Veterans Aging Cohort Study involving 82,459 adults, people living with HIV were reported to have a 50% increased risk of CVD beyond recognized traditional risk factors (Freiberg *et al.*, 2013). An imaging study using computed tomography angiography showed a higher prevalence of coronary atherosclerosis in young, asymptomatic men with HIV-1 compared to their HIV- seronegative counterparts (Lo *et al.*, 2010). Multiple studies show that HIV-1 infectionis associated with intrinsic characteristics that increase the risk of CVDs among affected people (So-Armah and Freiberg, 2014). This brings into question the biological mechanisms surrounding the development of CVD in PLWH HIV-1.

1.7. Endothelial dysfunction

1.7.1. Endothelial cell activation

Since the discovery of HIV-1 being the causative agent of AIDS, it is evident that chronic inflammation plays a role in the pathogenesis of HIV-1 infection (Deeks *et al.*, 2013). HIV-1 infection induces a pro-thrombotic state and pro-inflammation phenomena in the vascular endothelium that increases CVD risk (Hsue *et al.*, 2009; Mazzuca *et al.*, 2016).

The endothelium is a single layer of squamous cells that internally lines the walls of blood vessels, forming a barrier between blood and tissues (Brevetti *et al.*, 2008). Endothelial cell activation is defined by the induction of transcription factors and nuclear factor kappa-light-chain-enhancer of activated B cells (NF-κB) pathway, leading to enhanced expression of cell-surface adhesion molecules such as the intercellular adhesion molecule-1 (ICAM-1), vascular cell adhesion molecule-1 (VCAM-1) and endothelial leukocyte adhesion molecule-1 (ELAM-1 or E-selectin) on the outer membrane of endothelial cells (Figure 1.7; Liao, 2013). In response to endothelial activation by cytokines, the adhesion molecules bind to leukocytes to increase leukocyte affinity to the endothelial surface, thus increasing trans-endothelial migration into tissues (Cerutti and Ridley, 2017). The cytokine, tumour necrosis factor alpha (TNF-α), binds to its TNF-receptor (TNFR) on the outer membrane of endothelial cells. The binding of TNF-α to TNFR induces the kinase phosphorylation of NF-κB in the cytoplasm leading to the degradation of kappa light polypeptide gene enhancer in B-cells inhibitor alpha (IκBα) by proteasomes (Barnes & Karin, 1997). The degradation of IκBα allows the migration of NF-κB into the cell nucleus, where it binds to promoter regions of adhesion molecule genes to enhance the expression of cellular adhesion molecules (Steyers and Miller Jr, 2014).

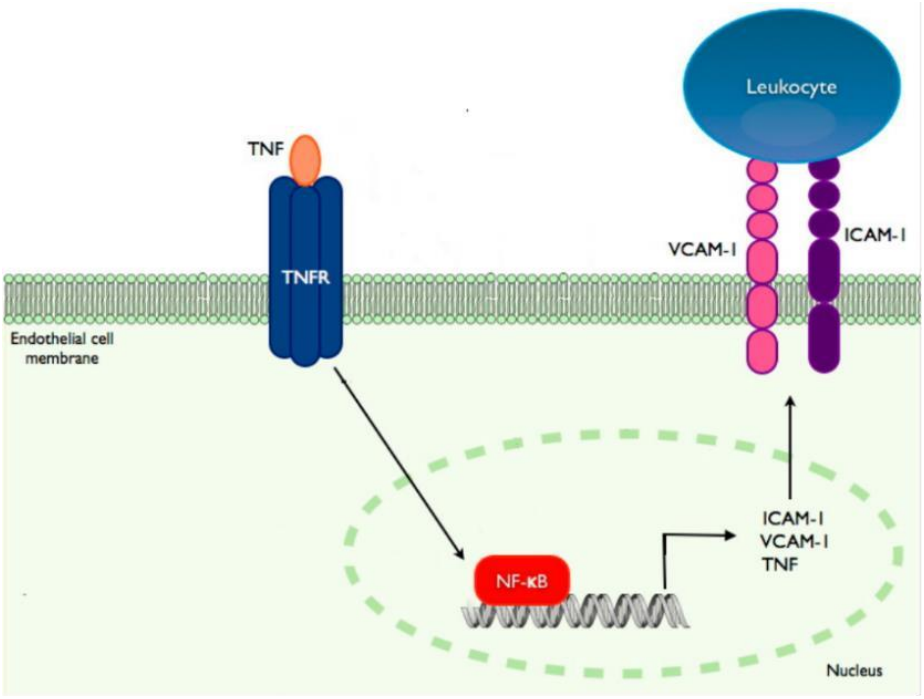

Figure 1.7: Endothelial cell activation pathways
Tumour Necrosis Factor-α (TNF-α) is known to target endothelial cells by binding to the TNF- receptor (TNFR) on the cellular membrane. Binding of the cytokine to its cell surface receptor leads to increased expression of cellular adhesion molecules ICAM-1 and VCAM-1, via migration of NF-κB into the nucleus. NF-κB in the nucleus binds to promoters than enhance the expression of cellular adhesion molecules. Figure adapted from Steyers and Miller Jr, (2014).

Increased levels of inflammation and vascular activation increases the production of reactive oxygen species (ROS), which inhibits endothelial nitric oxide synthase resulting in endothelial dysfunction (Liao, 2013). The latter leads to impaired regulation of vascular tone, cellular adhesion, vascular smooth muscle migration and resistance to thrombosis (Steyers and Miller Jr, 2014). Impairment of endothelial function is regarded as a precursor for the initiation of most CVDs (Biswas and Khan, 2020). Endothelial dysfunction is a pathological condition characterized by the detachment of ICAM-1 and VCAM-1 from the endothelial cell membrane (Mu *et al.*, 2007).

HIV-1 infection is associated with the release of cytokines including Interferon-A, Interferon-γ, inducible protein 10, Tumour Necrosis Factor (TNF), Interleukin-15 (IL- 15), IL-6 and IL-

10 (Stacey *et al.*, 2009; Deeks *et al.*, 2013), Reactive Oxygen Species (ROS) and, -oxidized low-density lipoprotein (LDL) (Steyers and Miller Jr, 2014), which either directly or indirectly activate endothelial cells. Multiple studies report elevated levels of these molecules in adults with HIV-1 (Francisci *et al.*, 2009; Arildsen *et al.*, 2012; Deeks, Tracy *et al.*, 2013), as well as in infected children, compared to their uninfected counterparts (Miller *et al.*, 2010).

1.7.2. Biomarkers of endothelial dysfunction

Endothelial dysfunction contributes to the pathogenesis of a variety of CVD, including atherosclerosis and thrombosis. However, endothelial activation often precedes endothelial dysfunction, and biomarkers of the activated endothelium may be detected in serum (Page and Liles, 2013). This can therefore be used as a measure to determine disease severity as well as prognosis. Several molecules and proteins have been identified as markers for the assessment of endothelial activation/dysfunction in individuals infected with HIV-1 with varying degrees of confidence. These include Angiopoietin-1 and -2 (Ang-1 and-2), von Willebrand factor (vWF), ICAM-1, VCAM-1, and E-selectin (Page and Liles, 2013).

1.7.2.1. Angiopoietin-1 and -2

Angiopoietin-1 and -2 (Ang-1 and -2) are well established biomarkers of endothelial activation/dysfunction in infectious diseases (Meurs *et al.*, 2009). Ang-1 is expressed in the pericytes and smooth muscle cells surrounding the endothelium, while Ang-2 is produced by endothelial cells and released from Weibel-Palade bodies upon inflammatory stimuli (Meurs *et al.*, 2009). Ang-1 and -2 operate as antagonistic ligands of the Tie-2 receptor on vascular epithelial cells (Figure 1.8; Fiedler and Augustin, 2006). Under normal physiological conditions, serum concentration of Ang-1 surpasses that of Ang-2, allowing Ang-1 to bind to the Tie-2 receptor (Fiedler *et al.*, 2003). This induces a pro-survival state and inhibits pro- inflammatory pathways (Lukasz *et al.*, 2008; Page and Liles, 2013).

However, during inflammation, the stimulated Weibel-Palade bodies release Ang-2 by exocytosis to allow preferential binding of Ang-2 to Tie-2 receptors, thus promoting pro-inflammatory and pro-thrombotic pathways (Fiedler and Augustin, 2006; Page and Liles, 2013). Angiopoietin dysregulation, as a consequence of chronic inflammation, is characterized by increased levels of Ang-2 over Ang-1, thus making it an excellent biomarker of endothelial activation/dysfunction (Fagiani and Christofori,2013).

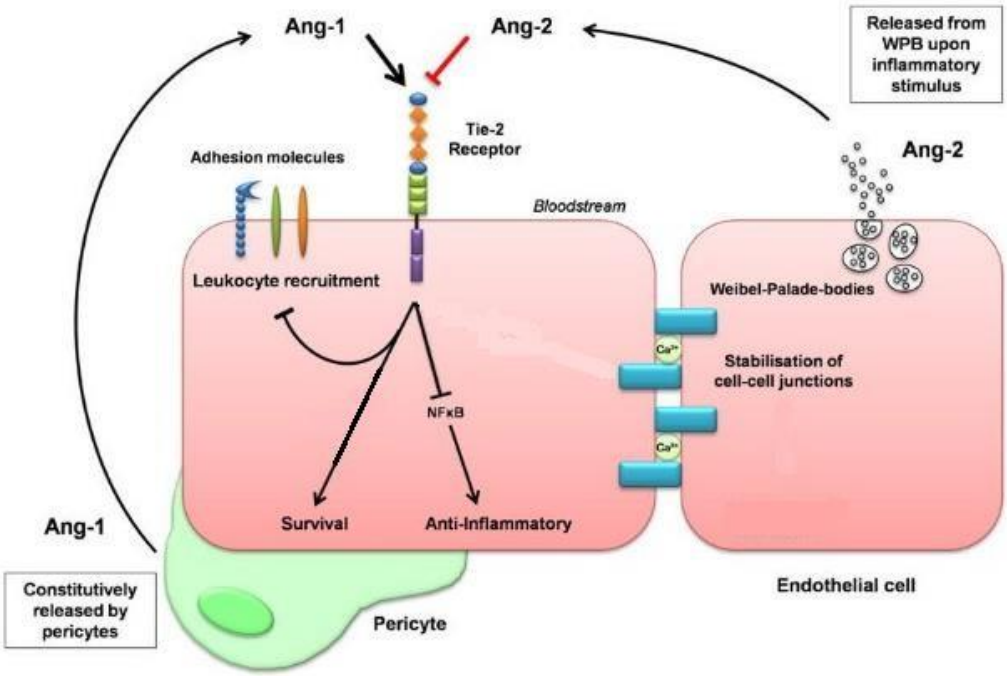

Figure 1.8: The angiopoietin and Tie-2 receptor system
Under normal physiological conditions, serum concentration of Ang-1 released pericytes surpasses that of Ang-2, allowing Ang-1 to bind to the Tie-2 receptor, maintaining the quiescent resting state of the endothelium. This induces a pro-survival state and inhibits pro- inflammatory pathways. However, during inflammation, the stimulated Weibel-Palade bodies in endothelial cells release Ang-2 by exocytosis to allow preferential binding of Ang-2 to Tie- 2 receptors, thus destabilizing the quiescent endothelium and promoting pro-inflammatory and pro-thrombotic pathways. Figure adapted from Fiedler and Augustin, (2006).

1.7.2.2. Von Willebrand factor

Von Willebrand factor (vWF) is an adhesive glycoprotein synthesized by endothelial cells and stored in Weibel-Palade bodies (Peyvandi *et al*., 2011). It is released upon endothelial

activation to stabilize adhesion of platelets at sites of vascular injury (Page and Liles, 2013). The role of vWf as a biomarker of CVD is controversial as multiple studies cite a weak association between high levels of vWF and the risk of CVD (Spiel *et al*., 2008; Arildsen *et al*., 2013; Gragnano *et al*., 2017). However, within the context of HIV-1 infection, a 10 year study by Dries *et al*., (2015) involving 198 participants with HIV-1 of which 71% were males and 183 subjects were on treatment, reported 60 documented thrombotic events in 14,026 person years of observation occurred (PYO), resulting in an incidence rate of 2.50 (arterial), 2.21 (venous) and 4.28 (combined) thrombotic events per 1000 PYO. The vWF level was elevated in most cases compared to controls. A prospective study of 20 treatment-naïve PLWH HIV-1 conducted by Arildsen *et al*. (2013) examined patients before and after 3 months of treatment. The data revealed that treatment- naïve patients with HIV-1 exhibited endothelial dysfunction with flow-mediated dilation (FMD) at 108% vs 111% [$P< 0.05$]; C-reactive protein (CRP) 24 vs 8.6 nmol/L and vWF 2.0 vs 0.9 U/l, for HIV- infected vs HIV-negative control groups (Arildsen *et al*., 2013). The low FMD reading among PLWH means that the arteries do not dilate past their basal diameter upon responding to increased blood flow, which suggests low levels of nitric oxide are released by the endothelial cells (Raitakaari and Celermajer, 2000). This is as a result of endothelial dysfunction. However, initiation of therapy resulted in normalization of FMD and decreased endothelial activation and serum CRP levels (Arildsen *et al*., 2013). These findings may explain the weak association between vWF and risk of CVD, as treatment may reverse the release of vWF from endothelial cells.

1.7.2.3. Adhesion Molecules

The most studied markers of endothelial function are the blood-based markers, and more specifically, the cellular adhesion molecules ICAM-1, VCAM-1 and E-selectin (Graham *et*

al., 2013). ICAM-1 and VCAM-1 are expressed on the cell surface of both hematopoietic and non-hematopoietic cells (Yu *et al.*, 2020), while E-selectin is exclusively expressed on endothelial cells upon cytokine activation (Milestone *et al.*, 2000). During inflammation, these molecules are up regulated resulting in the increased recruitment of leukocytes to the endothelium, promoting trans endothelial migration (Cerutti and Ridley, 2017). Increased movement across the endothelium results in endothelial shear stress, causing endothelial shedding which promotes the detachment of cellular surface proteins into the surrounding environment (Chatzizisis*et al.*, 2007).

Cellular adhesion molecules are excellent biomarkers of endothelial activation/dysfunction as they are found in low concentrations on the cellular membrane of endothelial cells at basal conditions, however, they are not simultaneously expressed or always suppressed (Cybulsky *et al.*, 2001). Multiple studies investigating levels of vascular biomarkers during HIV-1 infection report elevated levels of cellular membrane-detached soluble forms of ICAM-1, VCAM-1 and E-selectin in the blood (Fourie *et al.*, 2011; Miller *et al.*, 2012; Graham, Mwilu and Liles, 2013; Hunt, Lee and Siedner, 2016; Mosepele *et al.*, 2018). A study conducted by Baker and Duprez (2010) reported change in plasma levels, specifically the soluble form of VCAM-1, to be associated with increased HIV-1 viral replication following interrupted treatment. Furthermore, studies conducted by Hwang *et al.* (1997) and Ridker *et al.* (1998) report an association between elevated levels of ICAM-1 and E-selectin with increased risk of coronary heart disease. Although results from the studies have been inconsistent, they may go well to show that different pathways are activated in response to different inflammatory diseases, with varying effects on the expression of cellular adhesion molecules (Page and Liles, 2013).

1.7.3. Role of HIV-1 Nef in endothelial dysfunction

The emergence of HIV-1 infection as an independent contributor of CVDs in the population infected with HIV-1 has led to investigations which aim to understand the mechanism of action (Figure 1.9; Triant *et al.*, 2007). The presence of HIV-1 gp120 and Tat in endothelial cells, and the interdependent actions of these proteins with HIV-induced cytokines, has shed some light into this phenomenon (Ullrich *et al.*, 2000; Toborek *et al.*, 2003). HIV-1 gp120 and Tat negatively affect endothelial function by inducing the release of the potent vasoconstrictor, endothelin-1, increasing the expression of cellular adhesion molecules and inducing apoptosis in endothelial cells (Kline and Sutliff, 2008). HIV-1 Nef became of great interest as Appay *et al.* (2002) observed ongoing expression of HIV-1 Nef despite prolonged and clinically successful antiretroviral therapy. A study conducted by Marecki *et al*. (2005) supported the theory that Nef may play a role in the development of CVD after observing the development of HIV-related pulmonary hypertension in Macaques infected with only the recombinant chimeric Simian Immunodeficiency Virus (SIV)/HIV constructs containing the HIV-1 *nef* gene as opposed to those infected with SIV strains (Marecki *et al.*, 2005). This observation was corroborated in a subsequent study (Marecki *et al.*, 2006) where Nef was detected in vascular cells of patients with HIV-related pulmonary hypertension, and not in patients with idiopathic pulmonary arterial hypertension.

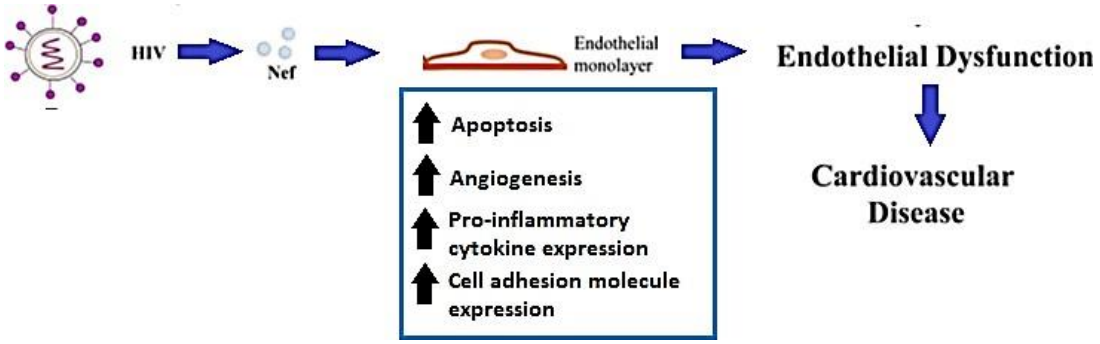

Figure 1.9: HIV-1 Nef and its effect on endothelial function
The transfer of HIV-1 Nef by circulating HIV-infected cells to endothelial cells leads to apoptosis, angiogenesis, increased expression of inflammatory cytokines and cell adhesion molecules. These events are characteristic of endothelial dysfunction which is known to predict a potential CVD event. Figure adapted from Anand *et al.*, (2018).

Multiple studies suggest Nef can be transferred from HIV-1 infected cells to bystander cells by either a cell-cell contact-independent mechanism (via tunnelling nanotubes and exosomes, Sowinski *et al.*, 2008; Lenassi *et al.*, 2010; Shelton *et al.*, 2012), or via a cell-cell contact-dependent mechanism (Luo *et al.,* 2015). Endothelial and other bystander cells are in direct contact with circulating HIV-infected cells that release the Nef protein into the blood, placing them in prime position for Nef transfer (Muratori *et al.*, 2009). Nef has been detected in endothelial cells of patients infected with HIV-1, despite HIV-1 not being an endothelium-tropic virus (Mazzuca *et al.*, 2016).

Within the endothelium, Nef contributes to endothelial dysfunction via two independent mechanisms; (1) apoptosis of endothelial cells through a nicotinamide adenine dinucleotide phosphate (NADPH) oxidase-dependent mechanism, and (2) by the production of monocyte chemoattractant protein-1 (MCP-1) through the NF-κB signalling pathway (Wang *et al.*, 2014). Nef can activate NADPH oxidase with its SH3 binding site to decrease nitric oxide production and increase superoxide anion production (Duffy *et al.*, 2009), thus

contributing to ROS production and inducing apoptosis (Lam *et al.*, 2010; Mazzuca *et al.*, 2016). This mechanism is independent of NF-κB activation (Wang *et al.*, 2014). A study by Acheampong *et al.* (2005) demonstrated that Nef was able to induce apoptosis in human brain microvascular endothelial cells (MVECs) in a dose-dependent manner. Gene microarray analysis showed increased expression of caspases, which only occur during programmed cell death (Acheampong *et al.*, 2005). They suggested that Nef- induced apoptosis may have more than one pathway, as both mitochondrial and Fas/FasL apoptotic pathway genes were up-regulated (Acheampong *et al.*, 2005). The NF-κB pathway requires the activation of NF-κB by dissociation of IκBα from NF- κB, allowing for NF-κB translocation from the cytosol to the nucleus (Hiscott *et al.*, 2001). HIV-1 Nef induces the activity of IκB kinase which phosphorylates Ⅰ κBα, marking the inhibitor for degradation by ubiquitination (Liu and Kumar, 2015). Once in the nucleus NF-κB binds to DNA, enhancing the expression of MCP-1 in endothelial cells, recruiting monocytes during atherosclerosis development (Ramji and Davies, 2015). MCP-1 can induce the monocyte and foam cell apoptosis, causing the release and build-up of lipid content in the arteries, building up the lipid core in the atherosclerotic plaque (Anand *et al.,* 2018)

1.8. HIV-1 Nef sequence variations on Nef activity

Extensive sequence variation in HIV-1 is attributed to the lack of proofreading by the error-prone reverse transcriptase enzyme, recombination, and short generation time (Andrews and Rowland-Jones, 2017). This has resulted in the inability of the host‘s immune system to control and eradicate the virus and provides major challenges in the development of suitable drugs and vaccines (Johnston and Fauci, 2008). The highly variable nature of HIV-1 presents a conflict between diversifying viral sequences and maintaining viral protein functions that are critical to replication and infectivity (Poon *et al.*, 2010). Sequence variations from the consensus *nef* sequence may lead to no significant effect on Nef

function while other variations may lead to either increased or decreased Nef function. However, in long-term non progressors (LTNP), sequence variations have led to defects in the ability of HIV-1 to replicate and infect more cells (Wang *et al.*, 1996). When comparing the patient derived HIV-1 Nef sequences to HIV-1 subtype C sequence, Walker *et al.* (2007) observed that deviation from the consensus HIV-1 subtype C sequence resulted in less effective HIV-1 Nef, which resulted in slow progressing HIV-1 infections. This results in attenuation of HIV-1 Nef functions in LTNP (Mwimanzi *et al.,* 2013).

Sequence defects in HIV-1 *nef* have varying effects on disease outcome of PLWH (Kuang *et al.*, 2014). Kirchhoff and colleagues (1995) observed that the defects in *nef* sequences were common among LTNP living with HIV-1. A study by Geffin *et al.* (2000) reported large deletions in the *nef* gene sequence in one out of five non-progressor perinatally children living with HIV-1, while the other had a higher frequency of mutations, as compared to rapid progressors. Similar findings were reported by Walker and colleagues (2007), in which they conducted *nef* sequence analysis from clinical isolates obtained from 34 treatment-naïve HIV- infected South African children (Walker *et al.*, 2007). Furthermore, research conducted by Zuo *et al.* (2012) on *nef* genes from adolescent and adult survivors of perinatal HIV-1 infection demonstrated a loss in the ability of mutated Nef to downregulate CD4 and MHC-I molecules. HIV-1 Nef polymorphisms such as G2A, D123A, LL165AA (Foster *et al.*, 2001) and C55S, K94E, H116N, V148L and S163R (Jin *et al.*, 2019), have been shown to lower Nef‘s ability to antagonize SERINC5. These findings show that elite controller and slow progressors have HIV-1 Nef sequence variations that have reduced Nef functionality due to their deviation from the consensus sequence. Even so, studies have shown higher levels of chronic inflammation and an increased risk of CVD amongst elite controllers and LTNP compared to their HIV-negative controls (Hsue *et al.*, 2009; Migueles and Connors, 2010; Pereyra *et al.*, 2012; Crowell *et al.*, 2015). This may suggest that loss

of HIV-1 Nef ability to downregulate CD4 and MHC-I molecules may not be associated with its ability to increase inflammation and the risk of CVD.

In the context of CVD, naturally occurring mutations in Nef have given rise to HIV-1 *nef* signature sequences that are associated with pulmonary hypertension (Almodovar *et al.*, 2012). In a study involving PLWH with and without pulmonary hypertension, HIV-1 Nef polymorphisms (i.e., R19K, R21Q, H40Y, A53P, L58V, E63G, M79I, T80N and Y81F) were overrepresented in persons infected with HIV-1 with pulmonary hypertension compared to persons with HIV-1 without pulmonary hypertension (Almodovar *et al.*, 2012). In a study conducted by Mezoh and colleagues (2018) involving 77 South African adults living with HIV-1 with no history of CVD, six polymorphisms (i.e., V16I, H40Y, T50A, E59Q, S169N and R188Q) were associated with higher levels of ICAM-1 compared to reference HIV-1 subtype C Nef sequence. Furthermore, in a second validation cohort consisting of 120 patients infected with HIV-1, 40H was found to be significantly associated with high values of carotid intima media thickness, indicative of increased CVD risk (Mezoh *et al.*, 2018). These findings therefore solicit more research on HIV-1 Nef in the context of CVD.

1.9. Problem statement

Advances in HIV therapy has increased the life span of people infected with HIV-1, similar to the general population. However, deaths amongst patients infected with HIV-1 are now attributed to non-communicable illness, with cardiovascular disease being the leading cause of death within this population. This trend is on the increase as PLWH reach ages above 45 years old. People living with HIV are twice more likely to develop CVD than their unaffected counterparts (Shah *et al.*, 2018). Antiretroviral drugs were once thought to be the cause of the observed increased risk of CVD in PLWH (Nsagha *et al.*, 2015), but recent findings show HIV-1 infection to be an independent contributor to the development of CVD.

Individuals living with HIV-1 have a higher risk of CVD in both the absence and presence of suppressive viral therapy (Wang *et al.*, 2015). Research into the aetiology of CVD in PLWH revealed chronic inflammation and HIV viral proteins, especially HIV-1 Nef, to be the main contributors by inducing endothelial dysfunction (Section 1.3.4; Marecki *et al.*, 2005). HIV-1 Nef is known to be transferred from infected cells to bystander cells like endothelial cells, with detrimental effects including apoptosis, increased expression of inflammatory cytokines and cellular adhesion molecules (Figure 1.3; Mazzuca *et al.*, 2016). These events lead to endothelial dysfunction, which is a precursor for future CVD events.

Research conducted on cohorts including PLWH show varying degrees of endothelial dysfunction in this population (Miller *et al.*, 2010; Fourie *et al.*, 2011; Graham *et al.*, 2013). The high variable nature of HIV-1 sequences has led to studies looking at Nef polymorphisms, as sequence variations in Nef have been attributed to differential phenotypic outcomes (Section 1.3.5; Kuang *et al.*, 2014). Residue deletions, insertions and mutations at functional domains have resulted in disease non-progressing individuals living with HIV-1. A study by Almodovar *et al.* (2012) reported HIV-1 Nef mutations that were associated with pulmonary hypertension, while Mezoh *et al.* (2018) reported mutations that were associated with increased plasma concentrations of biomarkers of endothelial dysfunction, ICAM-1 and VCAM-1. Identifying PLWH with a higher risk of developing CVD compared to other unaffected individuals is essential to reducing CVD-related deaths within the HIV affected population. This requires knowledge of how HIV-1 Nef polymorphisms influence endothelial dysfunction. Thus, the current project is a functional *in vitro* study which seeks to determine the effect of the H40Y HIV-1 subtype C Nef polymorphism, identified by both Almodovar *et al.* (2012) and Mezoh *et al.* (2018), on endothelial function. The H40Y mutation is of interest as it was found among PLWH and pulmonary

hypertension, and was associated with higher concentrations of plasma biomarkers of endothelial dysfunction, therefore suggesting that it could be critical in the development of CVD. We therefore hypothesize that the HIV-1 subtype C Nef 40H polymorphism is associated with endothelial dysfunction.

1.10. Project aim and objectives

The general aim of the project is to investigate the association between HIV-1 subtype C Nef H40Y polymorphism and endothelial function. The objectives of the study were therefore as follows:

1. Generate the HIV-1 *nef* mutant in a reference HIV-1 subtype C *nef* expression vector.
2. Stably express the mutated HIV-1 Nef protein in a continuous mammalian cell line
3. Determine the impact of the HIV-1 Nef mutant on endothelial cell function *in vitro*

Chapter 2: Materials and Methods

2. Methodology

2.1. Ethical clearance

A human research ethics waiver, Ref: W-CBP-190802-01, was obtained from the Human Research Ethics Committee (Medical), at the University of Witwatersrand on 02/08/2019 (Appendix A1). The Biosafety clearance was granted by the Institutional Biosafety Committee of the University of the Witwatersrand on 22/10/2019 (AppendixA2).

2.2. Materials

2.2.1. Mediums and supplements

Dulbecco's Modified Eagle Medium (DMEM), fetal bovine serum (FBS), 50 mg/ml gentamicin, 1 M hepes buffer and 100*X G*lutaMax were purchased from Thermofisher Scientic (Walthem, Massachusetts, U.S.A.). The DMEM contained 25 mM glucose, 4 mM L-glutamine and 1 mM sodium pyruvate. Endothelial Cell Medium (ECM), endothelial cell growth supplement 100X (EGCS), 5000 U/mL penicillin-streptomycin solution and 1 mg fibronectin were purchased from ScienceCell Research Laboratories (California, U.S.A). All bacterial culture materials were purchased from Glentham Life Science (Corsham, England). The Luria broth (LB) media was prepared in house, containing 1.0% (w/v) tryptone, 0.5% (w/v) yeast, 1.0% (w/v) NaCl in deionized water, with the addition of 1.5% (w/v) agar to make LB culture plates. Working concentration of ampicillin antibiotic was 100 µg/ml and it was purchased from Glentham Life Science (Corsham, England).

2.2.2. Antibodies

Rabbit polyclonal anti-DDDDK antibodies (α-FLAG) [WB 1:500 dilution] were purchased from Abcam (Cambridge, MA, U.S.A.) and the goat raised anti-rabbit horseradish

peroxidase conjugated antibody [WB 1:10000 dilution] was purchased from Sigma-Aldrich (St Louis, MO, U.S.A). Mouse monoclonal HIV-1 anti-Nef antibody was purchased from Abcam (Cambridge, MA) [WB 1:1000 dilution] and goat raised anti-mouse horseradish peroxidase conjugated antibodies [WB 1:10000 dilution] were purchased from Abcam (Cambridge, MA, U.S.A.).

2.2.3. Reagents

The Q5® High-Fidelity 2X Master mix and One*Taq*® 2X Master Mix with Standard Buffer were purchased from New Englad BioLabs (Massachussetts, U.S.A.). Restriction enzymes 20000 units/mL BamHI, 20000 units/mL AgeI, 20000 units/ml EcoRI, and 2000 units/ml FatI were purchased from New Englad BioLabs (Massachussetts, U.S.A.). The Zymoclean Gel DNA Recovery Kit and Zippy™ Plasmid Miniprep Kit were purchased from Zymo Research (California, U.S.A.). The Lipofectamine LTX reagent was purchased from Invitrogen. Polyethleneimine (PEI) [1 mg/ml] was purchased from Polysciences, Inc (Pennsylvania, U.S.A.). TGX™ FastCast™ Acrylamide Kit, 12% and Clarity™ ECL Western Blotting Substrate were purchased from Bio-Rad Laboratories (California, U.S.A.). QuikChange™ II XL Site-Directed Kit was purchased from Aligent (California, U.S.A.). LunaScript® RT SuperMix Kit and Luna® Universal qPCR Master Mix kit were purchased from New England Biolabs (Massachusetts, U.S.A.). All PCR and site-directed mutagenesis primers were ordered from Inqaba Biotechnical Industries (Pretoria, South Africa). Recombinant human tumour necrosis factor alpha (TNF-α) protein [200 µg/ml] was purchased from Abcam (Cambridge, MA). Dr Eleanor Cave from the Department of Chemical Pathology at the University of Witwatersrand gifted the 80 µg/ml X-gal and 20 mM Isopropyl-β-D-thiogalactoside (IPTG). Human soluble VCAM-1 (sVCAM-1) enzyme-linked immunosorbent assay (ELISA) kit was purchased from Thermofisher Scientic (Walthem, Massachusetts, U.S.A.).

2.2.4. Plasmids and Nef clones

The *nef* gene coding for HIV-1 Subtype C Nef (*nef* 40H) obtained from a clinical isolate (P0144), mammalian expression vectors pcDNA™ 3.1(+) (Appendix A3, Figure A1), pSelect-GFPZeo-mcs (Appendix A3, Figure A2) and pLKO.dCMV,TetO.3xFlag (Appendix A3, Figure A3) plasmids were obtained from Dr Genevieve Mezoh from the Department of Chemical Pathology at the University of Witwatersrand. The pSelect-GFPZeo-mcs was used as a transfection control vector as it expressed a Green fluorescent protein independently of the cloned-in gene of interest. A wild-type reference *nef* of a subtype C strain (*nef* MJ4) from pMJ4 was obtained from Dr Adriaan E. Basson from the Department of Molecular Medicine and Haematology at the University of Witwatersrand. The pGEM®-T Easy Vector system was purchased from Promega Corporation (Wisconsin, U.S.A.).

2.2.5. Cell lines

A HEK293T cell line was obtained from Dr Adriaan E. Basson from the Department of Molecular Medicine and Haematology at the University of the Witwatersrand. The HEK29T cells were used to evaluate the recombinant plasmids' ability to express the HIV-1 Nef proteins. The Human pulmonary microvascular endothelial cells (HPMEC) were a gift from Dr Allison Seeger from the Wellcome Centre for infectious Diseases Research in Africa (CIDRI-Africa), University of Cape Town. The HPMECs were used to evaluate the effect of HIV-1 Nef variants on endothelial dysfunction.

2.3. Methods

2.3.1. Construction of stable HIV-1 Nef expressing plasmids

The pLKO.dCMV.TetO.3xFlag plasmid was used to generate stable HIV-1 Nef expression plasmids. The *PO144* (*nef*-40H) patient sample excised from a patients' DNA living with HIV-1 was selected for this study because it had all the five amino acid residues (16V, 40H, 50T, 169N, and 188Q) previously identified to be associated with high levels of ICAM-1 in HIV-infected ART-naïve South African individuals (Mezoh *et al*., 2021). The *nef*-MJ4 gene was used as the HIV-1 subtype C *nef* reference strain and had amino acid residues (16V, 40H, 50A, 188H) associated with an elevated concentration of ICAM-1 (Ndung'u *et al*., 2001). HIV-1 *nef* genes were amplified by Polymerase Chain Reactions (PCR) using Hi-Fi *Taq* to introduce the *Age*I and *Eco*RI restriction sites with the forward and reverse primers, respectively (Table 2.1). The Q5® High-Fidelity 2X Master mix was used for PCR reactions and a master mix for 5 PCR reactions were prepared for each template DNA (Table 2.2). The master mix was aliquoted in 5 PCR tubes with a final volume of 19 µl each. A microliter of DNA template was added to 4 of the tubes while one tube was used for the no-template control, where 1 µl of deionized water was added in place of the template DNA. The reagents were mixed and centrifuged to collect all liquids to the bottom of the PCR tube. The PCR tubes were transferred to a T100 thermal cycler (Bio-Rad Laboratories, California, U.S.A) and programmed as described in Table 2.3. Following thermocycling, the PCR products were analysed on a 1% (w/v) agarose gel. The 1% (w/v) agarose gel was prepared by dissolving 0.5 g of agarose in 50 ml TAE (1X) buffer (40 mM, 20 mM acetic acid and 1 mM EDTA) and heated with shaking. The agarose was allowed to cool, after which 5 µl of ethidium bromide [10 mg/ml] was added to the mixture and then poured into a casting tray with a preplaced comb and allowed to polymerize at room temperature. The comb was removed from the solidified gel and the casting tray placed in

an electrophoresis chamber filled with TAE (1X) buffer. Four microliters of 6x DNA loading buffer were added to each 20 µl restriction digest mixture and then loaded into the pre-cast wells of the gel. Five microliters of 1 kb DNA ladder [0.1 µg/µl] (New England Biolabs, Massachusetts, U.S.A.) was loaded into one well. Electrophoresis was conducted at one hundred volts for one hour. The gel was then visualized by UV light using the ChemiDoc XRS+ GelImaging system (Bio-Rad Laboratories, California, U.S.A).

Table 2.1: PCR Primers for amplification of HIV-1 *nef*

Strain	**PCR primer sequence**	**Features**
MJ4	F1: 5‘- CTGaccggtATGGGGGGCAAGTGGT -3‘	*Age*I
	R1: 5‘- Ggaattc TCAGCAGTCTTTGTAA-3‘	*Eco*RI
PO144	F1_PO144-FLG: 5‘- CTGaccggt ATGGGGGGCAAATTAT -3‘	*Age*I
	R1_P0144-EcoRI: 5‘- Ggaattc TCAGCAGTCTTTGTAG -3‘	*Eco*RI

The underlined characters represent nucleotides that constitute the restriction site.

Table 2.2: PCR reaction preparation

Reagents	**1X**	**5X**
Q5® High-Fidelity 2X Master mix	10 µl	50 µl
DNA template	< 1,000 ng	Variable
Forward primer [10 µM]	1 µl	5 µl
Reverse primer [10 µM]	1 µl	5 µl
dH_2O	7 µl	35 µl
Total	19 µl	95 µl

Table 2.3: Thermocycling conditions for PCR

Step	Temperatures	Time	Number of cycles
Initial denaturation	94 ˚C	2 minutes	1
Denaturation Annealing Elongation	94 ˚C 60 ˚C 68 ˚C	15 seconds 30 seconds 4 minutes	35
Final elongation	68 ˚C	15 minutes	1

2.3.2. DNA recovery from agarose gel

The DNA amplicons corresponding to *nef* 40H and *nef* MJ4 were recovered from the aforementioned agarose gel using a Zymoclean Gel DNA Recovery Kit (Zymo Research, California, U.S.A.). For the recovering of PCR products, the agarose gel was placed on the transilluminator drawer on the ChemiDoc XRS+ Gel Imaging system (Bio-Rad Laboratories, California, U.S.A) where the band excision option is selected to allow the visualization of the DNA bands. The ethidium bromide in the gel is excited by ultraviolet light at 210 nm and 285 nm and emits orange light (DNA bands) with a wavelength of 605 nm. The DNA bands of interest was excised from the agarose gel using a blade and transferred into a 1.5 ml microcentrifuge tube. Three times the volume of ADB to each volume of excised agarose was added to the tube and incubated at 55 ˚C for 10 minutes for the gel to dissolve. The melted agarose solution was transferred to a Zymo-Spin™ Column and centrifuged for 60 seconds at 10000 x *g*. The flow-through was discarded and 200 µl of DNA Wash buffer was added to the spin column and centrifuged for 30 seconds at 10000 x *g*, this step was repeated twice. The spin column was placed in a new labelled 1.5 ml tube and 10 µl of DNA Elution buffer was added to the column. The DNA was eluted by centrifugation for 60 seconds at 10000 x *g* and the pure DNA was collected in the labelled 1.5 mL tube. The concentration and quality of the recovered DNA was measured using a NanoDrop™ One/One C Microvolume UV-Vis Spectrophotometer (Thermofisher Scientific, U.S.A.). DNA

with a reading of ~1.8 for the ratio of absorbance at 260 nm and 280 nm was deemed to be pure and of excellent quality and used in subsequent procedures.

2.3.3. Restriction digestion of HIV-1 nef products and vector

The amplicons and the pLKO.dCMV,TetO.3xFlag vector were digested with AgeI and EcoRI restriction enzymes (New England Biolabs, Massachusetts, U.S.A.) in restriction digest reactions (Table 2.2). The reactions were incubated for 1 hour at 37 ˚C in a heating block. The digested products were electrophoresed on a 1% (w/v) agarose gel as mentioned previously. DNA corresponding to *nef* 40H, *nef* MJ4 and the digested vector were recovered from the aforementioned agarose gel using a Zymoclean Gel DNA Recovery Kit (Zymo Research, California, U.S.A.) and the concentrations were measured as described previously.

Table 2.4: Restriction digests reaction preparation

Components	**Tube 1 Control (uncut vector)**	**Tube 2 Linearized vector (AgeI)**	**Tube 3 linearized vector (EcoRI)**	**Tube 4 Double cut vector**	**Amplicons**	
					Tube 5 144-40H	**Tube 6 MJ4**
Buffer	2 µl	2 µl	2 µl	2 µl	2 µl	2 µl
AgeI [20000 units/ml]	-	1 µl	-	1 µl	1 µl	1 µl
EcoRI [20000 units/ml]	-	-	1 µl	1 µl	1 µl	1 µl
DNA [0.4 µg]	2 µl	2 µl	2 µl	2 µl	2 µl	2 µl
dH_2O	16 µl	15 µl	15 µl	14 µl	14 µl	14 µl

.

2.3.4. Ligation of HIV-1 nef into pLKO vector

The *nef* amplicons were cloned into the restricted pcDNA™ 3.1(+) vector using T4 DNA ligase (Promega Corp, Wisconsin, U.S.A.). The ligation reactions were prepared by mixing

1 µl T4 DNA ligase, 3:1 ratio of digested *nef* amplicons to vector and dH_2O until reaction is 10 µl in total volume in a PCR tube. The reactions were incubated at 37 ˚C for 1 hour in a heating block, yielding the pLKO.dCMV,TetO.3xFlag/Nef-40H and pLKO.dCMV,TetO.3xFlag/Nef-MJ4 constructs which were then used for Nef expression (Figure 2.1).

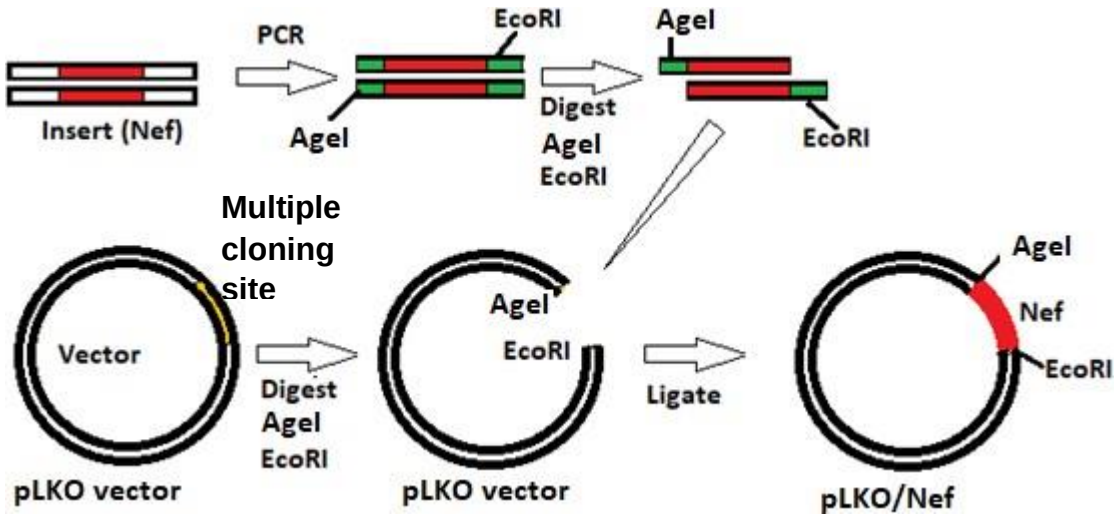

Figure 2.1: PCR cloning of Nef into pLKO.dCMV,TetO.3xFlag vector
Construction of Nef-expressing plasmids using PCR to amplify the *nef* genes. The *nef* genes and pLKO.dCMV,TetO.3xFlag vector are digested with restriction enzyme AgeI and EcoRI so the digested products could be joined together by a ligation reaction. The resulting products are FLAG-tagged Nef expressing plasmids. Figured adapted from Spiliotis (2012).

2.3.5. Preparation and transformation of chemically competentcells

Multiple copies of pLKO.dCMV,TetO.3xFlag/Nef-40H and pLKO.dCMV,TetO.3xFlag/Nef-MJ4 constructs plasmids were produced after the ligation reaction. This was done by transformation, were exogenous genetic material, in the form of the Nef-expressing plasmids, is taken up and incorporated by competent *E.coli* cells. The competent cells were prepared chemically to give them the ability to absorb the exogenous plasmid DNA. The competent cells were prepared by taking *E. coli* glycerol stocks of JM109 cells and streaking on an antibiotic-free LB agar plate (1.0% (w/v) tryptone, 0.5% (w/v) yeast, 1.5%

(w/v) agar, 1.0% (w/v) NaCl in deionized water) and incubated overnight at 37˚C. A single colony from the plate was picked and transferred into 20 ml of antibiotic-free LB broth. The inoculum was allowed to grow overnight in an incubator set at 37 ˚C with shaking at 180 rpm. The overnight starter culture broth was transferred into 30 ml of fresh antibiotic-free broth and incubated for 2 hours at 37 ˚C with shaking. The culture was collected a 50 ml tube and centrifuged for 10 minutes at 5000 x *g* at 4 ˚C after which the pellet was suspended on ice. The pelleted cells were resuspended in 10 ml of 0.1 M $MgCl_2$ and incubated for 30 minutes on ice. The suspension was centrifuged at 5000 x *g* at 4 ˚C for 10 minutes and the supernatant was discarded. The pelleted cells were resuspended with 10 ml 0.1 M $CaCl_2$ and incubated on ice for 4 hrs. The suspension mixture was centrifuged at 5000 x *g* at 4 ˚C for 10 minutes. The pellet was resuspended in a mixture of 3 ml of 0.1 M $CaCl_2$ and 3 ml of 30% glycerol and incubated on ice for 15 minutes. Following incubation, the cells were aliquoted at 100 µL per tube into labelled microcentrifuge tubes and stored at -80 ˚C. The transformation of the competent cells with the Nef-expression plasmids was done by thawing the competent cells on ice and transferring a 25 µl aliquot of chemically prepared *E. coli* JM109 competent cells in a fresh labelled 1.5 mL tube placed on ice. Two microliters of pLKO.dCMV,TetO.3xFlag/Nef DNA 1 µg/µl was added to their corresponding tubes. For the controls, empty pLKO.dCMV,TetO.3xFlag plasmid DNA was added to the chemically competent *E. coli* JM109 cells in a different tube as a positive control, while distilled water was added as a negative control. The tubes were incubated in ice for 30 minutes and then heat shocked at 42 ˚C for 60 seconds in a heating block. The tubes were then placed back in ice and incubated for 10 minutes. Five hundred microliters of antibiotic-free LB broth were added into each tube. The mixture was incubated for 1 hour at 37 ˚C with shaking at 180 rpm. Following incubation, 150 µL of the culture was streaked onto LB agar plates supplemented with 100 µg/ml ampicillin. The plates were

labelled accordingly and incubated overnight at 37 ˚C. Five colonies were picked from each LB agar plate, inoculated into separate 50 mL tubes with fresh 15 mL LB broth supplemented with ampicillin [100 µg/ml] and cultured overnight at 37 ˚C with shaking.

2.3.6. Plasmid DNA extraction

Following the incubation in section 2.3.2, the plasmid DNA was extracted from the overnight cultures using the Zyppy™ Plasmid Miniprep Kit (Zymo Research, California, U.S.A.). The cultures were centrifuged for 10 minutes at 4500 x *g* to pellets the cells and discard the supernatant. Six hundred microliters of distilled water were added to resuspend the cells and transferred to a fresh labelled 1.5 mL tube. A hundred microliters of 7X lysis buffer added into the same tube. The solutions were thoroughly mixed and incubated for 2 minutes. The reaction was neutralized by adding pre-chilled Neutralization buffer and mixed thoroughly. The mixture was centrifuged for 4 minutes at 14000 x *g*. The supernatant was transferred into a Zymo-Spin™ INN column, centrifuged for 15 seconds at 14000 x *g* and theflow through discarded. Subsequently, Endo-Wash buffer was added to the column and the column was centrifuged for 30 seconds at 14000 x *g*. Four hundred microliters of Zyppy™ Wash buffer was then added to the column and centrifuged for 1 minute at 14000 x *g*. Following centrifugation, the column was transferred into a clean labelled 1.5 ml microcentrifuge tube and 30 µl of Zyppy™ Elution buffer was added directly to the column matrix and incubated for 1 minute at room temperature. The plasmid DNA was eluted by centrifugation for 1 minute at 14000 x *g*. The concentration and purity of the plasmid DNA was measured by using a NanoDrop One/One C Microvolume UV-Vis Spectrophotometer (Thermofisher Scientific, U.S.A.). The Zyppy™ Elution buffer was used to blank the machine. DNA with a reading of ~1.8 for the ratio of absorbance at 260 nm and 280 nm was deemed to be pure and of excellent quality. The plasmids were stored at -20 ˚C.

2.3.7. Confirmation of Nef-expressing constructs

To confirm the cloning of the pLKO.dCMV,TetO.3xFlag/Nef-40H and pLKO.dCMV,TetO.3xFlag/Nef-MJ4 constructs, the plasmids were digested using the restriction enzymes AgeI and EcoRI. The restriction digest reaction was prepared as described in Section 2.3.3, table 2.4 (tube 1-4). Restriction products were analysed by electrophoresis on a 1% (w/v) agarose gel. Successful cloning would be confirmed by the presence of two DNA fragments of the same sizes as the *nef* gene amplicon and the digested pLKO.dCMV,TetO.3xFlag vector, as seen in section 2.3.3. The identity of the insert was validated by Sanger sequencing using the pLKO sequencing primers listed in table 2.5 at Inqaba Biotechnical Industries (Pretoria, South Africa). The resulting sequences were confirmed by sequence alignment and running a BLAST search on the National Center for Biotechnology Information (NCBI) (https://blast.ncbi.nlm.nih.gov/Blast.cgi).

Table 2.5: pLKO sequencing primers

Primer name	Sequence
Puro-F	5‘- GCAACCTCCCCTTCTACGAGC-3‘
Puro-R	5‘- GTGGGCTTGTACTCGGTCAT-3‘

2.3.8. *In vitro* expression of HIV-1 Nef

The constructs expressing the wild-type and a mock plasmid (empty pLKO.dCMV,TetO.3xFlag plasmid), were transfected into HEK293T cells using the Invitrogen Lipofectamine LXT Reagent (Thermofisher Scientific, U.S.A.) or PEI [1 mg/ml] in 12-well culture plates. The transfection of the HEK293T cells was to evaluate the ability of the constructs to produce recombinant Nef proteins. Prior to transfection of adherent HEK293T, the cells were maintained in a T75 flask (Sigma-Aldrich, U.S.A) with Gibco™ Dulbecco's Modified Eagle Medium (DMEM) supplemented with 10% (v/v) Glutamax and

10% (v/v) Fetal Bovine Serum (FBS) (Thermofisher Scientific, U.S.A.) and incubated in a humidified atmosphere incubator at 37 ˚C with 5% CO_2. The cells were passaged every two days. All cells were between passage 5 and 10 for the transfection. The day before transfection, the culture medium was removed, and the cells were washed with 5 ml phosphate buffered saline (PBS) solution. The cells were detached from the flask by trypsinization. One millilitre of TrypLE™ Express Enzyme (Thermofisher Scientic, U.S.A.) was added to the flask and incubated until the cells began to slide off the flask surface. Five millilitres of complete medium were added to stop the trypsinization and the cells were collected in a 15 ml conical tube (Thermofisher Scientific, U.S.A.). The cells were counted in a haemocytometer by diluting 20 µl of cells in 20 µl of 0.4% Trypan Blue stain (Thermofisher Scientic, U.S.A.). The cells were seeded into a 12-well plate, plating at $2.5x10^5$ cells per well and 1 ml of growth medium was added to each well to a final volume of 1.4 ml per well. The cells were incubated until they reached 80% confluency on the day of transfection. For each well to be transfected, 1 µg of Nef-expressing plasmids, mock plasmid (negative control) or pSelect-GFPzeo/Nef-HXB2 plasmid (transfection positive control) were diluted in 100 µl of Opti-MEM™ I Reduced Serum media (Thermofisher Scientific, U.S.A.) within a labelled 1.5 ml tube. The pSelect-GFPzeo plasmid was used as a transfection control as it expressed a green fluorescent protein which was visualized using an Olympus BX41 Phase Contrast & Darkfield Microscope (Microscope Central, U.S.A.) to confirm successful transfection. Three microliters of Invitrogen™ Lipofectamine LTX Reagent or PEI [1mg/ml] was added to each tube as seen in Table 2.6. The mixture was incubated for 30 minutes at room temperature. Following the incubation period, 100 µl of the DNA-Lipofectamine or PEI mixture was added directly to each well containing the cells and mixed by gently rocking the plate back and forth. The cells were incubated at 37 ˚C in a 5% CO_2 incubator for 48 hours. The transfections were done in duplicates for each

Nef-expressing plasmid.

Table 2.6: Transfection protocol used on HEK29T cells

Plasmids	Nef-HXB2	Nef-40H	Nef-MJ4
Cell vessel	12-well	12-well	12-well
Volume Medium	1 ml	1 ml	1 ml
Cells per Well	$2.5x10^5$ cells	$2.5x10^5$ Cells	$2.5x10^5$ Cells
Volume dilution Medium	100 µl	100 µl	100 µl
DNA	1 µg	1 µg	1 µg
Transfection Reagent	3 µl	3 µl	3 µl

2.3.9. Confirmation of *in vitro* HIV-1 Nef expression

The transformed *E.coli* cells described in section 2.3.8 were harvested 48 hours post transfection to analyse for Nef expression using Western blot analysis. Crude cell lysates were prepared for SDS-PAGE by adding 100 µl of SDS sample buffer (0.25% (w/v) Coomassie Brilliant blue, 2% (w/v) SDS, 10% (v/v) glycerol, 100 mM tris, and 1% (w/v) β-mercaptoethanol) to the cells in a ratio of 1:1. The mixture was heated for 10 minutes at 95 ˚C in a heating block. The proteins were resolved using 12% TGX™ FastCast™ Acrylamide kit (Stacker: 1 ml stacker A, 1 ml stacker B, 10 µl 10% (w/v) Ammonium Persulfate (APS), 2 µl TEMED; Resolver: 3 ml resolver A, 3 ml resolver B, 30 µl 10% (w/v) APS, 3 µl TEMED) (Bio-Rad Laboratories, California, U.S.A). Gels were then transferred into a tank filled with SDS running buffer (25 mM Tris, pH 8.3 250 mM glycine and 0.1% (w/v) SDS). The prepared samples were loaded into their separate wells, with a single well housing 5 µl Precision Plus Protein Standard (Bio-Rad Laboratories, California, U.S.A).

Electrophoresis was conducted at 200 V for 60 minutes using the Bio-Rad Mini protein electrophoresis system (Bio-Rad Laboratories, California, U.S.A.). The gel was visualized using the stain-free protocol on the ChemiDoc XRS+ Gel Imaging system (Bio-Rad Laboratories, California, U.S.A). The stain-free gels use trihalo compounds that make proteins within the gel to fluorescent after a brief period of UV activation at 302 nm. After viewing the gel, the gel was immersed in western transfer buffer (25 mM Tris, 192 mM glycine, 20% (v/v) methanol in deionized water), along with two thick blot filter paper pads. In the interim, the PVDF membrane was activated by 30 second incubation in 100% (v/v) methanol, and then rinsed in water. The membrane was equilibrated in Western transfer buffer for 5 minutes. The preparation of the transfer was done as follows: A thick blot filter paper pad, PVDF membrane, gel and thick blot filter paper pad sandwich was prepared in the mentioned order, ensuring no air bubbles were trapped. The sandwich was placed in a Trans-Blot® SD Semi-Dry transfer Cell (Bio-Rad Laboratories, California, U.S.A.) and the transfer of the proteins to the PVDF membrane was performed at 25V for 25 minutes. Following protein transfer, the PVDF membrane was removed from the sandwich and blocked in 10 ml of 5% (w/v) non-fat milk in TBS (50 mM Tris, 150 mM NaCl in deionized water) for 30 minutes on a shaker at 100 rpm at 4 ˚C. The membrane was washed three times in TBS-Tween (1L TBS, 1 ml Tween 20) for 5 minutes followed by overnight incubation at 8 ˚C of the membrane with mouse monoclonal anti-Nef antibodies [1:1000 dilution] and rabbit polyclonal anti-DDDDK antibodies (α-FLAG) [1:500 dilution] as primary antibodies of the FLAG-tagged HIV-1 Nef protein. Unbound primary antibodies were washed off the membrane thrice with TBS-Tween for 5 minutes per wash. The membrane was incubated at room temperature for one hour with the secondary antibody, goat raised anti-mouse and goat raised anti-rabbit horseradish peroxidase conjugated antibodies [1:10000 dilution], followed by washing with TBS-Tween for 5 minutes. All incubations

were done on a shaker at 100 rpm. The Clarity™ ECL Western Blotting Substrate (Bio-Rad Laboratories, California, U.S.A.) is an extremely sensitive chemiluminescence substrate used for detecting Western blot membrane bound horseradish peroxidase (HRP) conjugated antibodies. The PVDF membranes were placed in a light-resistant box. Equal volumes of Clarity Western Peroxide reagent and Clarity Western Enhancer reagent were mixed to a total of 1.5 ml in a 2 ml tube. The mixture was poured over the membranes and incubated for 5 minutes in the dark box. Following incubation, the membrane was removed from the box and excess substrate solution removed using absorbent tissue. The membrane was covered with a transparent plastic wrap and placed in the ChemiDoc XRS+ Gel Imaging system (Bio-Rad Laboratories, California, U.S.A) for imaging. During the imaging process, the HRP enzyme reacts with the substrate to emit light at 428 nm. The light is captured by a digital imager after 30 seconds of exposure time.

2.4.1. Construction of transient HIV-1 Nef expressing plasmids

Nef genes were amplified by Polymerase Chain Reactions (PCR) using *Taq* to introduce the *Bam*HI and *Eco*RI restriction sites with the forward and reverse primers, respectively. In addition, an N-terminal FLAG purification tag was added through the forward primers. The PCR primers used for amplifying HIV-1 *nef* from the MJ4 and *PO144* strains (Table 2.7). The One*Taq*® 2X Master Mix with Standard Buffer was used for PCR reactions and a master mix for 5 PCR reactions were prepared for each template DNA, as shown in Table 2.8. The master mix was aliquoted in 5 PCR tubes with a final volume of 19 µl each. A microliter of DNA template was added to 4 of the tubes while one tube was used for the no-template control, where 1 µl of deionized water was added in place of the template DNA. The reagents were mixed and centrifuged to collect all liquids to the bottom of the PCR tube. The PCR tubes were transferred to a T100 thermal cycler (Bio-Rad Laboratories,

California, U.S.A) and it was programmed as described in Table 2.9. After the thermocycling, the PCR products were analysed with a 1% (w/v) agarose gel as previously described in section 2.3.1. The DNA amplicons corresponding to Flag/*nef* 40H and Flag/*nef* MJ4 were recovered as described in section 2.3.2.

Table 2.7: PCR Primers for amplification of HIV-1 *nef*

Strain	PCR primer sequence	Features
MJ4	F1: 5‘- ggatcc**ATGGATTACAAGGATGACGATGACAAG**ATGGGGGGCAA GTGGTC -3‘	*Bam*HI and **FLAG tag**
	R1: 5‘- GgaattcTCAGCAGTCTTTGTAA-3‘	*Eco*RI
PO144	F1_PO144-FLG: 5‘- ggatcc**ATGGATTACAAGGATGACGATGACAAG**ATGGGGGGCAA A -3‘	*Bam*HI and **FLAG tag**
	R1_P0144-EcoRI: 5‘- GgaattcTCAGCAGTCTTTGTAG -3‘	*Eco*RI

The underlined characters represent nucleotides that constitute the restriction site, while characters in bold represent nucleotides that encode the fusion tag.

Table 2.8: PCR reaction preparation

Reagents	1X	5X
One*Taq*® 2X Master Mix with Standard Buffer	10 µl	50 µl
DNA template	< 1,000 ng	Variable
Forward primer [10 µM]	1 µl	5 µl
Reverse primer [10 µM]	1 µl	5 µl
dH_2O	7 µl	35 µl
Total	19 µl	95 µl

Table 2.9: Thermocycling conditions for PCR

Step	Temperatures	Time	Number of cycles
Initial denaturation	94 ˚C	2 minutes	1
Denaturation Annealing Elongation	94 ˚C 60 ˚C 68 ˚C	15 seconds 30 seconds 4 minutes	35
Final elongation	68 ˚C	15 minutes	1

2.4.2. Ligation of HIV-1 *nef* amplicons with pGEM®-T Easy Vector

The recovered amplicons were ligated into the pGEM®-T Easy Vector using the T4 DNA ligase. The Taq polymerase added an extra adenine at the 3‘ end of the HIV-1 nef PCR products that bind to the thymidine overhangs at the 3‘ end of the pGEM®-T Easy vector. The ligation reactions were prepared by mixing 1 µl T4 DNA ligase, 3:1 ratio of digested *nef* amplicons to vector and dH_2O until reaction is 10 µl in total volume in a PCR tube. The reactions were incubated at 37 ˚C for 1 hour in a heating block, yielding the pGEMT+Nef-40H and pGEMT+Nef-MJ4 plasmids. The ligated products were transformed into *E.coli* JM109 chemically competent cells as described in section 2.3.5. The agar culture plates were supplemented with ampicillin [100 µg/ml], X-Gal [80 µg/ml] and 0.5 mM IPTG to facilitate blue/white screening of colonies. The plates were incubated overnight at 37˚C. Post incubation, the colonies would either appear blue or white in colour. The blue colonies represent colonies that did not have the HIV *nef* insert while the white colonies represented successful inactivation of the *β-galactosidase* gene by the HIV- 1 *nef* inserts. About 8 to 10 white colonies from each plate were picked and used during colony PCR as template DNA to confirm the cloning of HIV-1 *nef* genes into the pGEM®-T Easy vector. The colony PCR used the PCR primers listed in table 2.7 (section 2.4.1). Colonies that showed the correct size amplicons from the colony PCR were inoculated into fresh LB broth supplement with ampicillin [100 µg/ml] and incubated overnight with shaking at 37 ˚C. Post

incubation, the DNA plasmids were extracted using the method described in section 2.3.6.

2.4.3. Restriction digest of ligated pGEM®-T Easy Vector products and pcDNA™ 3.1(+) vector

The extracted pGEMT+Nef plasmids and the pcDNA™ 3.1(+) vector were digested with BamHI and EcoRI restriction enzymes (New England Biolabs, Massachusetts, U.S.A.) in restriction digest reactions prepared as shown in Table 2.10. The reactions were incubated for 1 hour at 37 ˚C in a heating block. The advantage of this cloning technique is that it allows for the screening of successfully ligated products based on the formation of blue and white colonies; secondly, it improves the efficiency of restriction enzymes as many restriction enzymes often do not cleave linear PCR products but rather circular DNA (Celie *et al*., 2016). The digested products were electrophoresed on a 1% (w/v) agarose gel as mentioned previously in section 2.4.1. DNA corresponding to *nef* 40H, *nef* MJ4 and the digested vector were recovered from the aforementioned agarose gel using a Zymoclean Gel DNA Recovery Kit as described in section 2.3.2 and theconcentrations were measured.

Table 2.10: Restriction digests reaction preparation

Components	**Tube 1 Control (uncut vector)**	**Tube 2 Linearized vector (BamHI)**	**Tube 3 linearized vector (EcoRI)**	**Tube 4 Double cut vector**	**pGEMT plasmids**	
					Tube 5 144-40H	**Tube 6 MJ4**
Buffer	2 µl	2 µl	2 µl	2 µl	2 µl	2 µl
BamHI [20000 units/ml]	-	1 µl	-	1 µl	1 µl	1 µl
EcoRI [20000 units/ml]	-	-	1 µl	2 µl	2 µl	2 µl
DNA [0.4 µg]	2 µl	2 µl	2 µl	2 µl	2 µl	2 µl
dH_2O	16 µl	15 µl	15 µl	14 µl	14 µl	14 µl

2.4.4. Ligation of HIV-1 *nef* genes and pcDNA™ 3.1(+) vector

The *nef* amplicons were cloned into the restricted pcDNA™ 3.1(+) vector using T4 DNA ligase (Promega Corp, Wisconsin, U.S.A.). The ligation reactions were prepared by mixing 5 µl 2X ligase buffer, 1 µl T4 DNA ligase, 3:1 ratio of digested *nef* amplicons to vector and dH_2O until reaction is 10 µl in total volume in a PCR tube. The reactions were incubated at 37 ˚C for 1 hour in a heating block, yielding the pcDNA™ 3.1(+)-FLAG/Nef-40H and pcDNA™ 3.1(+)-FLAG/Nef-MJ4 constructs which were then used for Nef expression (Figure 2.1). The ligated products were transformed in chemically competent cells and plated on agar plates supplemented with ampicillin [100 µg/ml] as described in section 2.3.5.

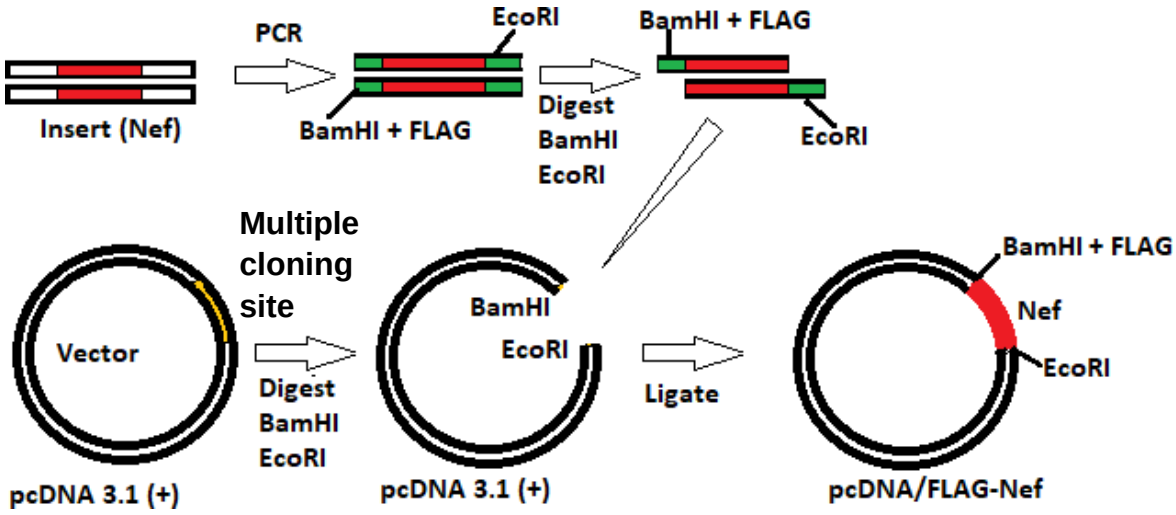

Figure 2.2: PCR cloning of Nef into pcDNA 3.1 (+) vector
Construction of Nef-expressing plasmids using PCR to amplify the *nef* genes. The *nef* genes and pcDNA 3.1 (+) vector are digested with restriction enzyme BamHI and EcoRI so the digested products could be joined together by a ligation reaction. The resulting products are FLAG tagged Nef expressing plasmids. Figured adapted from Spiliotis, (2012).

2.4.5. Confirmation of Nef-expressing constructs

Following the incubation of the agar plates, colony PCR was performed to confirm the successful cloning of HIV-1 *nef* genes into the pcDNA™ 3.1(+) vector using the PCR primers listed in table 2.7 (section 2.4.1). The colony PCR products were analysed on a

1% (w/v) agarose gel. Colonies that showed the correct size amplicons from the colony PCR were inoculated into fresh LB broth supplement with ampicillin [100 µg/ml] and incubated overnight with shaking at 37 ˚C. Post incubation, the DNA plasmids were extracted using the method described in section 2.3.6. The extracted plasmid DNA was used to confirm the cloning of the pcDNA™ 3.1(+)-FLAG/Nef-40H and pcDNA™ 3.1(+)-FLAG/Nef-MJ4 constructs. The plasmids were digested using the restriction enzymes BamHI and EcoRI and the restriction digest reaction were prepared as in table 2.10 (tubes 1-4) and incubated for 1 hour at 37 ˚C. Restriction products were analysed by electrophoresis on a 1% (w/v) agarose gel. Successful cloning would be confirmed by the presence of two DNA fragments of the same sizes as the *nef* gene amplicon and the digested pcDNA™ 3.1(+) vector, as seen in section 2.4.1. The identity of the insert was validated by Sanger sequencing using the PCR primers (Table 2.8) at Inqaba Biotechnical Industries (Pretoria, South Africa). The resulting sequences were confirmed by running a BLAST search on the National Centre for Biotechnology Information (NCBI) (https://blast.ncbi.nlm.nih.gov/Blast.cgi).

2.4.6. Production of the modified HIV-1 *nef* expressing plasmids

To assess the effects of the mutations in Nef proteins on endothelial function, a mutation had to be introduced into the wild-type strain. This would provide the same wild-type background for all strains. The QuikChange™ II XL Site-Directed Mutagenesis kit (Agilent, California, U.S.A.) was used to make a point mutation in the *nef* gene, changing base pair 127C to 127T. This mutation would change the amino acid sequence of the HIV-1 Nef protein at position 40 from Histidene (H) to Tyrosine (Y). In following with the kits manual, mutagenic primers were designed using the QuikChange™ Primer Design Program (https://www.agilent.com/store/primerDesignProgram.jsp) that makes the point mutation in

pcDNA™ 3.1(+)-FLAG/Nef-40H plasmid. The primers designed were optimized for the kit. Using the provided control primers and the designed sample primers, two master mix reactions were prepared as described in the table below (Table 2.11). The reactions were subsequently subjected to thermocycling in a T100 thermal cycler (Bio-Rad Laboratories, California, U.S.A) using the cycling parameters recommended by the manufacturer as shown in Table 2.12. Following completion of the thermocycling, 1 µl of *Dpn* I [10 U/µl] restriction enzyme was added to each tube. The mixture was gently mixed and incubated for 1 hour at37 ˚C in a heating to digest the parental (the nonmutated) plasmid DNA (Figure 2.2). The *Dpn* I-treated mutated plasmids were than transformed into the kit provided XL10-Gold ultracompetent cells using the protocol described in section 2.3.5 and plated on LB agar plate supplemented with 100 µg/ml ampicillin. The plates were incubated overnight at 37 ˚C.

Table 2.11: Preparation of mutagenesis reactions

Components	**Control reaction**	**Sample reaction**
10x Reaction buffer	5 µl	5 µl
Plasmid DNA [10 ng]	2 µl	2 µl
Forward primer [125 ng]	1.25 µl	1.25 µl
Reverse primer [125 ng]	1.25 µl	1.25 µl
dNTP mix	1 µl	1 µl
PfuUltra HF DNA polymerase [2.5 U/ µl]	1 µl	1 µl
QuikSolution reagent	3 µl	3 µl
dH2O	36.5 µl	36.5 µl
Total volume	50 µl	50 µl

Table 2.12: Cycling parameters for the QuikChange™ II XL kit

Segment	Number of cycles	Temperature	Time
1	1	95 ˚C	1 minute
2	18	95 ˚C	50 seconds
		60 ˚C	50 seconds
		68 ˚C	1 minute/kb of plasmid length
3	1	68 ˚C	7 minutes

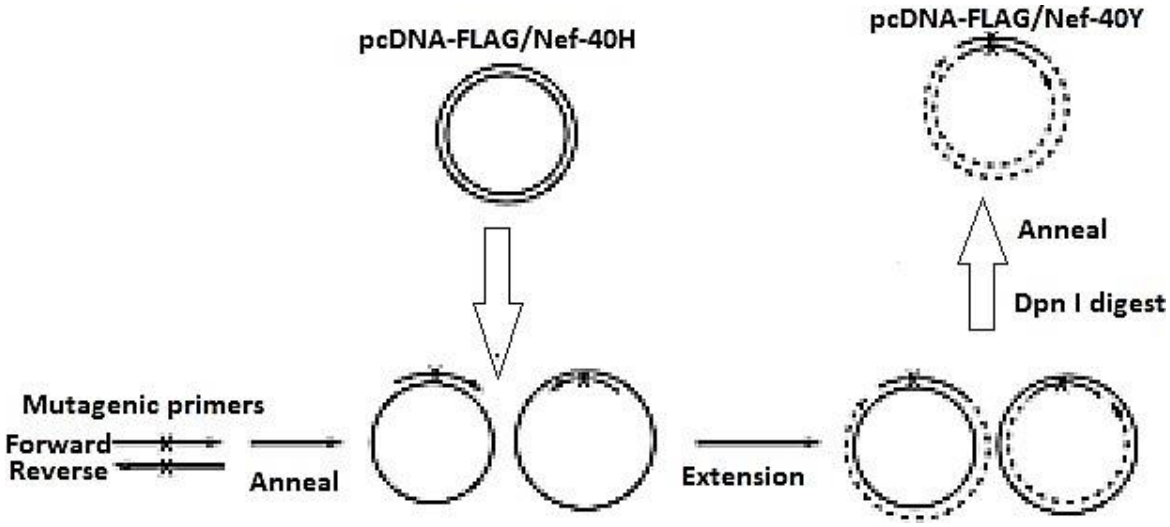

Figure 2.3: Site directed mutagenesis of Nef plasmid
Mutagenic primers designed with the mutation desired are used to introduce the mutation in a process similar to polymerase chain reaction. Post the extension cycle, the template plasmid (pcDNA 3.1-FLAG/Nef-40H) is digested by the Dpn I enzyme and allows the mutated strands to anneal. This results in new pcDNA-FLAG/Nef-40Y plasmids, figure adapted from Xia *et al*., (2014).

2.4.7. Confirmation of the site-directed mutagenesis

To confirm the presence of the mutation, 5 colonies were picked using pipette tips from the sample reaction agar plate to perform colony PCR using the *PO144* primers in table 2.7. Each pipette tip was dipped in a PCR tube with 19 µl of PCR master mix as described in section 2.4.1. The PCR products were analysed by electrophoresison a 1% (w/v) agarose gel as described in section 2.4.1. The *nef* gene products were recovered from the agarose gel using a Zymoclean Gel DNA Recovery Kit (Zymo Research, California, U.S.A.) as in section 2.3.2. The recovered PCR products were digested with FatI restriction enzymes for 1 hour at 55 ˚C in a heating block. Mutation screening using the FatI restriction enzyme was done because the FatI restriction site was present at the site of the mutation in the 144-40H gene but was absent inthe 140-40Y gene after the mutagenesis reaction. A 144-40H PCR product was used as a positive control as shown is table 2.13. The digested products would be analysed on a 2% (w/v) agarose gel, loaded with a 100 bp DNA ladder [0.1 µg/µl] (Solis Biodyne, Tartu, Estonia) performed under exact conditions as in section

2.4.1. The same pipette tips used in the colony PCR were used to inoculate 5 fresh 15 mL LB broth supplemented with 100 µg/ml ampicillin in 50 ml tube and cultured overnight at 37 ˚C with shaking at 150 rpm. Plasmid DNA was extracted using a Zippy Plasmid Miniprep Kit as mentioned in section 2.3.6. The integrity of the pcDNA™ 3.1(+)-FLAG/Nef-40H plasmid was confirmed by restriction digest using BamHI and EcoRI restriction enzymes The restriction products were analysed by electrophoresis on a 1% (w/v) agarose gel as previously described in section 2.4.1. Based on the analyses on the digested products described in table 2.7 only PCR products that differed from the control sample were validated by Sanger sequencing performed at Inqaba BiotechnicalIndustries (Pretoria, South Africa). The presence of the H40Y mutation was confirmed by performing a *nef* sequence alignment with constructed plasmids against the HXB2 *nef* wild-type sequence using the BioEdit software v.2.1 (http://www.mbio.ncsu.edu/BioEdit/bioedit.html.).

Table 2.13: Restriction digests reaction preparation

Components	**144-40H**	**PCR products**
20X Buffer	2 µl	2 µl
DNA [25 ng/ul]	2 µl	2 µl
FatI [2000 units/ml]	2 µl	2 µl
dH_2O	14 µl	14 µl
Total	20 µl	20 µl

2.4.8. Expression of recombinant HIV-1 Nef proteins

To determine the ability of the transient HIV-1 Nef expressing plasmids to produce recombinant HIv-1Nef proteins, the constructs, and a mock plasmid (empty pcDNA™ 3.1(+) plasmid), were transfected into HEK293T cells as described in section 2.3.8. Post incubation of the transfected cells, the expression of recombinant HIV-1 Nef proteins was analysed by SDS-PAGE and Western blot analysis as described in section 2.3.9.

2.4.9. *In vitro* expression of HIV-1 Nef in endothelial cells

The constructs expressing the wild-type and mutated HIV-1 *nef* genes, as well as a mock plasmid (empty pcDNA™ 3.1(+) plasmid), and pSelect-GFPzeo plasmid (transfection positive control) were transfected into HPMEC cells using the Invitrogen Lipofectamine LXT Reagent or PEI [1 mg/ml] in 12-well culture plates. Lipofectamine LXT reagent and PEI had similar transfection efficiency and decision on which one to use was based on availability. Prior to transfection of adherent HPMECs, the cells were maintained in a T75 flask (Sigma-Aldrich, U.S.A) with Endothelial cell medium (ECM) supplemented with 10% (v/v) FBS, 1% (v/v) Endothelial cell growth supplement (EGCS)[100X], 100 U/mL penicillin-streptomycin solution and 1mg/mL fibronectin (ScienceCell Research Laboratories, California, U.S.A) for HPMECs, incubated in a humidified atmosphere incubator at 37 ˚C with 5% CO^2. The cells were passaged every two days. All cells were between passage 5 and 10 for the transfection. The day before transfection, the cells were prepared for transfection as described in section 2.3.8. The cells were incubated until they reached 80% confluency on the day of transfection. Once confluent, half of the wells would be treated with TNF-α [10 ng/ml] and incubated for 6 hours to induce endothelial cell activation. Activated non-transfected endothelial cells and supernatant were used as a positive control for qPCR and ELISA respectively because TNF-α increased the expression of ICAM-1 and VCAM-1 independently of HIV-1 Nef. Post incubation, for each well to be transfected, 1 µg of Nef-expressing plasmids, mock plasmid or pSelect-GFPzeo plasmid were diluted in 100 µl of Opti-MEM™ I Reduced Serum media (Thermofisher Scientific, U.S.A.) within a labelled 1.5 ml tube. Three microliters of Invitrogen™ Lipofectamine LTX Reagent (Thermofisher Scientific, U.S.A.) or PEI [1mg/ml] was added to each tube as seen in Table 2.14. The mixture was incubated for 30 minutes at room temperature. Following the incubation period, 100 µl of the DNA-Lipofectamine mixture was added directly to each well

containing the cells and mixed by gently rocking the plate back and forth. The cells were incubated at 37 ˚C in a 5% CO_2 incubator for 48 hours. The transfections were done in duplicates for each Nef-expressing plasmid.

Table 2.14: Transfection protocol used on endothelial cells

	TNF-α treatment naïve endothelial cells			**6-hour TNF-α [10 ng/ml] treated endothelial cells**		
Plasmids	Nef-40H	Nef-40Y	Nef-MJ4	Nef-40H	Nef-40Y	Nef-MJ4
Cell vessel	12-well	12-well	12-well	12-well	12-well	12-well
Volume Medium	1 ml	1 ml	1 ml	1 ml	1 ml	1 ml
Cells per Well	$2.5x10^5$ Cells	$2.5x10^5$ cells	$2.5x10^5$ Cells	$2.5x10^5$ Cells	$2.5x10^5$ Cells	$2.5x10^5$ Cells
Volume dilution Medium	100 µl	100 µl	100 µl	100 µl	100 µl	100 µl
DNA	1 µg	1 µg	1 µg	1 µg	1 µg	1 µg
Transfection Reagent	3 µl	3 µl	3 µl	3 µl	3 µl	3 µl

2.4.10. Confirmation of *in vitro* HIV-1 Nef expression

Cells and culture media described in section 2.4.9 were harvested separately at 0, 3, 6, 9, 12, 24 and 48 hours post transfection to analyse for HIV-1 Nef expression. The culture medium was aspirated and stored in labelled 1.5 ml tubes at -20 ˚C, while the cells were scrapped of the surface of the well with a cell scraper (Thermofisher Scientific, U.S.A.) and collected with 200 µl PBS solution. The cells were divided in half, with 100 µl of the cells were used to analyse HIV-1 Nef expression using Western blot analysis as described in section 2.3.9. The remaining 100 µl of cells were centrifuged at 10000 x *g* for 10 minutes to pellet the cells. The supernatant was discarded, and the pellet was stored at -20°C to be

used in the quantitative-PCR (qPCR) analysis.

2.4.11. Quantification of biomarkers of endothelial function

2.4.11.1. Extraction of total RNA

Gene expression levels of the biomarker of endothelial function, ICAM1 and VCAM- 1, were assessed in the harvested cells from section 2.4.10 by quantitative-PCR (qPCR). A housekeeping gene (β-actin) was used as a loading control and to normalize the expression of ICAM-1 and VCAM-1 between the different harvested cells. The total RNA was extracted from the cells using the Quick-RNA™ Miniprep Kit (Zymo Research, California, U.S.A.). The pelleted stored cells mentioned in section 2.4.10 were thawed on ice. The pellet was resuspended in 100 µl of RNA Lysis Buffer. The lysed sample was then transferred into a Spin-Away Filter in a collection tubeand centrifuged at 16000 x *g* for 30 seconds to remove genomic DNA. The flow through was saved and 100 µl of 100% (v/v) ethanol added to the flow through. The mixture was then transferred into a Zymo-Spin IIICG Column in a collection tube and centrifuged for 30 seconds at 16000 x *g*. Following centrifugation, the flow-through was discarded and 400 µl of RNA Wash Buffer added to the column and centrifuged at 16000 x *g* for 30 seconds. Five microliters of DNase I [250 U] and 75 µl of DNA Digestion buffer were mixed in the column and incubated at room temperature for 15 minutes. After incubation, 400 µl of RNA Prep Buffer was addedto the column and centrifuged for 30 seconds at 16000 x *g*. The flow-through was discarded; following 700 µl of RNA Wash Buffer was added to the column and centrifuged for 30 seconds at 16000 x *g*. Complete removal of the wash buffer was achieved by adding 400 µl of RNA Wash buffer to the column and centrifuged for 1 minute at 16000 x *g*. The column was transferred to a labelled nuclease-free 1.5 ml tube, where 100 µl of DNase/RNase-Free Water was added directly onto the column matrix and centrifuged for 1 minute at 16000 x *g* to collect the mRNA. The purity of the RNA was measured by using a

NanoDrop™ One/One C Microvolume UV-Vis Spectrophotometer (Thermofisher Scientific, U.S.A.). The DNase/RNase-Free Water was used to blank the machine. RNA with a reading of ~2.0 for the ratio of absorbance at 260 nm and 280 nm was deemed to be pure and of excellent quality.

2.4.11.2. Complementary DNA synthesis

The LunaScript® RT SuperMix Kit (New England Biolabs, Massachusetts, U.S.A.) was used to synthesis complementary DNA (cDNA) used in a 2-step qPCR workflow. A cDNA synthesis reaction was prepared for each mRNA extracted (section 2.4.11.1) by adding 4 µl of LunaScript RT Supermix, 1 µl of RNA sample (section 2.4.11.1) and nuclease-free water up to 20 µl in a nuclease-free PCR tube. The tubes were incubated in a T100 thermal cycler (Bio-Rad Laboratories, California, U.S.A) set to the manufacturer's parameters, as shown in Table 2.15.

Table 2.15: Cycling parameters for the LunaScript® RT SuperMix Kit

Cycle Step	Temperature	Time	Cycles
Primer annealing	25˚C	2 minutes	1
cDNA synthesis	55˚C	10 minutes	
Heat inactivation	95˚	1 minute	

2.4.11.3. Real-time quantitative-PCR

The Luna® Universal qPCR Master Mix kit (New England Biolabs, Massachusetts, U.S.A.) was used for the qPCR. A master mix was created for each biomarker and β-actin to be analysed by adding the Luna Universal qPCR Master mix with the specific primers (Table 2.16) to the template cDNA. The β-actin Ct value obtained was used to standardize the Ct values of the biomarkers for the 2^-ΔΔCt calculations. The 2^-ΔΔCt calculations represent the fold change in mRNA expression relative to the control group used. The volumes for

each component were obtained from the manufacturer ‘s instruction, shown in Table 2.17. The master mix was thoroughly mixed, centrifuged, and aliquoted (19 µl each) into eight qPCR tubes. One microliter of template cDNA from section 2.4.11.2 was added to their corresponding tubes and mixed. The tubes were then placed in a Rotor-Gene Q (QIAGEN, Germany) real-time PCR instrument set to the kit manufacturer ‘s thermocycling parameter, as shown in Table 2.18. The Luna Universal qPCR Master Mix uses the SYBR® Green I dye for detection of the amplified DNA products which will be detected in the melt curve step. The intercalating SYBR® Green I dye gives a signal for detection only when bound to dsDNA and stops fluorescing when the dsDNA is separated into ssDNA.

Table 2.16: Primer sequences used in RT-PCR

Target	**Primer name and sequence**
ICAM-1	F1_ICAM: 5‘- AGCCAACCAATGTGCTATTCAAAC-3‘
	R1_ICAM: 5‘-CACCTGGCAGCGTAGGGTAA-3‘
VCAM-1	F1_VCAM: 5‘-CGAAAGGCCCAGTTGAAGGA-3‘
	R1_VCAM: 5‘-GAGCACGAGAAGCTCAGGAGAAA-3‘
β-actin	F1_B-actin: 5‘-TGGCACCCAGCACAATGAA-3‘
	R1_B-actin: 5‘-CTAAGTCATAGTCCGCCTAGAAGCA-3‘

Table 2.17: Reaction setup for qPCR

Components	**X1 Reaction**	**8x Reaction**
Luna Universal qPCR Master Mix	10 µl	80 µl
Forward Primer (10 uM)	0.5 µl	4 µl
Reverse primer (10 uM)	0.5 µl	4 µl
Template DNA	<100 ng	
Nuclease-free water	8 µl	64 µl
Total	19 µl	152 µl

Table 2.18: Thermocycling protocol for the Luna® Universal qPCR Master Mix

Cycle step	Temperature	Time	Cycles
Initial denaturation	95˚C	60 seconds	1
Denaturation	95˚C	15 seconds	40
Extension	60˚C	30 seconds	
Melt curve	60-95˚C	Various	1

2.4.12. VCAM-1 Protein expression study

A quantitative analysis of the concentration of soluble VCAM-1 in harvested culture supernatant in section 2.4.10 was done using an Enzyme-linked Immunosorbent Assay (ELISA). This was done to evaluate the levels of soluble VCAM-1 in the supernatant against their levels of expression as the levels of detached VCAM-1 from the cellular membrane may differ to their levels of expression. The supernatant from the transformed cultures mentioned in section 2.4.10 was harvested and centrifuged at 10000 rpm for 15 minutes to remove cells and debris. Soluble VCAM-1 were measured in the collected samples using the Human sVCAM-1 ELISA kit (Thermofisher Scientific, U.S.A.). Protein standards were established for the kit by performing serial dilutions sVCAM-1 [200 ng/ml] standard solutions. Microcentrifuge tubes (1.5 ml) were labelled, one for each standard point: S1, S2, S3, S4, S5 and S6. The 1:2 serial dilutions were prepared as follows, 225 µl of Assay buffer was pipetted into each tube and then 225 µl of standard was added to tube S1 thus giving the first standard a final concentration of 100 ng/ml. Tube S2 received 225 µl of the dilution in tube S1, resulting in a final concentration of 50 ng/ml. This was done until tube S6 and the concentrations for all standards were represented in table 2.19. The supernatant samples harvested were diluted 1:10 (10 µl sample + 90 µl sample diluent). Supernatant from the TNF-α treated non-transfected cells was used as positive control. Hundred microliters of each standard were pipetted into the respective microwell plates coated with monoclonal antibody to human sVCAM-1 in duplicates. Blanks wells were

prepared by adding 100 µl of Assaybuffer. Hundred microliters of the diluted supernatant samples were added to the remaining wells in duplicates. Fifty microliters of HRP-conjugated anti-human sVCAM-1 monoclonal antibodies were added to each well on respective plates. The plates were covered with adhesive film and incubated for 2 hours at room temperature. After incubation, the adhesive film was removed, and the wells were emptied. The plates were washed twice by adding 400 µl of Wash buffer per well. The Wash buffer was incubated for 15 seconds before aspiration. After the last wash, the Wash buffer was removed and the microwell plates were tapped on absorbent paper towel to remove the excess Wash buffer. TMB Substrate solution was added to all wells to a volume of 100 µl. The plates were incubated in a dark room for 10 minutes at room temperature, allowing the solution to develop a dark blue colour. The reaction was stopped by adding 100 µl of Stop solution to each well. The absorbance of each microwell was read on a Synergy™ HT microplate reader (Agilent, California, U.S.A.) using 450 nm as the primary wavelength and 620 nm as the reference wavelength. The mean absorbance readings for each standard were used to make a standard curve for each kit. The standard curve was used to extrapolate the concentrations of sVCAM-1 in each sample.

Table 2.19: Standard dilutions for the sVCAM-1 ELISA kits

Standard	Concentration (ng/ml)
	VCAM-1
S1	37.5
S2	16.7
S3	9.37
S4	4.69
S5	2.34
S6	1.17
S7	0.59

2.4.13. Statistical analysis

Statistical analysis was performed using Graphpad Prism software v8.4.3 (GraphPad, California, U.S.A.). Expression levels of ICAM-1 and VCAM-1 mRNA in HIV-1 Nef transfected HPMECs in the presence and absence of TNF-α were compared using a Student‘s unpaired *t* test. Levels of ICAM-1 and VCAM-1 mRNA expressed at varying time points (3, 6, 9, 12, 24 and 48hrs) in the absence and presence of TNF-α were compared to their respective negative control using ANOVA. The expression level of ICAM-1 and VCAM-1 were grouped by HIV-1 Nef variants and by each experimental condition, following which a Tukey‘s multiple comparisons test was used to compare across the 3 HIV-1 Nef variants (Nef-40H, Nef-40Y and Nef-MJ4) to determine significant differences in expression levels of adhesion molecules. The timepoint considered to give maximum expression of adhesion molecules (24hrs post transfection) was selected, and a Dunnett‘s multiple comparisons test wasperformed to determine significant differences in expression levels of ICAM-1 and VCAM-1 mRNA in HPMECs cultured in the absence of HIV-1 Nef and TNF-α (negative control) compared against HPMECs cultured in the presence of HIV-1 Nef and TNF-α, absence of HIV-1 Nef and presence of TNF-α, and HPMECs cultured in the

presence of HIV-1 Nef and absence of TNF-α. A Tukey‘s multiple comparisons test was equally performed to determine significant differences between levels of ICAM-1 and VCAM-1 mRNA expression in HIV-1 Nef transfected HPMECs in the presence of TNF-α against HPMECs cultured in the absence of Nef but presence of TNF-α, and HPMECs cultured in the presence of Nef but absence of TNF-α. This was done to determine if there was a cooperative relationship between HIV-1 variants and TNF-α. The same statistical analysis was performed on VCAM-1 protein expression profiling data. A value of statistical significance was defined as a $p<0.05$.

Chapter 3: Results

3.1. Construction of stable HIV-1 Nef expression plasmids

3.1.1. PCR amplification of HIV-1 *nef* encoding genes

The HIV-1 *nef* encoding sequences were amplified by a polymerase chain reaction using a Hi-Fi *Taq* with primers containing restrictions sites, *Age*I and *Eco*RI, to enable cloning into the pLKO.dCMV,TetO.3xFlag plasmid for stable expression in mammalian cells. The pMJ4 plasmid was used as the DNA template for the amplification of wildtype HIV-1 *nef* (*nef*-MJ4) (Figure 3.1, lane 1-4) while a clinical isolate (i.e., *PO144*) in the form of a PCR product was used for the amplification of the wildtype HIV-1 *nef* (i.e., 40H) (Figure 3.1, lane 5-6). Both produced amplicons of the correct size of approximately 640 bp, as well as some non-specific amplicons greater than 700bp.

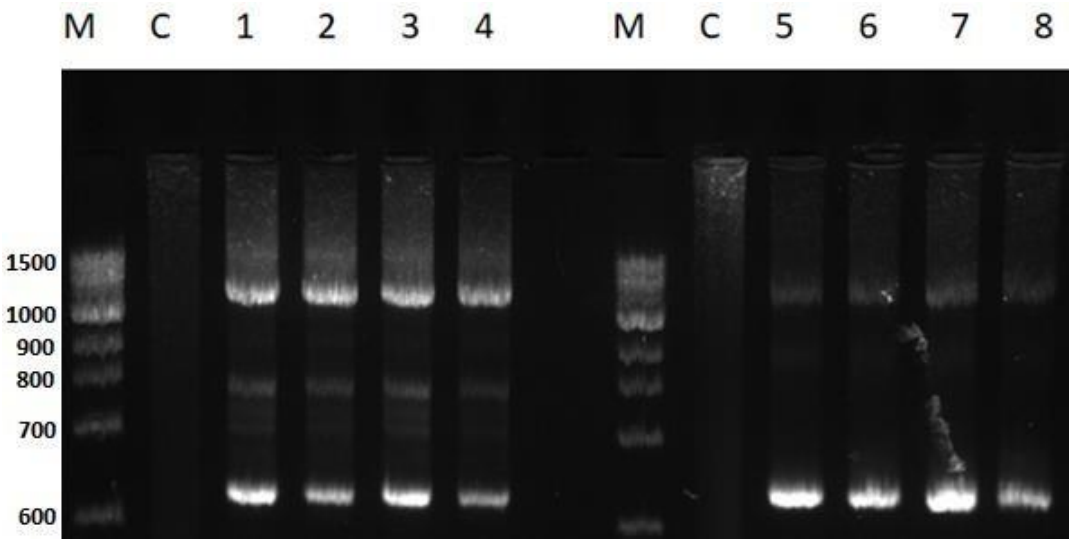

Figure 3.1: Agarose gel electrophoresis of HIV-1 Nef PCR products
HIV-1 *nef* PCR products resolved on a 1% (w/v) agarose gel. Lane M: Quick load 100 bp DNA ladder; lane C — negative control (no plasmid); lanes 1-4: HIV-1 *nef* MJ4 PCR products with *Age*I and *Eco*RI restriction sites; Lanes 5-8: HIV-1 *nef* 40H PCR products with *Age*I and *Eco*RI restriction sites. HIV-1 nef amplicons were approximately 640 bp in size, however non-specific amplicons greater than 700 bp were observed in lanes 1-4 but not seen in lanes 5-6.

3.1.2. Construction of recombinant HIV-1*nef* expression plasmids

The amplified HIV-1 *nef* gene was inserted into the multiple cloning site of the pLKO.dCMV,TetO.3xFlag plasmid by ligation, between the *Age*I and *Eco*RI restriction sites of the vector. To clone the HIV-1 *nef* gene inserts into the pLKO.dCMV,TetO.3xFlag vector, double digestion of the pLKO.dCMV,TetO.3xFlag vector and amplified HIV-1 *nef* products was performed with *Age*I and *Eco*RI restriction enzymes and analysed on a 1% (w/v) agarose gel. For the plasmid (Figure 3.2), restriction digest with either *Age*I (lane 3) or *Eco*RI (lane 4) resulted in a linearized pLKO.dCMV,TetO.3xFlag vector with a size of 8140 bp; while a double digest (lanes 1, 2) resulted in two fragments, 7519 bp and 621 bp in size, respectively corresponding to the pLKO.dCMV,TetO.3xFlag vector backbone and the AgeI and EcoRI fragment with the pLKO.dCMV,TetO.3xFlag vector (Figure 3.2, lane 1-2).

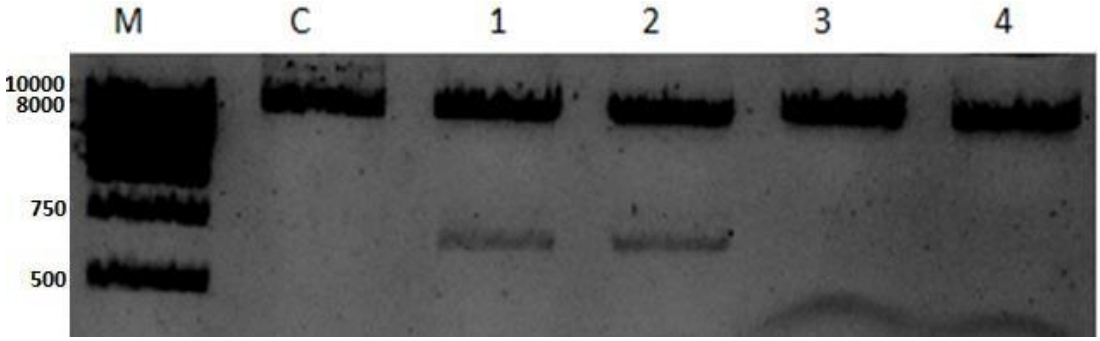

Figure 3.2: Restriction digest of pLKO.dCMV,TetO.3xFlag plasmids
Restriction digest of pLKO.dCMV,TetO.3xFlag plasmids resolved on a 1% (w/v) agarose gel. Lane M: 1 kb DNA ladder (Promega, U.S.A.); lane C: undigested pLKO.dCMV,TetO.3xFlag plasmid; lanes 1-2: duplicate reactions of double digested pLKO.dCMV,TetO.3xFlag plasmids with AgeI and EcoRI; lane 3: linearized pLKO.dCMV,TetO.3xFlag plasmid by single digest with AgeI; lane 4: linearized pLKO.dCMV,TetO.3xFlag plasmid by single digest with EcoRI.

For the amplicons (Figure 3.3), double digestion resulted in a fragment of approximately 630 bp for HIV-1 *nef*-MJ4 (Figure 3.3, lane 1-2) and 640 bp for HIV-1 *nef*-40H (Figure 3.3, lane 3-4), respectively. The sizes of the amplicons were estimated by adding the number of

base pairs of the restricted primers to the length of the HIV-1 *nef* genes.

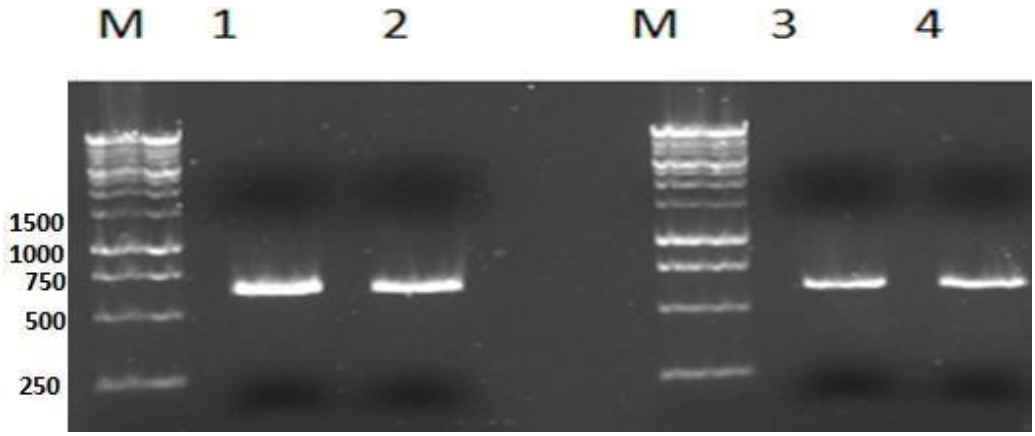

Figure 3.3: Restriction digest of HIV-1 *nef* PCR products

Restriction digestion of HIV-1 *nef* PCR products analysed on a 1% (w/v) agarose gel. Lane M: 1kb DNA ladder (Promega, U.S.A.); lanes 1-2: duplicate reactions of double digested *nef*-MJ4 PCR product with *AgeI* and *EcoRI* restriction enzymes; lanes 3-4: duplicate reactions of double digested *nef*-40H PCR product with *AgeI* and *EcoRI* restriction enzymes.

Colonies possibly containing the pLKO.dCMV,TetO.3xFlag/ plasmids with the desired Nef-MJ4 (Figure 3.4A) and Nef-40H (Figure 3.4B) inserts were observed on the plates.

A **B**

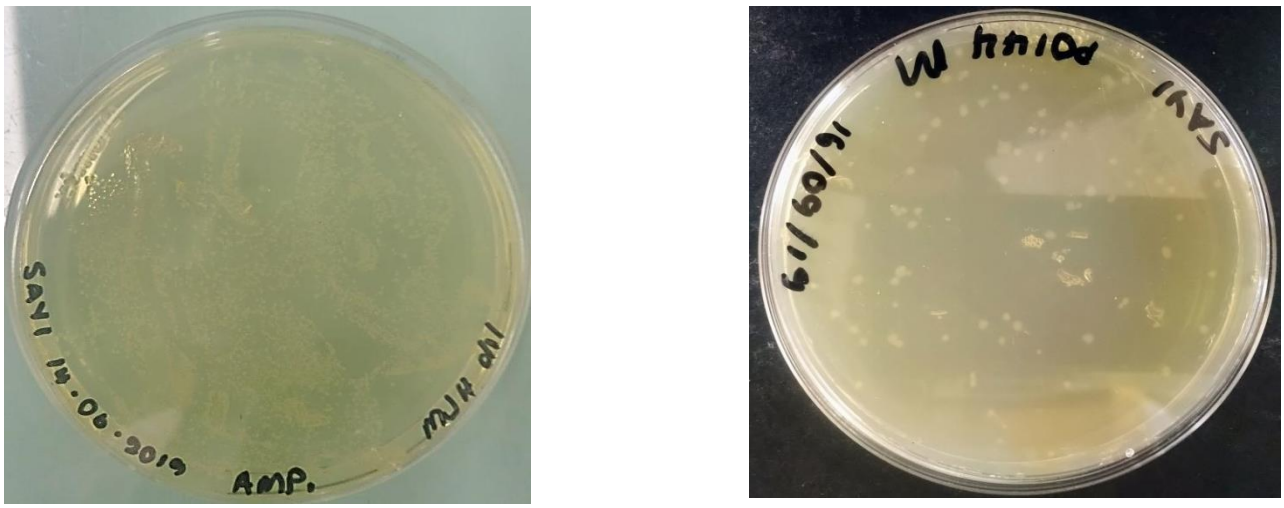

Figure 3.4: LB agar plates with Nef-expressing construct colonies

Transformed JM109 *E.coli* colonies with (A) pLKO.dCMV,TetO.3xFlag/Nef-MJ4 ligation reaction and (B) pLKO.dCMV,TetO.3xFlag/Nef-40H ligation reaction plated on ampicillin supplemented LB agar plates.

Three colonies from each plate were grown overnight and confirmed for the presence respective inserts by performing colony PCR. PCR was conducted on a double digested empty pLKO.dCMV,TetO.3xFlag plasmid and no amplicons were observed thus no amplification had taken place (Figure 3.5A, lane CV), similar to the no template control reaction (Figure 3.5A, lane NC). Colony PCR of the HIV-1 *nef*-MJ4 overnight culture produced amplicons that were greater in size than the HIV-1 *nef*-MJ4 genes (Figure 3.5A, lanes 1-3). This may have been due to non-specific binding of the primers, resulting in PCR products larger than the HIV-1 *nef*-MJ4 gene. Colony PCR of the HIV-1 *nef*-40H overnight culture showed amplicons with the size of HIV-1 *nef*-40H genes observed in Figure 3.5B, lane 1-3. However, amplicons of greater and smaller sizes to the gene of interest were produced (Figure 3.5B, lanes 1-3), due to non-specific binding. A positive PCR control setup using a digested PCR product produced a single band on the agarose gel (Figure 3.5B, lane PC). A no template PCR was used as a negative control (Figure 3.5B, lane NC).

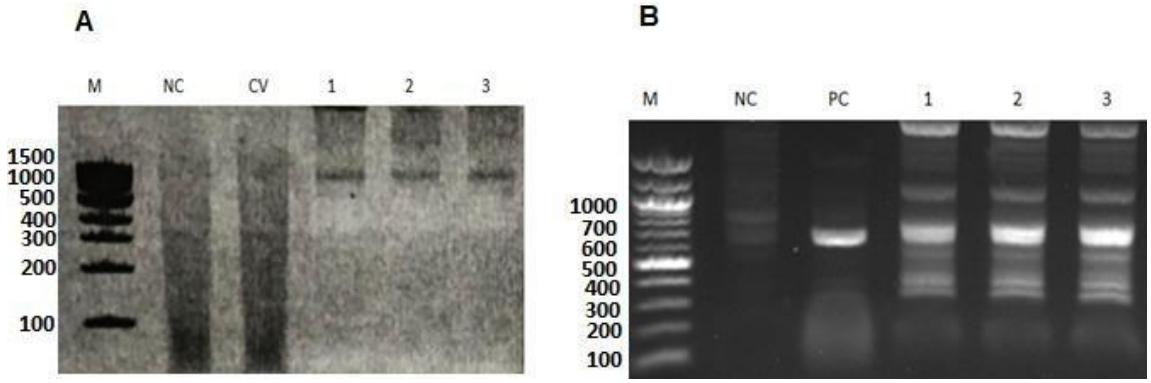

Figure 3.5: Colony PCR of transformed cells
Colony PCR of *E.coli* colonies transformed with (A) pLKO.dCMV,TetO.3xFlag/Nef-MJ4 constructs and (B) pLKO.dCMV,TetO.3xFlag/Nef-40H constructs. Lane M: Quick load 100 bp DNA ladder; lane NC: no plasmid control; lane CV: double digested empty pLKO.dCMV,TetO.3xFlag vector; lanes 1-3A: amplicons from the pLKO.dCMV,TetO.3xFlag/Nef-MJ4 construct; lane PC: positive control ; lanes 1-3B: successful pLKO.dCMV,TetO.3xFlag/Nef-40H clones.

Restriction digest was used to confirm successful cloning of the *nef* gene insert into the

pLKO.dCMV,TetO.3xFlag vector. Double digestion of the plasmid DNA obtained from colonies of pLKO.dCMV,TetO.3xFlag/Nef-MJ4 (Figure 3.6, lane 1) and pLKO.dCMV,TetO.3xFlag/Nef-40H (Figure 3.6, lane 2) with both *Age*I and *Eco*RI restriction enzymes resulted in two distinct DNA fragments of around 750 bp (*nef* inserts) and 7.5 kb (plasmid backbone).

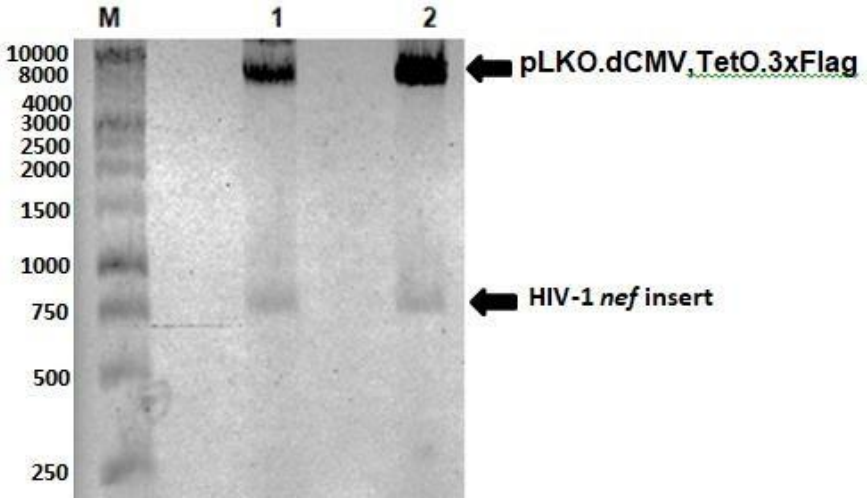

Figure 3.6: Confirmation of Nef-expressing plasmids

Restriction digest of pLKO.dCMV,TetO.3xFlag-*nef* expressing plasmids analysed on a 1% (w/v) agarose gel. Lane M: 1 kb DNA ladder (Promega, U.S.A.); lane 1: double digest of pLKO.dCMV,TetO.3xFlag/Nef-MJ4 with both AgeI and EcoRI enzymes; lane 2: double digest of pLKO.dCMV,TetO.3xFlag/Nef-40H with both AgeI and EcoRI enzymes. Bands of the HIV-1 *nef* inserts can be observed around the 750 bp marker.

3.1.3. Sequencing of Nef expression plasmids

Population-based Sanger sequencing of the pLKO.dCMV,TetO.3xFlag/Nef-MJ4 and pLKO.dCMV,TetO.3xFlag/Nef-40H plasmids extracted from the colonies was performed at Inqaba Biotech (Pretoria, South Africa) using the pLKO plasmid sequencing primers listed in section 2.3.1. Sequence alignment was performed on the sequencing data against the known HIV-1 *nef* sequences for nef-MJ4 (Figure 3.7A) and nef-40H (Figure 3.7B).

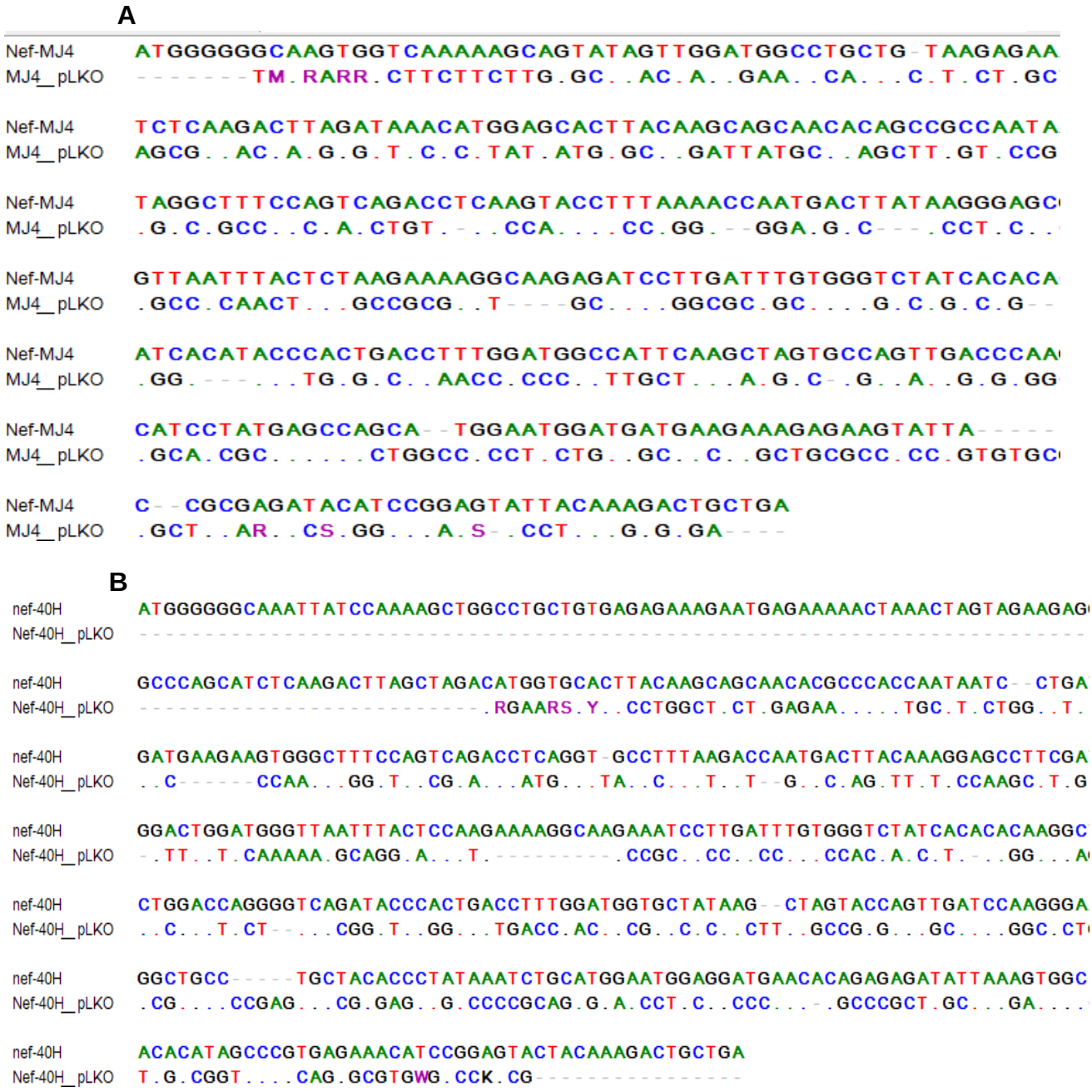

Figure 3.7: HIV-1 *nef* sequencing results
Sequences of HIV-1 *nef* inserts obtained from sequencing against the known HIV-1 nef sequences for (A) pLKO.dCMV,TetO.3xFlag/Nef-MJ4 and (B) pLKO.dCMV,TetO.3xFlag/Nef-40H using pLKO sequencing primers. The sequencing data was labelled nef-MJ4_pLKO and nef-40H_pLKO, while the known sequences were labelled *nef*-MJ4 and *nef*-40H. The ‗.' represented identical residues and ‗~' represent the gaps.

Sequence alignment of the obtained sequencing data against known sequences of HIV-1 *nef*-MJ4 and HIV-1 *nef*-40H did not yield any positive matches. Therefore, the Basic Local

Alignment Search Tool (BLAST) online tool was used on the National Centre for Biotechnology Information (NCBI) website (https://blast.ncbi.nlm.nih.gov/Blast.cgi?PROGRAM=blastn&PAGE_TYPE=BlastSearch&LINK_LOC=blasthome) to search matching sequences. Results from the BLAST search did not correspond to known sequences of the HIV-1 *nef* gene (Figure 3.8) but corresponded with 98% identity to sequences from tripartite motif 11 (TRIM11). The human E3 ubiquitin-protein ligase called TRIM11 facilitates the degradation of insoluble ubiquitinated proteins (Ishikawa *et al*., 2006). The TRIM 11 gene did not form part of the pLKO.dCMV,TetO.3xFlag vector. This therefore suggests that the cloning of the *nef*-expressing plasmids was not successful. Despite the lack confirmation of sequence identity, the expression of recombinant Nef proteins from the pLKO.dCMV,TetO.3xFlag/Nef-MJ4 and pLKO.dCMV,TetO.3xFlag/Nef-40H followed.

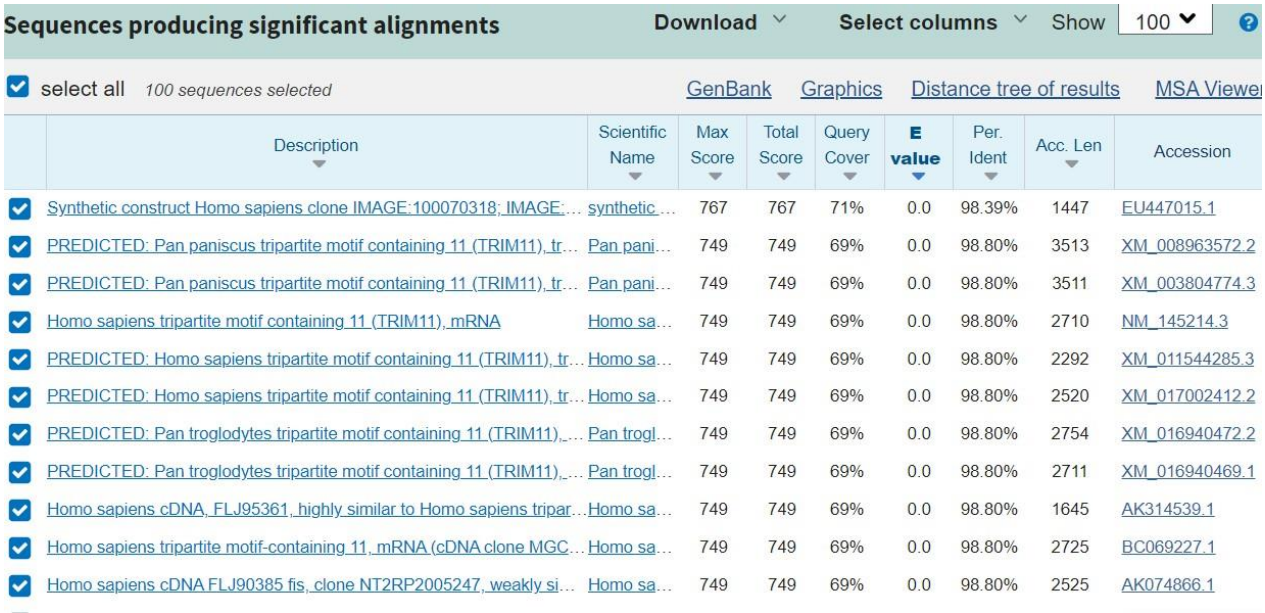

Sequences producing significant alignments Download Select columns Show 100

select all *100 sequences selected* GenBank Graphics Distance tree of results MSA Viewer

Description	Scientific Name	Max Score	Total Score	Query Cover	E value	Per. Ident	Acc. Len	Accession
Synthetic construct Homo sapiens clone IMAGE:100070318; IMAGE:…	synthetic…	767	767	71%	0.0	98.39%	1447	EU447015.1
PREDICTED: Pan paniscus tripartite motif containing 11 (TRIM11), tr…	Pan pani…	749	749	69%	0.0	98.80%	3513	XM_008963572.2
PREDICTED: Pan paniscus tripartite motif containing 11 (TRIM11), tr…	Pan pani…	749	749	69%	0.0	98.80%	3511	XM_003804774.3
Homo sapiens tripartite motif containing 11 (TRIM11), mRNA	Homo sa…	749	749	69%	0.0	98.80%	2710	NM_145214.3
PREDICTED: Homo sapiens tripartite motif containing 11 (TRIM11), tr…	Homo sa…	749	749	69%	0.0	98.80%	2292	XM_011544285.3
PREDICTED: Homo sapiens tripartite motif containing 11 (TRIM11), tr…	Homo sa…	749	749	69%	0.0	98.80%	2520	XM_017002412.2
PREDICTED: Pan troglodytes tripartite motif containing 11 (TRIM11),…	Pan trogl…	749	749	69%	0.0	98.80%	2754	XM_016940472.2
PREDICTED: Pan troglodytes tripartite motif containing 11 (TRIM11),…	Pan trogl…	749	749	69%	0.0	98.80%	2711	XM_016940469.1
Homo sapiens cDNA, FLJ95361, highly similar to Homo sapiens tripar…	Homo sa…	749	749	69%	0.0	98.80%	1645	AK314539.1
Homo sapiens tripartite motif-containing 11, mRNA (cDNA clone MGC…	Homo sa…	749	749	69%	0.0	98.80%	2725	BC069227.1
Homo sapiens cDNA FLJ90385 fis, clone NT2RP2005247, weakly si…	Homo sa…	749	749	69%	0.0	98.80%	2525	AK074866.1

Figure 3.8: Blast search results
Blast search results obtained from analysing the HIV-1 *nef* sequencing data, indicating the absence of HIV-1 nef in the submitted sequences.

3.1.4. Expression of recombinant Nef proteins

The ability of the cloned-in *nef* genes to produce HIV-1 subtype C Nef proteins was tested by transfecting HEK293T cells with the pLKO.dCMV,TetO.3xFlag/Nef-MJ4 and pLKO.dCMV,TetO.3xFlag/Nef-40H plasmids. The aim of the transfection was to assess whether the constructs were cable of producing proteins, and if so, check to see if the expressed Nef protein could be confirmed by Western blot using anti-Nef antibodies. The production of HIV-1 Nef proteins was analysed by SDS-PAGE and confirmed by Western blot analysis using mouse-raised monoclonal anti-Nef antibodies and rabbit-raised anti-Flag antibodies. SDS-PAGE analysis of the cell pellets from HEK293T cells transfected in duplicates with GFPZeo/Nef-HXB2 plasmid (Figure 3.9A, lane 1-2), pLKO.dCMV,TetO.3xFlag/Nef-MJ4 (Figure 3.9A, lane 3-4) and pLKO.dCMV,TetO.3xFlag/Nef-40H (Figure 3.9A, lane 5-6) plasmids retrieved during expression showed no distinctive bands when compared to the negative (untransfected) control HEK293T cells (Figure 3.9A, lane -C). Western blot using anti-Nef antibodies confirmed only expression of the Nef-HXB2 protein (Figure 3.9B, lane 1-2) but could not confirm expression of the HIV-1 Nef-MJ4 and Nef-40H proteins (Figure 3.9B, lane 3-6) as no intense bands could be observed around the expected location with reference to the Nef-HXB2 control protein. Western blot analysis confirmed no expression of the HIV-1 Nef protein by untransfected HEK293T cells (Figure 3.9B, lane –C). Western blot analysis performed using the anti-Flag antibodies could also not detect Flag-tagged HIV-1 Nef proteins (Figure 3.9C) which suggested that the cloning of the HIV-1 *nef*-expressing genes into the pLKO.dCMV,TetO.3xFlag vector was not successful. Another possible reason for thefailed detection could be due to the 3/16 amino acid mismatch in the Nef-MJ4 and 6/16 amino acid mismatch in the Nef-40H protein compared to the anti-Nef antibody epitope. The HIV-1 Nef antibody [3D12] is said to bind to HIV-1 subtype B and C Nef proteins

recognizing the amino acids at positions 35-50. A study by Poon and colleagues reported this region to be of high sequence variation (Poon *et al*., 2010). The high occurrence of variations in this region could negatively affect the ability of the monoclonal HIV-1 Nef antibody to bind to the HIV-1 Nef-40H and Nef-MJ4 proteins. Since the pSelect-GFPZeo/Nef-HXB2 plasmid did not contain a Flag tag, the anti-Flag antibodies were not expected to bind to this protein, as observed in the blot.

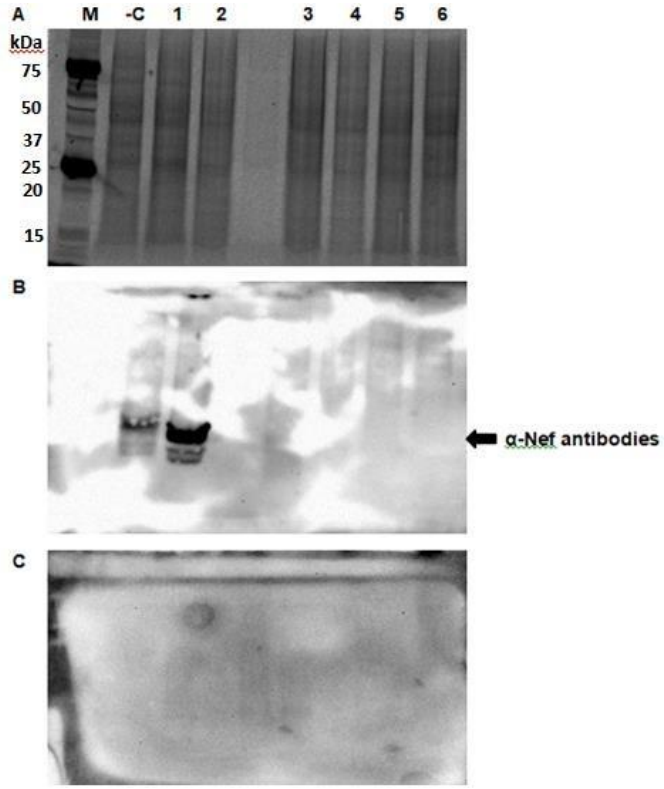

Figure 3.9: Analysis of recombinant Nef expression
Analysis of recombinant Nef expression. SDS-PAGE (12%) analysis of cells pellets from HEK293T cells transfected with the Nef-expressing plasmids (A). Western blot analysis of transfected cells using anti-Nef antibodies (B). Western blot analysis using anti-Flag antibodies (C). Lane M: Precision plus protein standard; lane -C: untransfected HEK293T cells; lane 1-2: pSelect-GFPZeo/Nef-HXB2 plasmid transfected cells; lanes 3-4: pLKO.dCMV,TetO.3xFlag/Nef-MJ4 plasmid transfected cells; lanes 5-6: pLKO.dCMV,TetO.3xFlag/Nef-40H plasmid transfected cells.

3.2. Construction of transient HIV-1 Nef expression plasmids

Cloning of HIV-1 *nef* genes into pLKO.dCMV,TetO.3xFlag vector and expression of HIV-1 proteins was not achieved. Changing of experimental design was chosen over troubleshooting because the pLKO.dCMV,TetO.3xFlag plasmid was a gift of which its identity was not confirmed prior to its use. A new transient mammalian expression vector was thus used for the expression of HIV-1 Nef proteins. A transient expression was chosen over stable expression because the transient expression vector sequence was identified and confirmed prior to its use. Additionally, transient expression produced large amounts of recombinant proteins in a shorter time compared to the more labour-intensive and lengthy pooling time involved with stable expression (Duong-Ly & Gabelli, 2014). The transient expression vector selected was under the control of the human cytomegalovirus (CMV) promoter, which is known to produce high levels of mRNA and protein expression in transient transfections (Xia *et al*., 2006).

3.2.1. PCR amplification of HIV-1 *nef* encoding genes

The HIV-1 *nef* encoding gene from the *PO144* clinical isolate and pMJ4 plasmid was amplified by PCR using *Taq* and visualised on a 1% (w/v) agarose gel. Amplification of the *nef* gene with the primers listed in Table 2.1 enabled addition of a FLAG tag protein on the N-terminal end of the HIV-1 *nef* genes, as well as *Bam*HI and *Eco*RI restriction sites on the 5‘- and 3‘-ends, respectively. The *nef*-MJ4 (Figure 3.10, lane 1) and *nef*-40H (Figure 3.10, lanes 2-4) genes were successfully amplified and were used downstream for cloning into the pGEM®-T Easy vector.

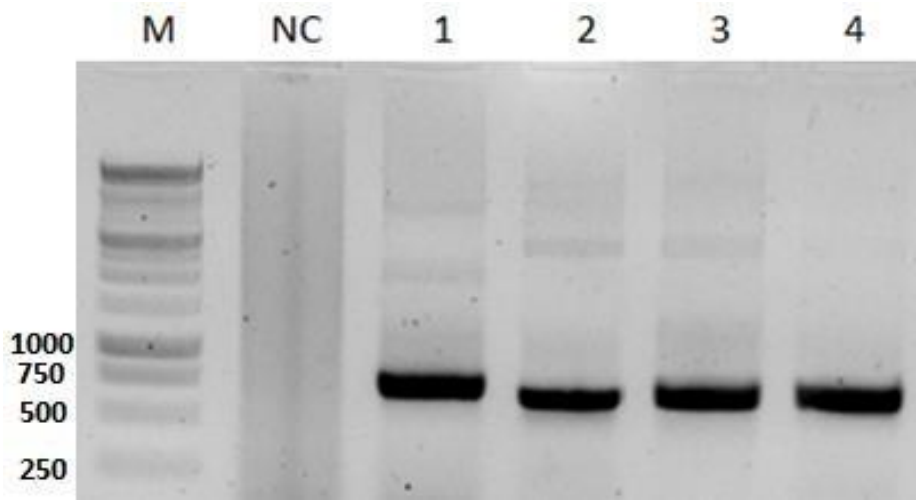

Figure 3.10: PCR products from *nef* amplification
Analysis of HIV-1 *nef* PCR products on 1% (w/v) agarose gel. Lane M: 1 kb DNA ladder (Promega, U.S.A.); lane NC: no template control; lanes 1: HIV-1 *nef*-MJ4 PCR product with introduced FLAG tag and *Bam*HI/*Eco*RI restriction sites; lane 2-4: triplicates of HIV-1 *nef*- 40H PCR product with introduced FLAG tag and *Bam*HI/*Eco*RI restriction sites.

3.2.2. Construction of recombinant HIV-1 Nef expression vectors

The amplified HIV-1 *nef* encoding PCR products were first cloned into a pGEM®-T Easy vector, followed by sub-cloning into the pcDNA™ 3.1(+) vector between the *Bam*HI and *Eco*RI restriction sites in cloning site. The cloning into pGEM®-T Easy vector was to allow for screening of successful clones and improve the efficiency of the restriction enzymes. The amplified HIV-1 *nef* genes were ligated to a pGEM®-T Easy vector using a 1:3 vector to insert ratio in the ligation reaction. The ligated products were transformed into chemically prepared JM109 *E.coli* competent cells and plated on LB agar plates supplemented with ampicillin, X-gal and IPTG to facilitate screening of colonies with the correct insert. A few blue colonies were observed on the *nef*-MJ4+pGEMT plate (Figure 3.11A) amongst the white colonies. Two blue colonies were seen on the *nef*-40H+pGEMT plate (Figure 3.11B) amongst the white colonies present.

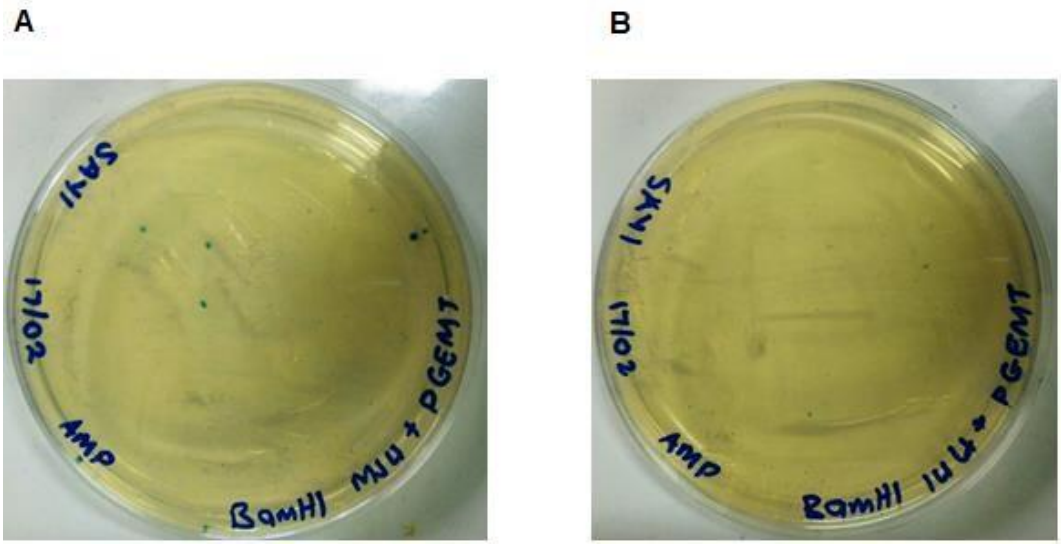

Figure 3.11: LB agar plates with pGEMT-Nef plasmids
Blue/White colony screening of (A) *nef*-MJ4+pGEMT plasmids and (B) *nef*-40H+pGEMT plasmids on LB agar plates supplement with ampicillin, X-gal and IPTG.

About 5 - 8 white colonies were picked from each plate and colony PCR performed to confirm successful cloning of the nef plasmid. One colony showed successful cloning of *nef*-MJ4 into the pGEM®-T Easy vector (Figure 3.12A, lane 2), with an amplicon of approximately 630bp. Four colonies showed successful cloning of *nef*-40H into the pGEM®-T Easy vector (Figure 3.12B, lane 3 to 6), with amplicons of approximately 640 bp.

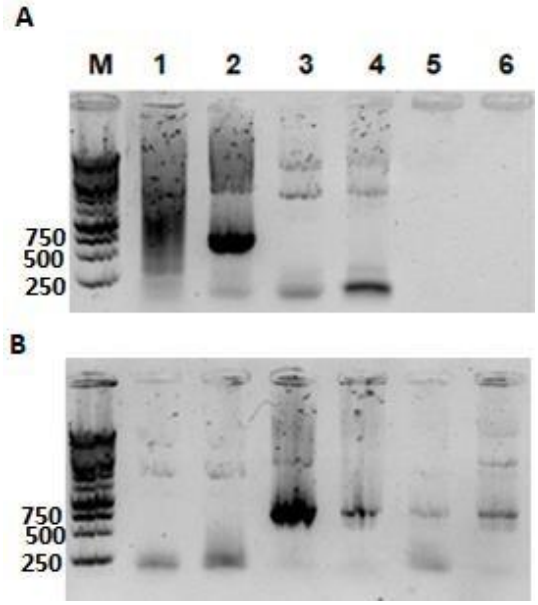

Figure 3.12: Colony PCR of Nef-pGEMT colonies
Colony PCR of *E.coli* colonies transformed with (A) *nef*-MJ4+pGEMT clones and (B) *nef*-40H+pGEMT clones. Lane M: 1 kb DNA ladder (Promega, U.S.A.); lanes 1-4 (A): *nef*-MJ4+pGEMT colonies; lane 1-6 (B): *nef*-40H+pGEMT colonies.

Colonies that showed correct sized amplicons for the colony PCR were inoculated in fresh LB broth, supplemented with ampicillin, and incubated overnight. Plasmid DNA was extracted from the overnight culture to perform a restriction digest. Double digestion of the plasmid DNA was conducted using restriction enzymes, BamHI and EcoRI, to excise the *nef* inserts from the pGEMT vector. Restriction digest of the *nef*- MJ4+pGEMT plasmids was successful, resulting in two fragments of approximately 3000 bp and 630 bp (Figure 3.13, lanes 1-5), corresponding to the empty pGEMT vector and the *nef*-MJ4 insert, respectively. Meanwhile, successful digestion of the *nef*-40H+pGEMT plasmids yielded two DNA bands of approximately 3000 bp and 640 bp (Figure 3.13, lane 6,-8,10), corresponding to the empty pGEMT vector and *nef*-40H insert, respectively.

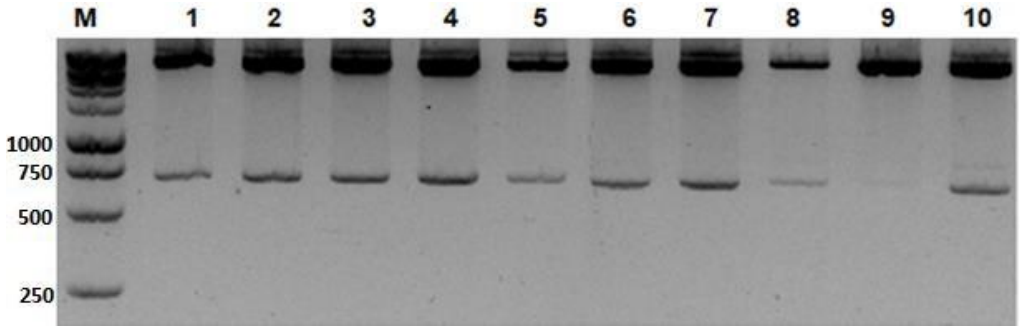

Figure 3.13: Restriction digest of Nef+pGEMT plasmids
Restriction digest of *nef*+pGEMT plasmids analysed on 1% (w/v) agarose gel. Lane M: 1 kb DNA ladder (Promega, U.S.A.); lanes 1-5: double digest of *nef*-MJ4+pGEMT plasmids with BamHI and EcoRI enzymes; lane 6-10: double digest of *nef*-40H+pGEMT plasmids with BamHI and EcoRI enzymes.

The digested HIV-1 *nef* products were electrophoresed, recovered from the agarose gel, and subsequently cloned into the pcDNA™ 3.1(+) plasmid for mammalian expression. Restriction digest of an empty pcDNA™ 3.1(+) plasmid (Figure 3.14) was carried out using restriction enzymes BamHI and EcoRI and verified on a 1% (w/v) agarose gel. The undigested pcDNA™ 3.1(+) plasmid produced three bands, corresponding to the open-circular, coiled and supercoiled confirmations on intact plasmid DNA (Figure 3.14, lane 1). Restriction digest with either the BamHI or EcoRI restriction enzyme resulted in a linearized plasmid at 5428 bp. However, BamHI could not completely digest the plasmid, resulting in two fragments in lane 3, corresponding to the linearized and supercoiled confirmation of the plasmid (Figure 3.14, lane 3). Double digestion using BamHI and EcoRI resulted in one fragment corresponding to the cut pcDNA™ 3.1(+) vector at 5405 bp, however, the smaller fragment of 23 bp in size could not be seen in the gel as it was 23 bp in size (Figure 3.14, lane 4).

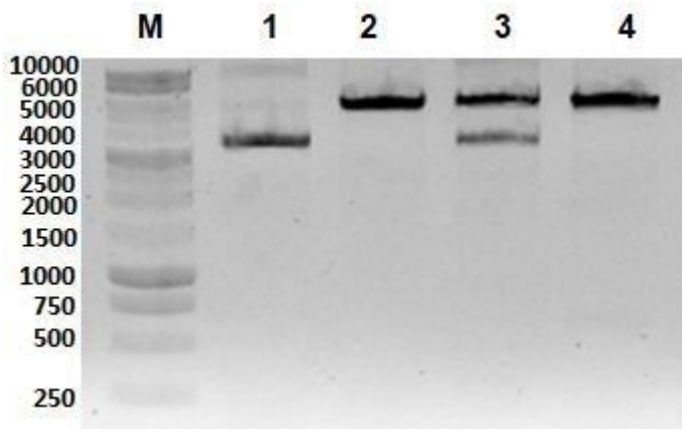

Figure 3.14: Restriction digest of pcDNA 3.1(+) vector
Restriction digest of pcDNA 3.1(+) plasmids resolved on a 1% (w/v) agarose gel. Lane M: 1 kb DNA ladder (Promega, U.S.A.); lane 1: undigested pcDNA 3.1(+) plasmid; lane 2: linearized pcDNA 3.1(+) plasmid by single digest with BamHI; line 3: linearized pcDNA 3.1(+) plasmid by single digest with EcoRI; lane 4: double digested pcDNA 3.1(+) plasmids with BamHI and EcoRI.

Post successful restriction digest, the digested products were recovered from the agarose gel and used in ligation reactions. A 1:3 ratio of plasmid to HIV-1 *nef* amplicon was used in the ligation reaction. The ligation products were transformed into chemically competent JM109 *E.coli* cells and incubated overnight on LB agar plates supplemented with ampicillin. The resulting colonies had pcDNA™ 3.1(+)- FLAG/Nef-MJ4 plasmid (Figure 3.15A) and pcDNA™ 3.1(+)-FLAG/Nef-40H plasmid (Figure 3.15B).

A

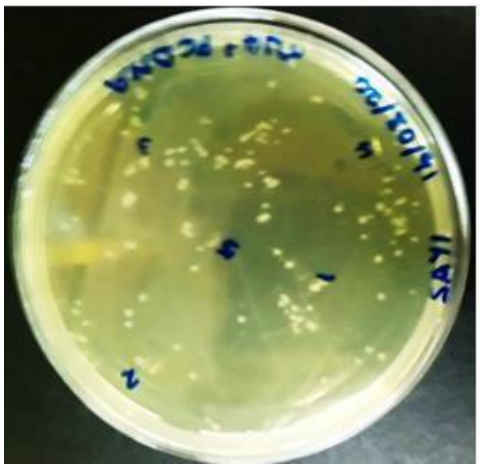

B

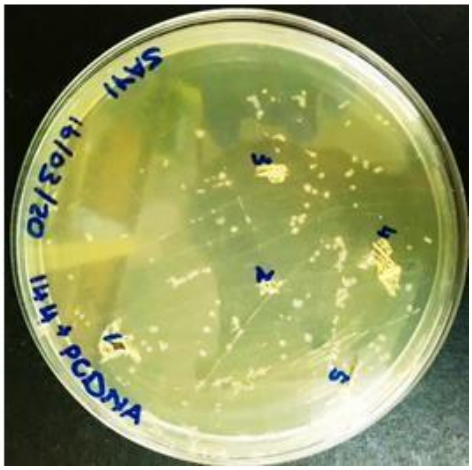

Figure 3.15: LB agar plates with pcDNA Nef-expressing construct colonies
Transformed JM109 *E.coli* colonies with (A) pcDNA™ 3.1(+)-FLAG/Nef-MJ4 plasmids and (B) pcDNA™ 3.1(+)-FLAG/Nef-40H plasmid plasmids plated on ampicillin supplement LBagar plates.

3.2.3. Confirmation of the pcDNA FLAG Tag Nef plasmids

To confirm successful ligation of HIV-1 *nef* to the pcDNA™ 3.1(+) vector, two colonies were selected from each plate and used to perform a colony PCR. A *nef*-40H PCR product, obtained from section 2.3.1 was used as a positive control (Figure 3.16, lane C). Results of the colony PCR showed successful amplification of *nef*-MJ4 (Figure 3.16, lane 1-2) and *nef*-40H (Figure 3.16, lane 3-4), thereby confirming the presence of our gene of interest.

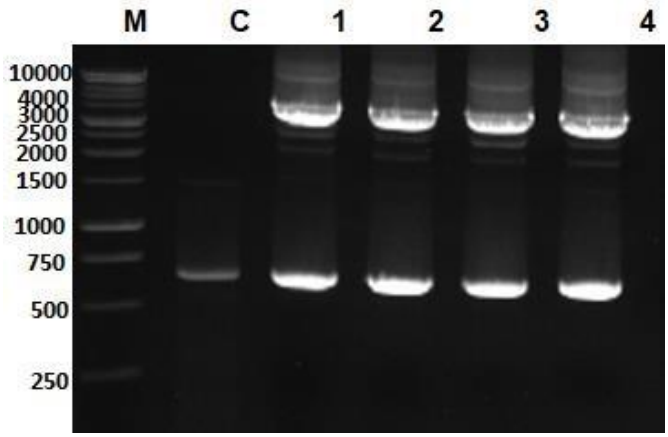

Figure 3.16: Colony PCR of transformed cells
Colony PCR of *E.coli* colonies transformed with pcDNA™ 3.1(+)-FLAG/Nef-MJ4 and pcDNA™ 3.1(+)-FLAG/Nef-40H. Lane M: 1 kb DNA ladder (Promega, U.S.A); lane C: *nef*-40H PCR product positive control; lanes 1-2: successful clones of pcDNA™ 3.1(+)-FLAG/Nef-MJ4 construct; lanes 3-4: successful clones of pcDNA™ 3.1(+)-FLAG/Nef-40H construct.

Positive colonies containing the HIV-1 *nef* genes were inoculated in fresh LB broth supplemented with ampicillin and incubated overnight. Post incubation, HIV-1 *nef* encoding plasmids were extracted from the *E.coli* culture and integrity of the plasmids confirmed by restriction digest with BamHI and EcoRI restriction enzymes. Double digestion of the pcDNA™ 3.1(+)-FLAG/Nef-40H plasmid resulted in two fragments of 5405 bp and 666 bp, corresponding to the pcDNA™ 3.1(+) expression vector and FLAG/*nef*-40H insert, respectively (Figure 3.17B).

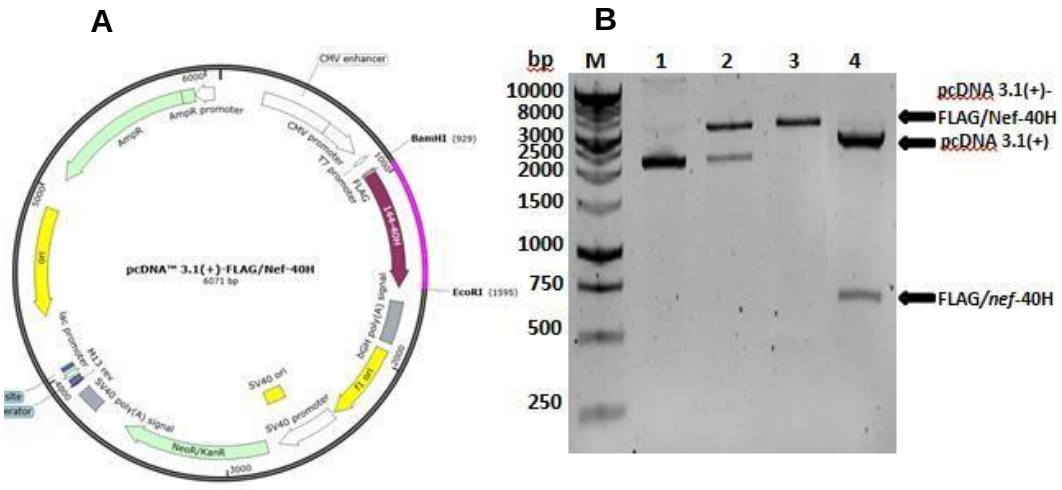

Figure 3.17: pcDNA™ 3.1(+)-FLAG/Nef-40H plasmid map and restriction agarose gel

The cloning of pcDNA™ 3.1(+)-FLAG/Nef-40H was verified using BamHI and EcoRI. (A) pcDNA™ 3.1(+)-FLAG/Nef-40H plasmid map showing site of FLAG/Nef-40H insertions into the pcDNA™ 3.1(+) expression vector. (B) Agarose gel of restriction digest of pcDNA™ 3.1(+)-FLAG/Nef-40H with either restriction enzymes EcoRI (Figure 3.1B, lane 2) or BamHI(Figure 3.1B, lane 3). Lane 4: double digestion of pcDNA™ 3.1(+)-FLAG/Nef-40H with BamHI and EcoRI resulting in fragments of 5405 bp and 666 bp corresponding to thepcDNA™ 3.1(+) expression vector and the excised FLAG/Nef-40H coding sequence. Lane M — 1 kb DNA ladder (Promega, U.S.A.). With regards to the pcDNA™ 3.1(+)-FLAG/Nef-MJ4 plasmid, double digestion with both BamHI and EcoRI resulted in two fragments of 5405 bp and 657 bp, corresponding to pcDNA™ 3.1(+) expression vector and FLAG/*nef*-MJ4 insert, respectively (Figure 3.18B).

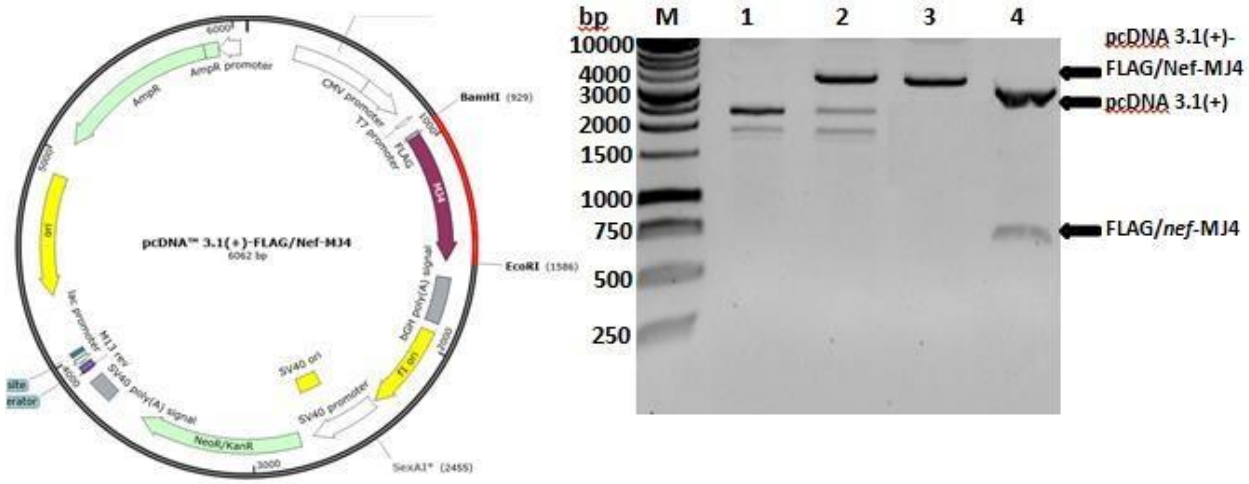

Figure 3.18: pcDNA™ 3.1(+)-FLAG/Nef-MJ4 plasmid map and restriction agarose gel

Restriction analysis of pcDNA™ 3.1(+)-FLAG/Nef-MJ4 plasmid resolved on 1% (w/v) agarose gel. (A) Plasmid map of pcDNA™ 3.1(+)-FLAG/Nef-MJ4 showing site of insertion of the FLAG/Nef-MJ4 coding sequence. (B) Restriction agarose gel of pcDNA™ 3.1(+)-FLAG/Nef- MJ4. Lane 1: undigested DNA plasmid. Lane 2: single digest with EcoRI of pcDNA™ 3.1(+)- FLAG/Nef-MJ4. Lane 3: BamHI single digestion. Lane 4: double digestion with both BamHI and EcoRI, representing pcDNA™ 3.1(+) expression vector (5405 bp) and FLAG/*nef*-MJ4 (657 bp) insert. Lane M — 1 kb DNA ladder (Promega, U.S.A.).

3.3. Site-directed mutagenesis of pcDNA™ 3.1(+)-FLAG/Nef-40Y plasmid

Site-directed mutagenesis was performed on the pcDNA™ 3.1(+)-FLAG/Nef-40H plasmid to change the Histidine amino acid at codon 40 (40H, wild-type) to a Tyrosine (40Y, mutant) residue. The substitution was done by changing the Cytosine (C) nucleotide of the

FLAG/Nef-40H coding sequence, positioned at 127 bp, toThymine (T). This resulted in the pcDNA™ 3.1(+)-FLAG/Nef-40Y plasmid. Following site-directed mutagenesis (Section 2.3.5), four colonies were selected and subjected to colony PCR with the *PO144* PCR primers (section 2.3.1) and electrophoresed on a 1% (w/v) agarose gel to confirm presence of the pcDNA™ 3.1(+)-FLAG/Nef-40Y plasmid (Figure 3.20A). A point mutation on HIV-1 *nef*-40H from C to T removes a restriction site for the enzyme *FatI.* The HIV-1 nef-40H had 3 FatI restriction sites (Figure 3.19A) while the mutant HIV-1 Nef-40Y had 2 FatI restriction sites (Figure 3.19B). FatI restriction sites were represented by the yellow box.

Figure 3.19: *FatI* restriction sites in HIV-1 nef-40 sequences

FatI restriction sites in HIV-1 *nef*-40 genes. Wild-type HIV-1 nef-40H sequence had 3 *FatI* restriction site represented by the yellow boxes (A). Mutant HIV-1 *nef*-40Y sequence had 2 *FatI* restriction sites represented by the yellow boxes (B).

To validate colonies with the mutated nucleotide 127-T, the PCR products of 673 bp in size were recovered and a restriction digest performed with the *FatI* restriction enzyme. A single restriction digest of the PCR product with *FatI* resulted in4 fragments of 396 bp, 154 bp, 118 bp and 5 bp in size for the HIV-1 nef-40H. Restriction digest of the HIV-1 nef-40Y PCR product with the FatI restriction enzyme would result in single 3 fragments of 550 bp, 118 bp and 5 bp in size. Agarose gel analysis of the FatI restriction enzyme PCR products showed either fragments approximately 550 bp in size (Figure 3.20B, lane 1 and 3) or 400 bp in size (Figure 3.20B, lane 2 and 4). Lanes 1 and 3 fragments suggested the digestion of the HIV-1 nef-40Y PCR products, while lanes 2 and 4 fragments suggested the digestion of HIV-1 nef-40H PCR products. The smaller fragments of 154 bp, 118bp and 5

bp could not be visualized on the agarose gel.

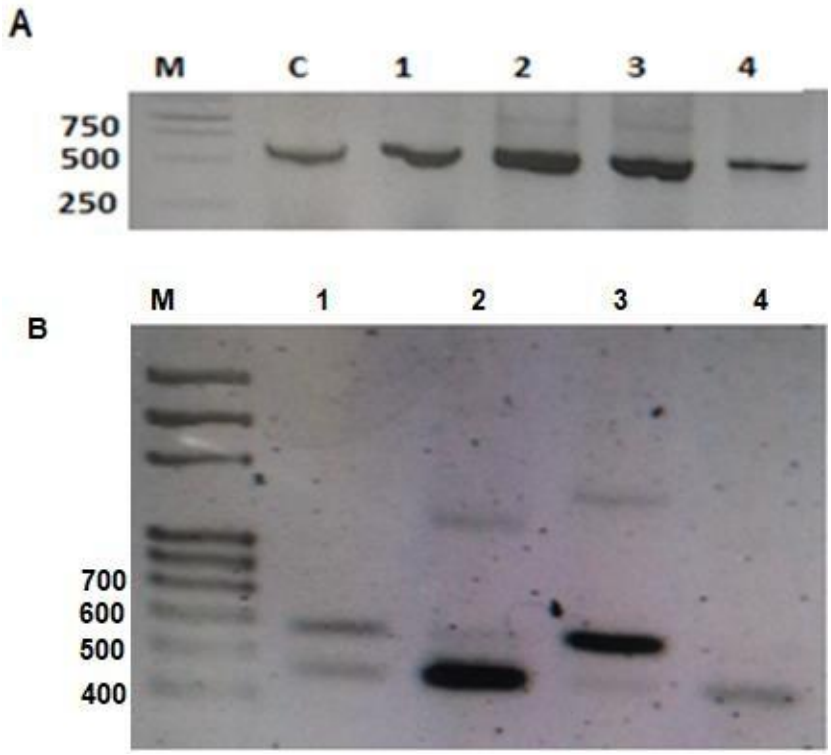

Figure 3.20: Agarose gel of colony PCR and restriction digest
PCR of successfully transformed competent *E.coli* cells with the site-directed mutagenesis reaction products (A). (A) Lane M: 1 kb DNA ladder (Promega, U.S.A). (B) 100 bp DNA ladder (Solis Biodyne, Estonia); lane C: Undigested FLAG/*nef*-40H PCR product; lane 1-4 (A): colony PCR products from the 4 picked colonies; lane 1-4 (B): Single *FatI* enzyme restriction digest product on 2% (w/v) agarose gel.

3.4. Sequencing of Nef-expressing constructs

The HIV-1 *nef* inserts in the pcDNA™ 3.1(+)-FLAG/Nef-40H, pcDNA™ 3.1(+)- FLAG/Nef-40Y and pcDNA™ 3.1(+)-FLAG/Nef-MJ4 plasmids were sequenced by Sanger sequencing at Inqaba Biotech (Pretoria, South Africa) using the PCR primers listed in Table 2.1. Sequencing data was analysed with BioEdit to confirm the *nef* sequence (Figure 3.21).

A

BamHI Flag tag

GGATCCATGGATTACAAGGACGACGATGACAAGATGGGGGGCAAATTATCCAAAAGCTGGCCTGCTGTGAGAGAAAGAATGAG
AAAAACTAAACTAGTAGAAGAGGAAGCAGGAGCAGCAGCAGTGGGAGTAGGCCCAGCATCTCAAGACTTAGCTAGACATGGTG
CACTTACAAGCAGCAACACGCCCACCAATAATCCTGATTGTGCCTGGCTGCAAGCACAAGAGGAGGATGAAGAAGTGGGCTTT
CCAGTCAGACCTCAGGTGCCTTTAAGACCAATGACTTACAAAGGAGCCTTCGATCTCGGCTTCTTTTTAAAAGAAAAGGGGGG
ACTGGATGGGTTAATTTACTCCAAGAAAAGGCAAGAAATCCTTGATTTGTGGGTCTATCACACACAAGGCTACTTCCCTGATT
GGCAGAACTACACACCTGGACCAGGGGTCAGATACCCACTGACCTTTGGATGGTGCTATAAGCTAGTACCAGTTGATCCAAGG
GAAGTGGAAGAGACCAACGAAGGAGAGGATGGCTGCCTGCTACACCCTATAAATCTGCATGGAATGGAGGATGAACACAGAGA
GATATTAAAGTGGCAATTTGACAGTCAACTAGCTCGCAGACACATAGCCCGTGAGAAACATCCGGAGTACTACAAAGACTGCT
GAGAATTC

EcoRI

B

BamHI Flag tag

GGATCCATGGATTACAAGGACGACGATGACAAGATGGGGGGCAAATTATCCAAAAGCTGGCCTGCTGTGAGAGAAAGAATGAG
AAAAACTAAACTAGTAGAAGAGGAAGCAGGAGCAGCAGCAGTGGGAGTAGGCCCAGCATCTCAAGACTTAGCTAGACATGGTG
CACTTACAAGCAGCAACACGCCCACCAATAATCCTGATTGTGCCTGGCTGCAAGCACAAGAGGAGGATGAAGAAGTGGGCTTT
CCAGTCAGACCTCAGGTGCCTTTAAGACCAATGACTTACAAAGGAGCCTTCGATCTCGGCTTCTTTTTAAAAGAAAAGGGGGG
ACTGGATGGGTTAATTTACTCCAAGAAAAGGCAAGAAATCCTTGATTTGTGGGTCTATCACACACAAGGCTACTTCCCTGATT
GGCAGAACTACACACCTGGACCAGGGGTCAGATACCCACTGACCTTTGGATGGTGCTATAAGCTAGTACCAGTTGATCCAAGG
GAAGTGGAAGAGACCAACGAAGGAGAGGATGGCTGCCTGCTACACCCTATAAATCTGCATGGAATGGAGGATGAACACAGAGA
GATATTAAAGTGGCAATTTGACAGTCAACTAGCTCGCAGACACATAGCCCGTGAGAAACATCCGGAGTACTACAAAGACTGCT
GAGAATTC

EcoRI

C

BamHI Flag tag

GGATCCATGGATTACAAGGACGACGATGACAAGATGGGGGGCAAGTGGTCAAAAAGCAGTATAGTTGGATGGCCTGCTGTAAG
AGAAAGAATAAGAACAACTGAGCCAGCGGCAGAGGGAGTAGGAGCAGCATCTCAAGACTTAGATAAACATGGAGCACTTACAA
GCAGCAACACAGCCGCCAATAATGCTGACGTTGCCTGGCTGGAACCGCAAGAGGAGGAAGGGGCGGTAGGCTTTCCAGTCAGA
CCTCAAGTACCTTTAAAACCAATGACTTATAAGGGAGCGGTGGATCTAGGCTTCTTTTTAAAAGAAAAGGGGGGACTGGAAGG
GTTAATTTACTCTAAGAAAAGGCAAGAGATCCTTGATTTGTGGGTCTATCACACACAAGGCTACTTCCCTGACTGGCAAAACT
ACACACCGGGACCAGGGATCACATACCCACTGACCTTTGGATGGCCATTCAAGCTAGTGCCAGTTGACCCAAGGGAAGTAGAA
GAGGCCAACAATGGAGAGAACAACTGTTTGCTACATCCTATGAGCCAGCATGGAATGGATGATGAAGAAAGAGAAGTATTAAC
ATGGAAGTTTGACAGTCACCTAGTACACAGACCCATGGCCCGCGAGATACATCCGGAGTATTACAAAGACTGCTGAGAATTC

EcoRI

Figure 3.21: HIV-1 *nef* sequencing results
Sequences of Nef inserts obtained from sequencing (A) pcDNA™ 3.1(+)-FLAG/Nef-40H, (B) pcDNA™ 3.1(+)-FLAG/Nef-40Y and (C) pcDNA™ 3.1(+)-FLAG/Nef-MJ4 using PCR primers. Red box: *Bam*HI restriction site; yellow box: *Flag* tag; blue box: *Eco*RI restriction site. HIV-1 nef genes appeared to be rich in A/T residues.

To ensure the presence of only amino acid mutation of the 40H residue to 40Y in pcDNA™ 3.1(+)-FLAG/Nef-40, a multiple sequence alignment was performed with the translated HIV-1 *nef* gene sequences (Figure 3.22). HIV-1 Nef-MJ4 was used a HIV-1 subtype C reference protein. Results of the multiple sequence alignment of the HIV-1 Nef amino acid sequences showed that the mutagenesis reaction did not cause any unwanted protein

sequence alterations between the HIV-1 Nef-40H and HIV-1 Nef-40Y clones. This therefore showed evidence of a good background for downstream application in which the proteins were to be compared against each other.

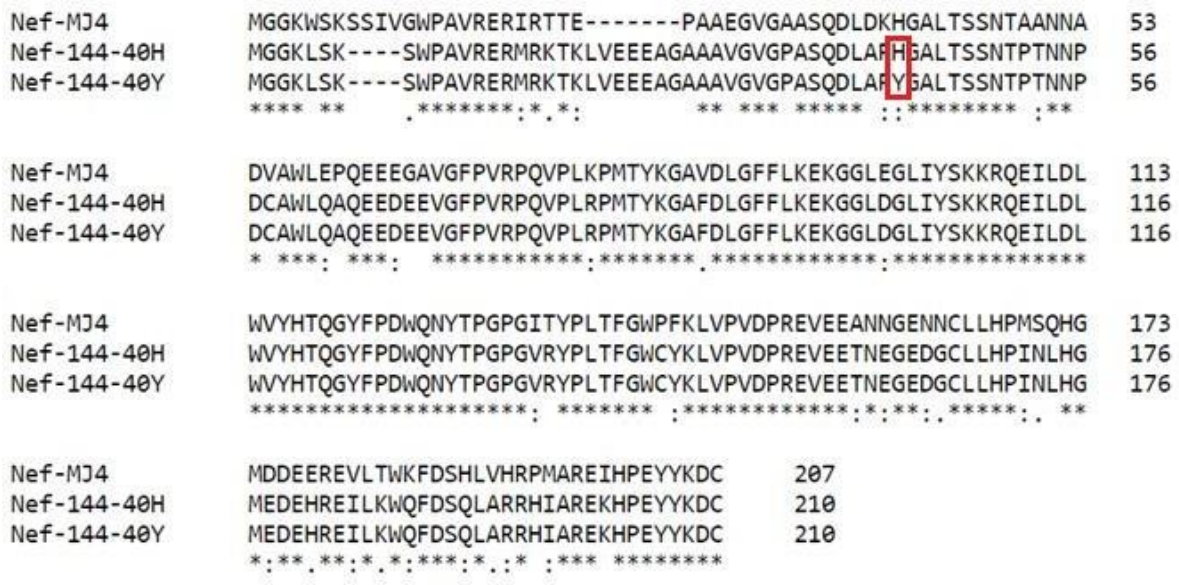

Figure 3.22: Multiple sequence alignment of Nef proteins
Multiple sequence alignment of HIV-1 Nef proteins. Protein sequences of translated sequencing data from the HIV-1 Nef-expressing plasmids were used to perform multiple sequence alignment. The amino acid substitution after the mutagenesis reaction from 40H to 40Y is presented in the red box. Identical residues between the three proteins were represented by '*', whilst ':' represented the conserved substitution and '.' represented the semi-conserved substitution that has occurred between the three proteins. The multiple sequence alignment was performed on ClusterW online tool (https://www.ebi.ac.uk/Tools/msa/clustalo/).

3.5. Expression of recombinant HIV-1 Nef proteins

To confirm the ability of the constructed HIV-1 *nef* plasmids to express HIV-1 Nef proteins, HEK293T cells were transfected with the HIV-1 *nef* plasmids and HIV-1 Nef production confirmed by Western blot analysis using anti-Flag antibodies. Results from the SDS-PAGE showed increased expression of a protein of approximately 24 kDa (Figure 3.22A), in agreement with the expected size for this protein (27-35 kDa) (Geyer *et al*., 2001). The negative control (empty pcDNA™ 3.1(+) plasmid transfected with HEK293T cells)

showed bands of similar size of the HIV-1 Nef proteins but there was no corresponding band on the Western blot analysis. Western blot analysis confirmed the protein at 24 kDa to be HIV-1 Nef (Figure 3.23B). Faint bands of greater than 24 kDa were equally observed on the Western blot, which could be a result of high antibody concentration or non-specific binding due to insufficient blocking of non-specific sites.

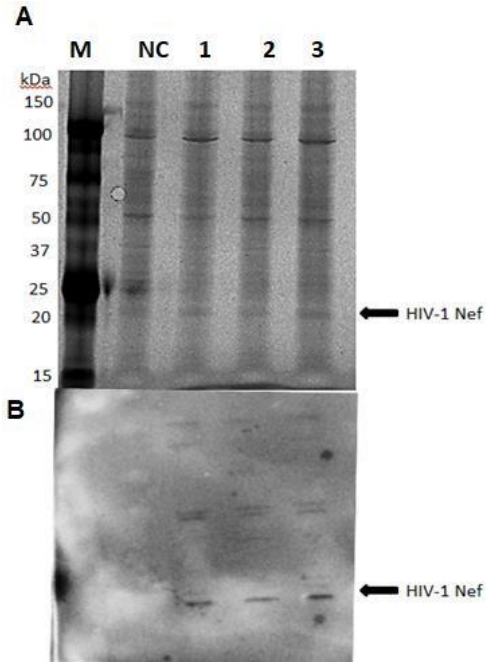

Figure 3.23: Expression of recombinant HIV-1 Nef proteins
HIV-1 Nef proteins were expressed in HEK293T cells transfected with Flag-tagged Nef plasmids. SDS-PGE (10%) and Western blot analyses of the expression of the recombinant HIV-1 Nef proteins. Lane M: Precision plus protein standard in kDa; lane NC: crude lysate of cells transfected with the empty pcDNA™ 3.1(+) plasmid; lane 1: total cell extract of cells transfected with the pcDNA™ 3.1(+)-FLAG/Nef-MJ4 plasmid; lane 2: total cell extract of cells transfected with pcDNA™ 3.1(+)-FLAG/Nef-40H plasmid and lane 3: total cell extract of cells transfected with pcDNA™ 3.1(+)-FLAG/Nef-40Y plasmid.

3.6. Maintenance and transfection of endothelial cells

This study required maintenance of Human Pulmonary Microvascular Endothelial Cells (HPMECs) in supplemented endothelial cell medium (Section 2.3.6) and treatment of cells with TNF-α for 6 hours prior to transfection to activate the endothelial cells. To test the cells' ability to grow in supplemented endothelial cell medium in the presence of TNF-α, the cells

were incubated for 24 hours with (Figure 3.24, A1 top) and without TNF-α (Figure 3.24, A2 top). The confluency of endothelial cells grown in the presence of TNF-α following a 24-hour incubation period (Figure 3.24, A1 bottom) seemed similar to that of the endothelial cells cultured in the absence of TNF- α (Figure 3.24, A2 bottom). Transfection efficiency of the available transfection reagents, Lipofectamine LTX and Polyethyleneimine, was tested by transfecting HPMECs with the pSelect-GFPZeo- mcs plasmid (Figure 3.24B). Fluorescence seemed similar in cells transfected with the plasmid using either the Lipofectamine LTX reagent (Figure 3.24, B1) or PEI (Figure 3.24, B2), thus suggesting similar transfection efficiency for the transfection reagents under the same conditions.

A1 **A2**

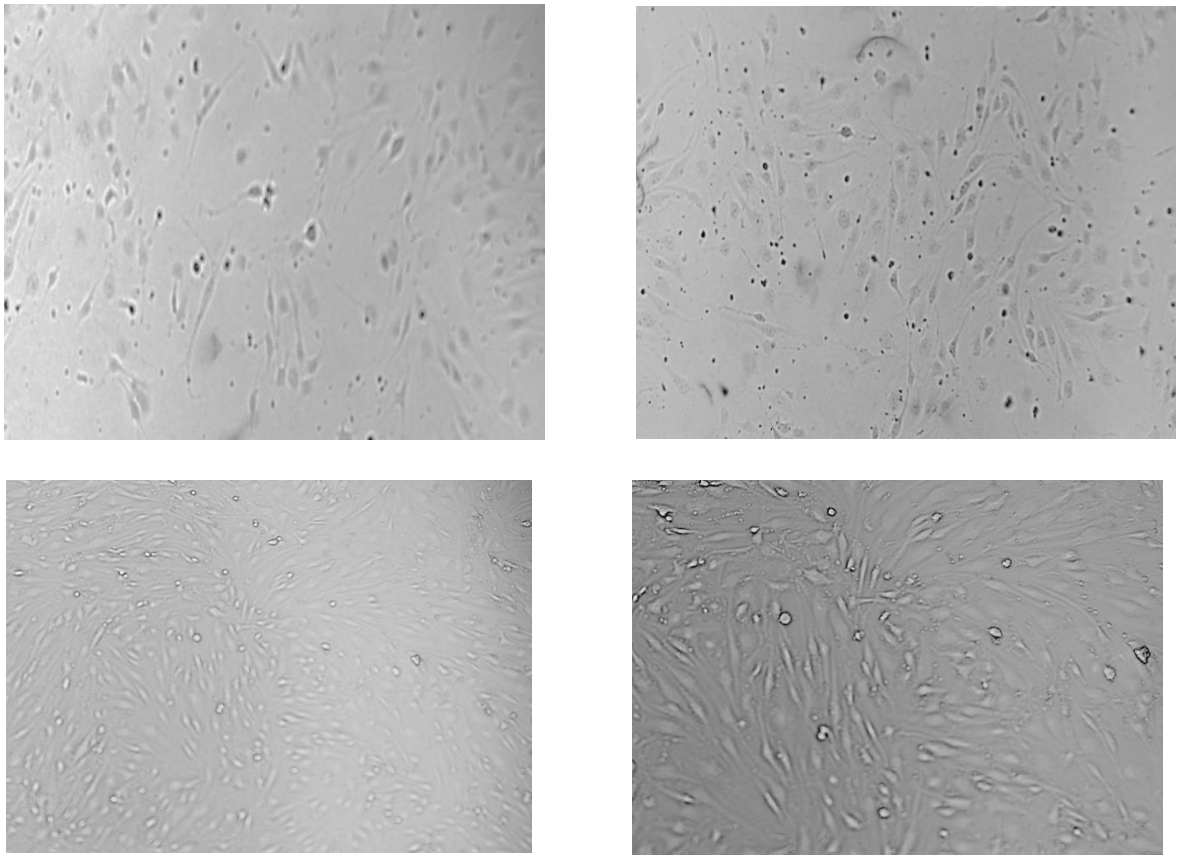

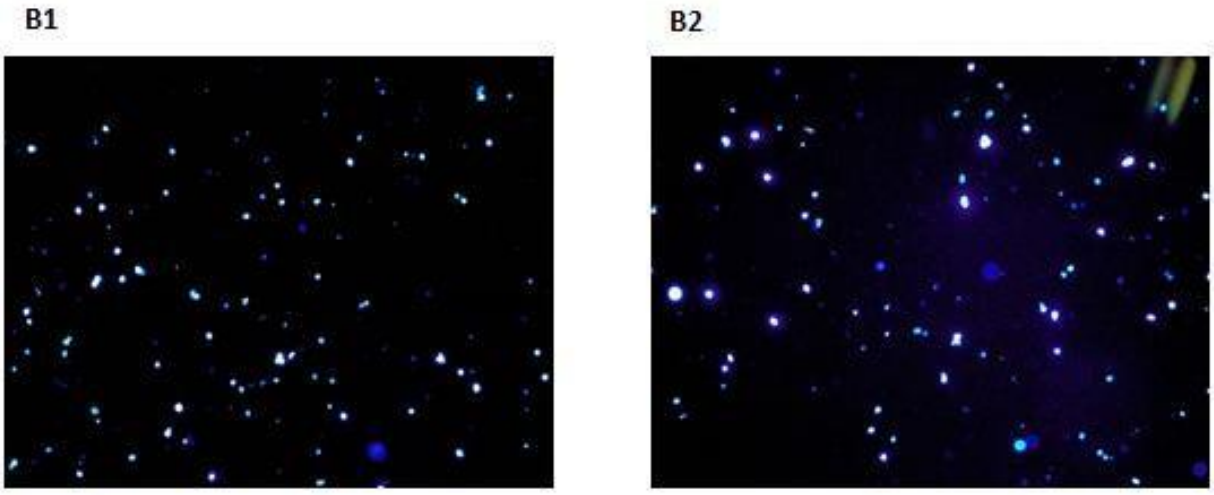

Figure 3.24: Maintenance and transfection of HPMEC cells
The growth rate of HPMEC in supplemented endothelial cell growth medium with TNF-α was compared to the growth of untreated cells (A). Confluency of cells (A1 and A2 top) before theTNF-α treatment. The confluency of TNF-α treated cells (A1 bottom) was similar to the untreated cells (A2 bottom). Transfection efficiency of the transfection reagents used was compared (B). Visually, Lipofectamine LXT reagent (B1) had similar transfection efficiency as PEI (B2) when GPF fluorescence was compared in cells transfected with the pSelect- GFPZeo-mcs plasmid using the two transfection reagents.

3.7. Expression of recombinant HIV-1 Nef proteins

3.7.1. Expression of HIV-1 Nef-40 proteins

Following transfection of both the TNF-α treated and untreated HPMECs with the pcDNA™ 3.1(+)-Flag/Nef-40H (Figure 3.25, A and B) and pcDNA™ 3.1(+)-Flag/Nef- 40Y plasmids (Figure 3.25, C and D), expression of the recombinant Flag tagged HIV-1 Nef proteins was accessed by SDS-PAGE and confirmed by Western blot using anti-Flag antibodies (Figure 3.25). Analysis of crude cell extracts by SDS- PAGE showed increased expression of a protein of approximately 24 kDa over time, with a peak intensity observed at 48 hours. As a negative control, TNF-α treated and untreated HPMECs were transfected with an empty pcDNA™ 3.1(+) plasmid. Under this experimental condition, analysis of crude lysate showed no proteins to be expressed of approximately 24 kDa. This therefore suggested the 24 kDa protein expressed by the HPMECs transfected with the HIV-1 Nef expressing plasmid to be the recombinant HIV-1 Nef proteins. Western blot with the peptide specific

Flag antibodies yielded positive bands, thus confirming expression of the Flag tagged recombinant HIV-1 Nef proteins. The expression of HIV-1 Nef proteins seemed notto be affected by the treatment of TNF-α when compared to the untreated HPMECs.

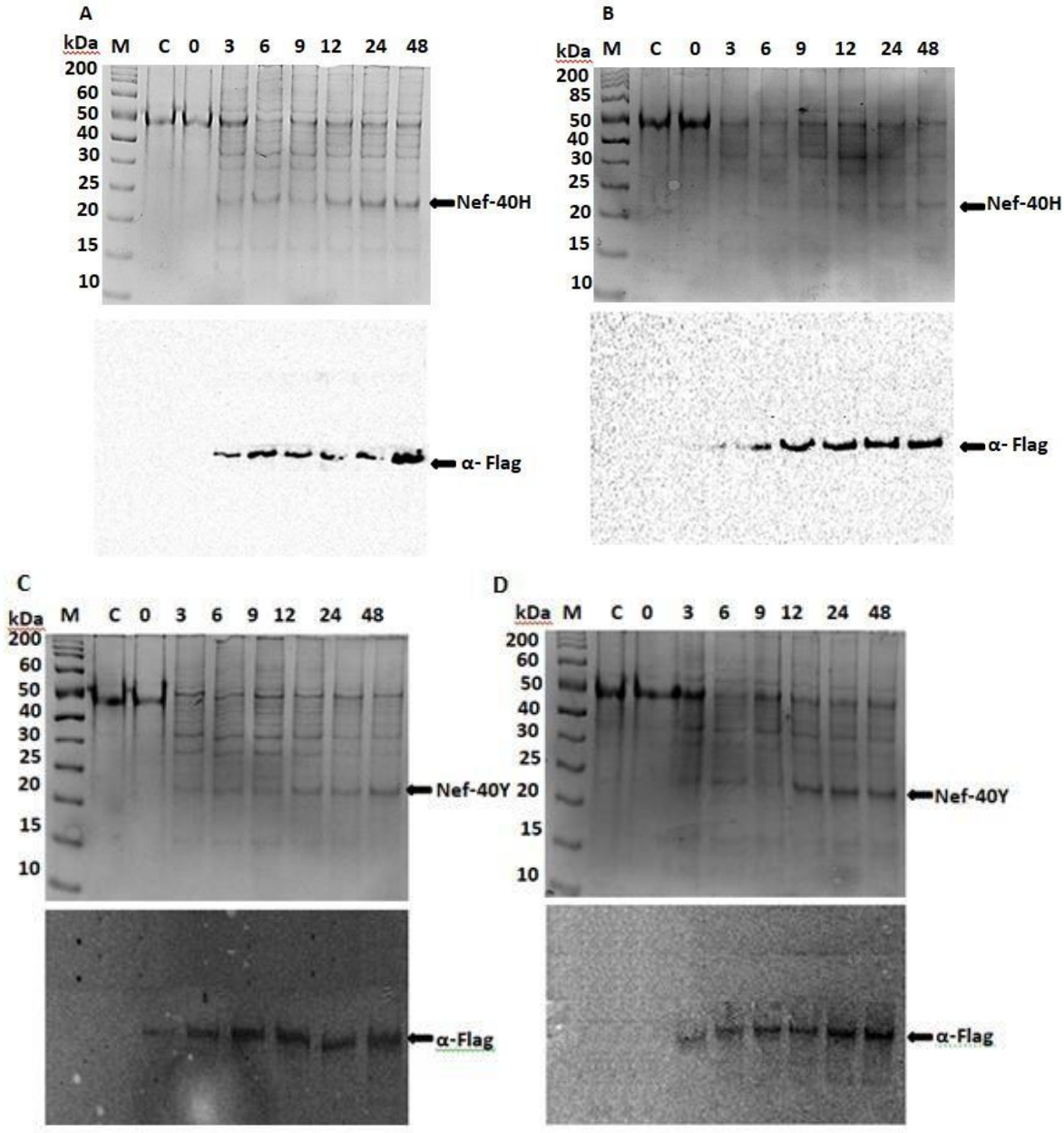

Figure 3.25: Expression of recombinant HIV-1 Nef-40 proteins
Flag-tagged HIV-1 Nef-40 proteins were expressed in HPMECs transfected with pcDNA™ 3.1(+)-Flag/Nef-40H and pcDNA™ 3.1(+)-Flag/Nef-40Y plasmids. SDS-PAGE (12%) and Western blot analyses of the expression of recombinant HIV-1 Nef-40H in HPMECs treated with TNF-α (A) and (B) untreated HPMECs. The expression of HIV-1 Nef-40Y proteins in TNF-α treated (C) and untreated (D) HPMECs were analysed by SDS-PAGE and Western blot. Lane M: Protein standard in kDa shown on the left-hand side; lane C: total cell lysate of cells transfected with empty with pcDNA™ 3.1(+) plasmid; lane 0,3 ,6 ,9 ,12 ,24 ,48: total cell lysate harvested at 0, 3, 6, 9, 12,24 and 48 hours post transfection.

3.7.2. Expression of recombinant HIV-1 Nef-MJ4

The HPMECs were transfected with the pcDNA™ 3.1(+)-Flag/Nef-MJ4 plasmid and expression of HIV-1 Nef-MJ4 assessed by SDS-PAGE and confirmed by Western blot using peptide specific antibodies for detection of Flag tagged proteins. Analysis of the SDS-PAGE showed a band of approximately 24 kDa, of which the intensity increased over time (Figure 3.26). No bands were observed at approximately 24 kDa in HPMECs transfected with an empty pcDNA™ 3.1(+) plasmid (Figure 3.25, lane NC). This suggests that the bands observed around 24 kDa were HIV-1 Nef-MJ4 proteins. Western blot analysis confirmed expression of the Flag tagged recombinant HIV-1 Nef-MJ4 proteins. The highest expression was observed at 48 hours for the both TNF-α treated HPMECs (Figure 3.26A) and untreated cells (Figure 3.25B). The expression of HIV-1 Nef-MJ4 proteins seemed not to be affected the treatment of TNF-α when compared to the transfected TNF-α untreated HPMECs.

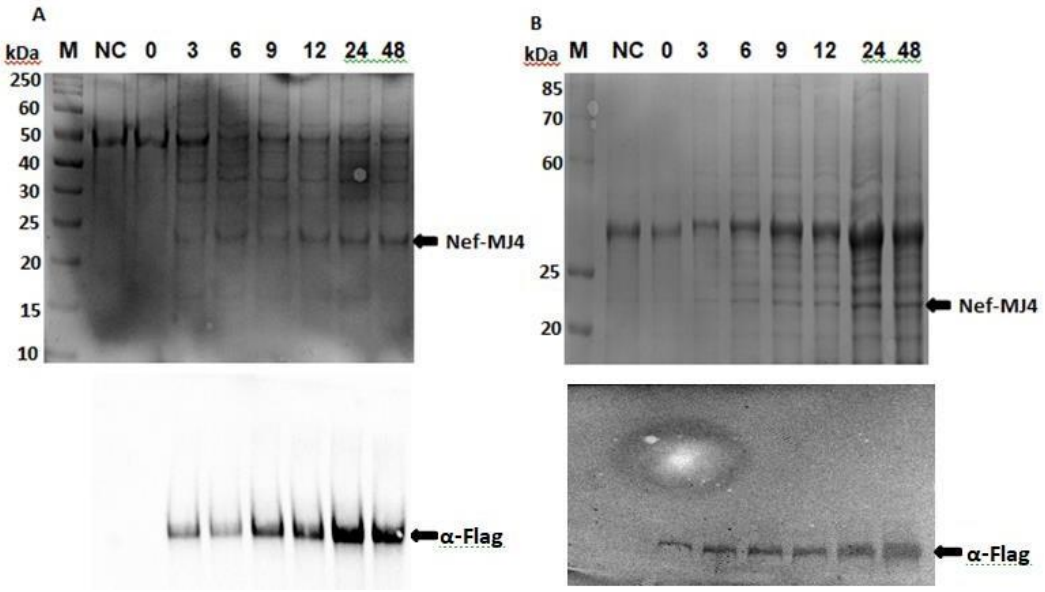

Figure 3.26: Expression of recombinant Nef-40Y expression
FLAG-tagged HIV-1 Nef-MJ4 was expressed in HPMEC cells transfected with pcDNA™ 3.1(+)-FLAG/Nef-MJ4 plasmid. SDS-PAGE (12%) and Western blot analyses of the expression of recombinant Nef-MJ4 in HPMEC cells treated with TNF-α (A) and (B) untreated HPMECs. Lane M: Protein standard in kDa shown on the left-hand side; lane C: total cell lysate of cells transfected with empty with pcDNA™ 3.1(+) plasmid; lane 0, 3, 6, 9,

12, 24, 48: total cell lysate harvested at 0, 3, 6, 9, 12, 24 and 48 hours post transfection.

3.8. Effect of HIV-1 Nef proteins on ICAM-1 and VCAM-1expression

3.8.1. Gene expression profiling of adhesion molecules

The ability of the HIV-1 Nef proteins to activate endothelial cells was evaluated by assessing expression of the biomarkers of endothelial activation, intercellular adhesion molecule-1 (ICAM-1) and vascular cell adhesion molecule-1 (VCAM-1), in HPMECs following transfection with Nef plasmids. The HPMECs were cultured for 6 hours in the presence and absence of TNF-α prior to transfection with Nef expressing plasmids (Section 2.3.6). The cells and culture supernatants were harvested at different time points after transfection, total RNA extracted from the cells and used downstream for cDNA synthesis. A reverse-transcriptase quantitative polymerase chain reaction (RT-qPCR) was performed to assess gene expression levels of ICAM-1 and VCAM-1 by the HPMECs.

Firstly, it was important to establish the expression levels of the adhesion molecules, ICAM-1, and VCAM-1, in the HPMECs before and after cell activation with TNF-α (Figure 3.27). The RT-PCR of non-transfected TNF-α treated and untreated cells was performed to establish ICAM-1 and VCAM-1 (Figure3.27A) controls. The RT- PCR analysis of β-actin was used to normalize the data. Real-time PCR analysiswith a threshold of 0.03 showed increased expression of ICAM-1 and VCAM-1 in the TNF-α treated cells by a fold change of 8.34 and 4.26, respectively, compared to the untreated cells (Figure 3.27, B2; B2).

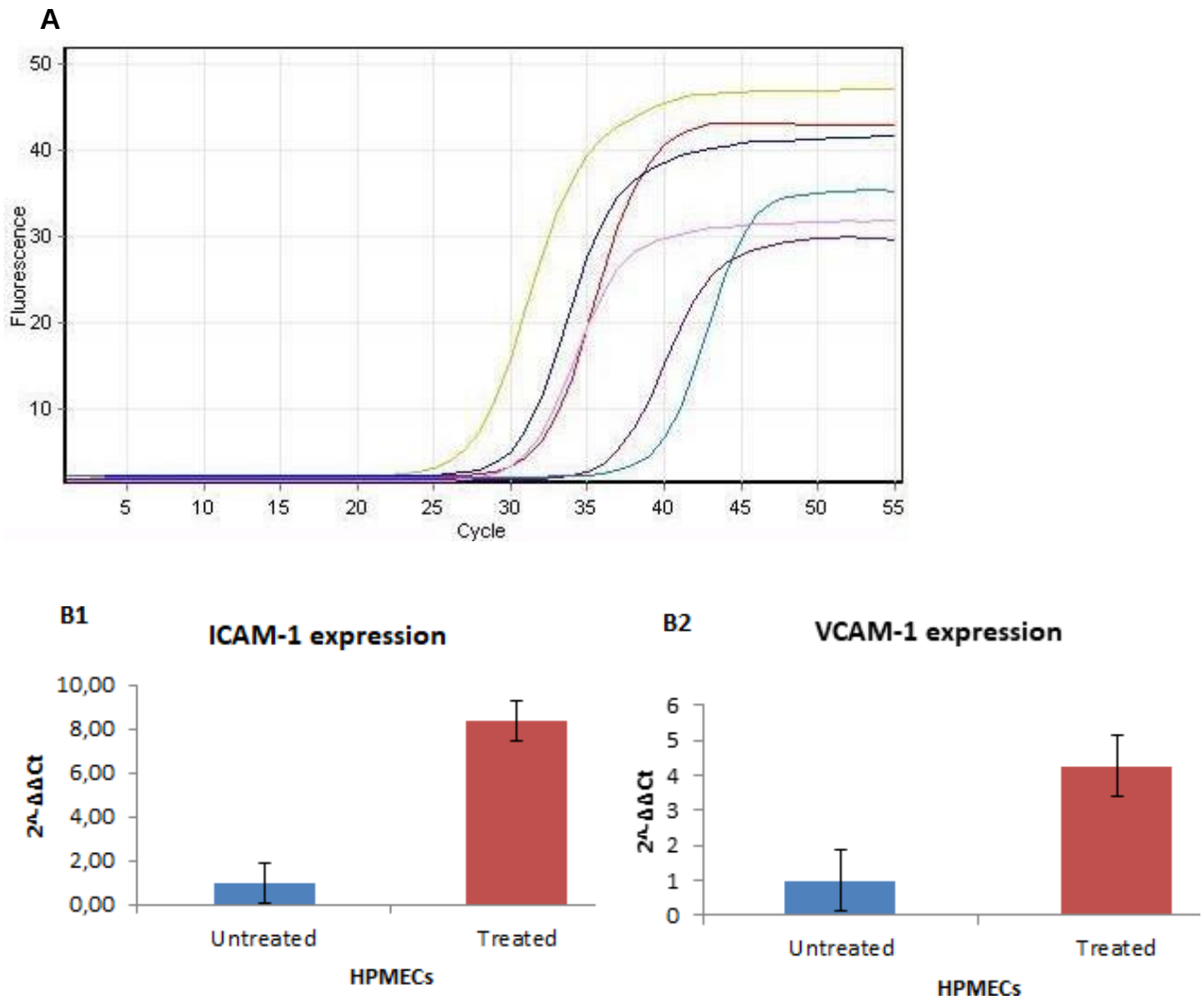

Figure 3.27: Quantitative real-time PCR of ICAM-1 and VCAM-1 expression

RT-PCR of ICAM-1 and VCAM-1 expression in non-transfected untreated HPMECs (A). (B1) Comparison of ICAM-1 expression in TNF-α untreated cells and TNF-α treated cells. (B2) Comparison of VCAM-1 expression in TNF-α untreated cells and TNF-α treated cells. Error bars represents standard deviation obtained from duplicate assays.

To assess differences in ICAM-1 mRNA expression levels following Nef-induced endothelial activation, ICAM-1 mRNA expression following transfection of HPMECs with the wildtype strains, HIV-1 Nef-40H and HIV-1 Nef-MJ4, were compared against each other. In addition, ICAM-1 mRNA expression following transfection of HPMECs with the Nef-40H wildtype strain was compared to that of the mutant strain, HIV-1 Nef-40Y. Results from the RT-PCR analysis performed showed a difference in ICAM-1 mRNA expression levels in the

untreated HPMECs transfected with the HIV-1 Nef-40H plasmid compared to cells transfected with either HIV-1 Nef-40Y or Nef-MJ4 (Figure 3.28, B1). The ICAM-1 mRNA expression in HIV-1 Nef-40H untreated HPMECs was greater than the expression in HIV-1 Nef-40Y cells at hours 3, 6, 9, 24 and 48(Figure 3.28, B1). However, the expression of ICAM-1 in HIV-1 Nef-40Y transfected untreated cells was greater than that of HIV-1 Nef-40H at 12 hours (Figure 3.28, B1). The ICAM-1 mRNA expression levels in HIV-1 Nef-MJ4 untreated cells were higher than in HIV-1 NEF-40Y cells after hours 6 and 12 (Figure 3.28, B1).

Analysis of VCAM-1 mRNA expression levels in the untreated HPMECs transfected with HIV-1 Nef-MJ4 showed a difference in expression compared to cells transfected with either HIV-1 Nef-40H or Nef-40Y (Figure 3.28, B2). The VCAM-1 mRNA levels in Nef-MJ4 untreated HPMECs increased in a time-dependent manner from hours 0 to 12, following which expression decreased at 24 and 48 hours. The untreated HIV- 1 Nef-40Y cells expressed more VCAM-1 mRNA at a greater level than HIV-1 Nef- 40H in a time dependent manner from hours 3 to 24 (Figure 3.28, B2). However, after 48 hours, VCAM-1 expression in HIV-1 Nef-40H was higher than in Nef-40Y cells (Figure 3.28, B2). Although the expression of VCAM-1 mRNA in HIV-1 Nef-40H untreated cells was lower than HIV-1 Nef-40Y and Nef-MJ4 cells, the expression levels were always above the negative control except for hour 6 (Figure 3.28, B2).

The expression of ICAM-1 and VCAM-1 mRNA in HIV-1 Nef expressing untreated HPMECs was higher than the expression of the biomarkers in untransfected cells (p<0.0001). Comparison of ICAM-1 mRNA expression in untreated Nef-40H cells was higher than in Nef-40Y cells (p<0.0001). The ICAM-1 mRNA levels in the HIV-1 Nef-40H variant were

higher than the levels observed in the HIV-1 Nef-MJ4 expressing untreated cells (p<0.001). Multiple comparisons of VCAM-1 mRNA expression in HIV-1 Nef-40H versus Nef-40Y demonstrated that HIV-1 Nef-40H variant had a significantly lower expression than the HIV-1 Nef-40Y variant (p<0.0001), HIV-1 Nef-40H VCAM-1 mRNA expression was lower than in HIV-1 Nef- MJ4 expressing cells (p<0.0001). The expression of VCAM-1 mRNA expression in the HIV-1 Nef-MJ4 variant was significantly higher compared to the expression in the HIV-1 Nef-40Y expressing untreated cells (p<0.0001).

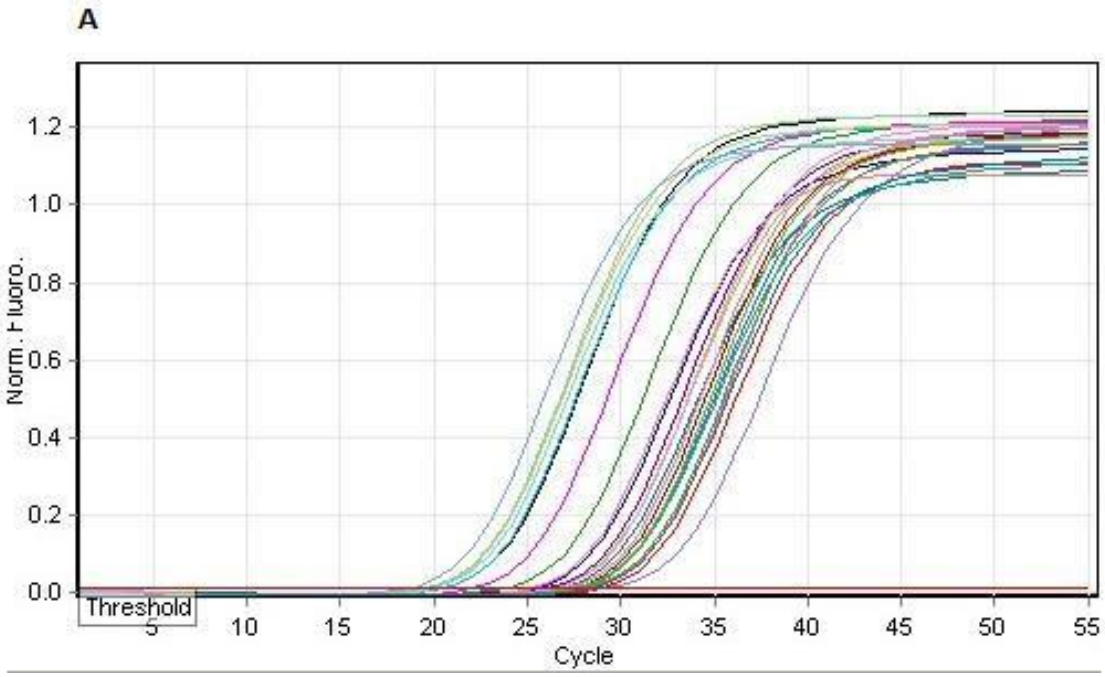

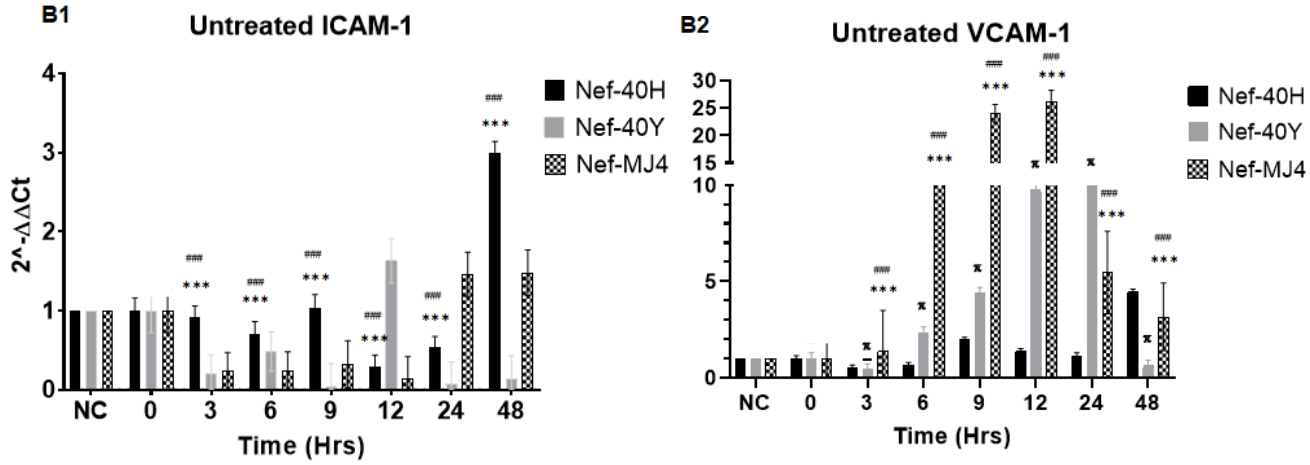

Figure 3.28: Quantitative real-time PCR of ICAM-1 and VCAM-1 expression
RT-PCR of ICAM-1 expression in untreated HPMECs with the HIV-1 Nef proteins (A). (B1) ICAM-1 expression in untreated HPMECs expressing the HIV-1 Nef proteins. (B2) VCAM-1 expression in untreated HPMECs expressing HIV-1 Nef proteins. (B1) ***p<0.0001 compared with HIV-1 Nef-40Y and ###p<0.0001 compared with HIV-1 Nef-MJ4. (B2) ***p<0.0001 compared with HIV-1 Nef-40H, ###p<0.0001 compared with HIV-1 Nef- 40Y and *p<0.0001 compared to HIV-1 Nef-40H. Error bars represent standard deviation obtained from duplicate assays.

Relative gene expression levels of ICAM-1 in the activated transfected HPMECs showed an increased expression of ICAM-1 with HIV-1 Nef-40H compared to either HIV-1 Nef-40Y or Nef-MJ4 transfected cells (Figure 3.29, B1). The expression of ICAM-1 mRNA levels was greater in HIV-1 Nef-MJ4 treated HPMECs than Nef-40Y cells from hours 9, 12 and 24 (Figure 3.29, B1). However, the ICAM-1 expression in HIV-1 Nef-40Y treated cells was greater than HIV-1 Nef-40H cells at hour 3 (Figure 3.29, B1). The ICAM-1 mRNA expression levels in all transfected treated cells were always below the levels of the negative control and 0-hour cells. Comparison of the ICAM-1 mRNA expression between the HIV-1 Nef expressing treated cells were statistically not significant.

The expression of VCAM-1 increased in a linear fashion within the HIV-1 Nef-MJ4 transfected activated HPMECs compared to either HIV-1 Nef-40H or Nef-40Y. The VCAM-1 expression in HIV-1 Nef-MJ4 decreased after 24 hours (Figure 3.29, B2). At 3 hours, the

expression levels of VCAM-1 mRNA in HIV-1 Nef-40Y and Nef-MJ4 were greater than in HIV-1 Nef-40H treated cells. The HIV-1 Nef-40Y expressing treated HPMECs had greater expression of VCAM-1 mRNA than the HIV-1 Nef-40H cells after hours 3, 6, 12 and 48 hours. However, HIV-1 Nef-40H transfected cells had higher expression of VCAM-1 mRNA expression than HIV-1 Nef-40Y at 9 and 24 hours (Figure 3.29, B2). The HIV-1 Nef-MJ4 transfected treated cells had significantly higher (p<0.0001) levels of VCAM-1 mRNA expression than HIV-1 Nef-40H and Nef- 40Y expressing treated HPMECs at all time points post transfection (Figure 3.29, B2). The mRNA expression levels of ICAM-1 and VCAM-1 were significantly higher in HIV-1 Nef-MJ4, Nef-40H and Nef-40Y transfected treated cells compared to their respective negative controls (p<0.01). The VCAM-1 mRNA expression with the HIV-1 Nef-40H variant was higher than with the HIV-1 Nef-40Y variant (p<0.01). The HIV-1 Nef-MJ4 variant significantly increased the expression of VCAM-1 mRNA compared to the HIV-1 Nef-40H variant (p<0.0001). The VCAM-1 mRNA expression was considerably lower with the HIV-1 Nef-40Y compared to the HIV-1 Nef-MJ4 expressing treated HPMECs (p<0.0001).

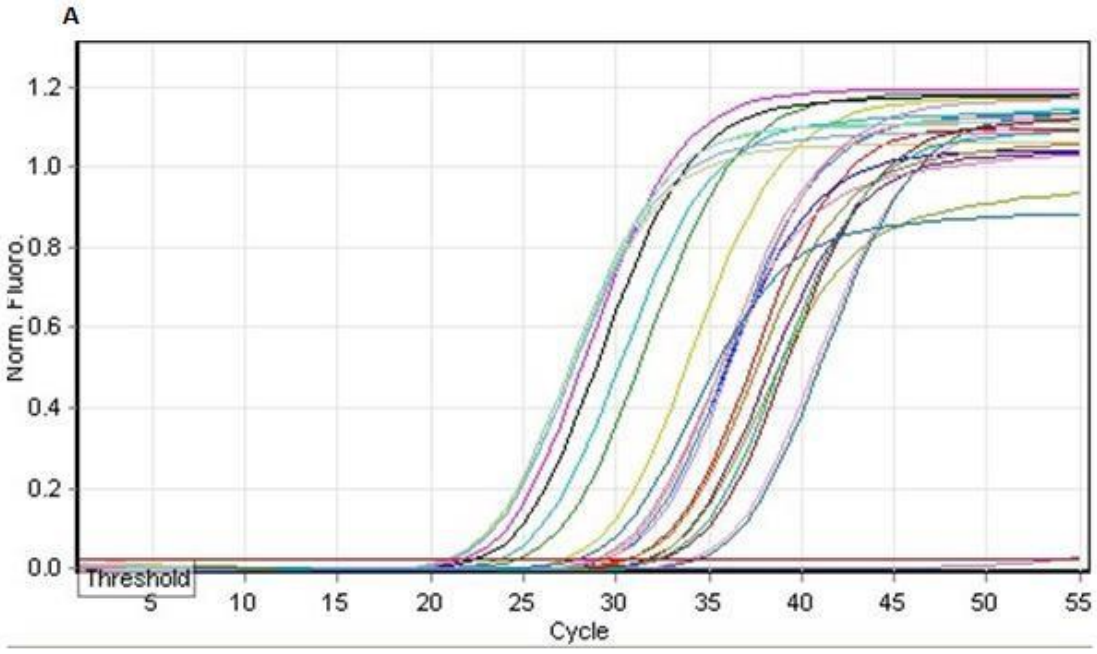

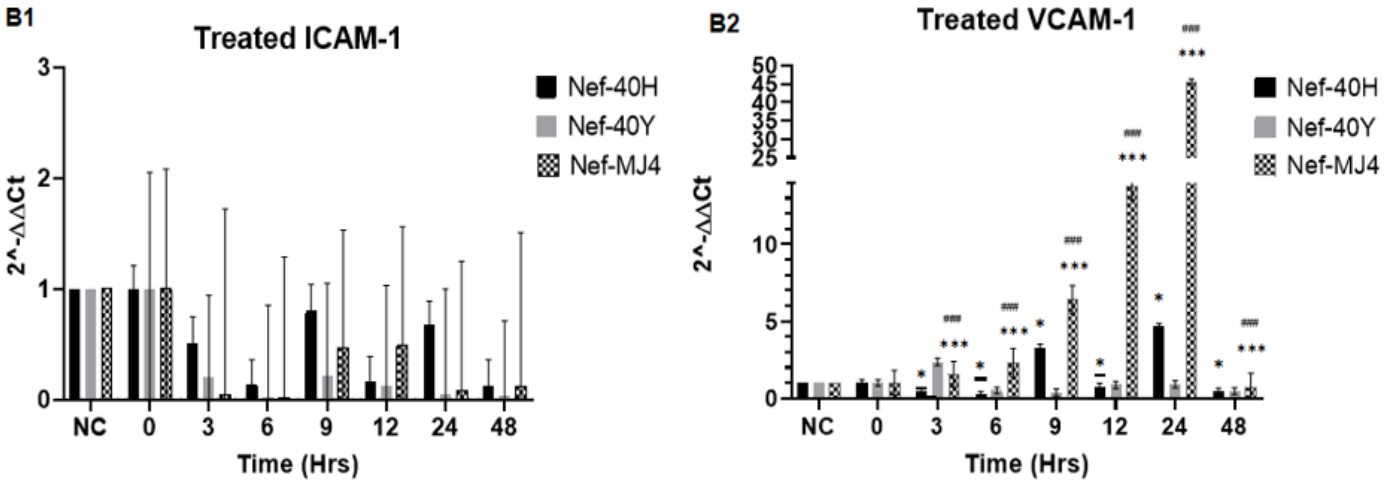

Figure 3.29: Quantitative real-time PCR of ICAM-1 and VCAM-1 expression
RT-PCR of ICAM-1 expression in TNF-α treated HPMECs with the HIV-1 Nef proteins (A). (B1) ICAM-1 expression in treated HPMECs expressing the HIV-1 Nef proteins. (B2) VCAM- 1 expression in treated HPMECs expressing HIV-1 Nef proteins. ***p<0.0001 compared with HIV-1 Nef-40H treated cells, ###p<0.0001 compared with HIV-1 Nef-40Y and *p<0.05 compared with HIV-1 Nef-40Y. Error bars represents standard deviation obtained from duplicate assays.

The time dependent study was used to compare mRNA expression of adhesion molecules following 48hrs transfection of HPMECs with Nef variants in order to identify the timepoint of optimal ICAM-1 and VCAM-1 mRNA expression. Optimal mRNA expression levels of ICAM-1 and VCAM-1 was observed at 24 hours post transfection (Figure 3.27 and 3.28). The ICAM-1 and VCAM-1 mRNA expression levels from the TNF-α treated and untreated HPMECs were compared against each other. It was established that TNF-α did in fact significantly increase (p<0.001) the expression of ICAM-1 in treated cells compared to untreated cells (Figure 3.26A). However, HIV-1 Nef-40H in untreated cells could not increase ICAM-1 mRNA expression levels above that of the untransfected untreated HPMECs. The combination of HIV-1 Nef-40H and TNF-α had no cooperative relationship that induced expression of ICAM-1 mRNA levels, as it was not of significant difference (3.30A). Similarly, to the effects of HIV-1 Nef-40H, HIV-1 Nef-40Y could not increase the expression levels of ICAM-1 above the levels of the negative control in untreated HPMECs. In TNF-α treated HPMECs, the HIV-1 Nef-40Y variant induced the expression of ICAM-1

mRNA, but to no statistical significance (Figure 3.30B). The ICAM-1 mRNA expression levels of HIV-1 Nef-MJ4 expressing treated cells were lower than the levels in the negative control cells (Figure 3.30C). The HIV-1 Nef-MJ4 variant and TNF-α had no synergistic relationship to increase expression of ICAM-1.

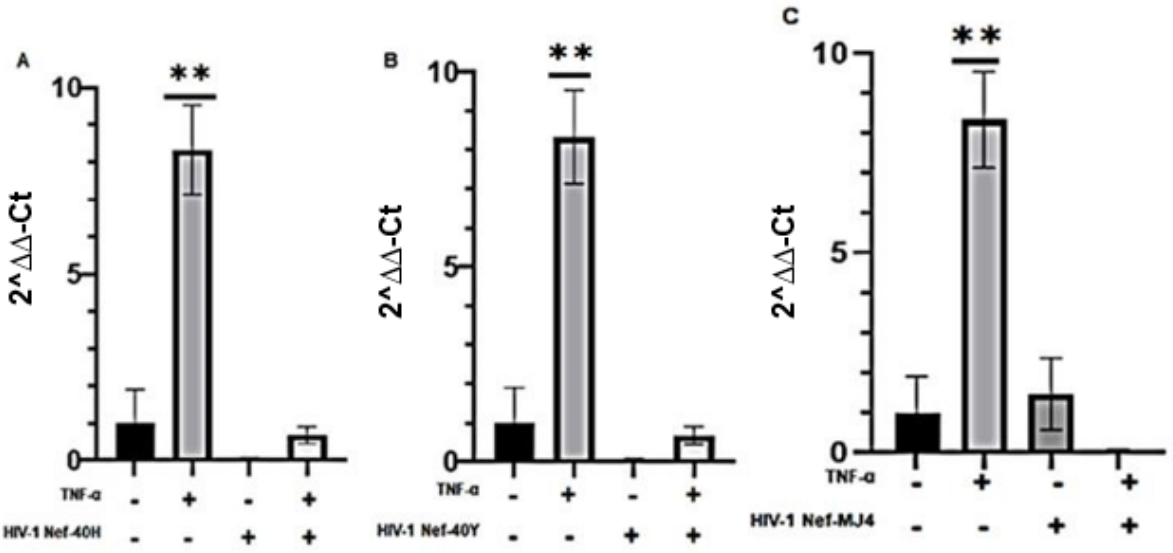

Figure 3.30: ICAM-1 mRNA Expression
The ICAM-1 mRNA expression levels after 24 hours post transfection in (A) HIV-1 Nef-40H, (B) HIV-1 Nef-40Y and (C) HIV-1 Nef-MJ4 expressing HPMECs. Statistical significance was established by comparing the cells against the untransfected untreated cells; ***p*<0.005 compared with untransfected untreated HPMECs. Standard deviation from duplicate assays represented by error bars.

The expression of VCAM-1 mRNA in TNF-α treated HPMECs was elevated when compared to the untreated cells. However, it was not of statistical significance. The HIV-1 Nef-40H expressing untreated HPMECs did induce expression of VCAM-1 mRNA, but to lower levels compared to the negative control cells. The VCAM-1 mRNA expression levels in HIV-1 Nef-40H expressing treated HPMECs were significantly increased *(p*<0.01) when compared to the negative control cells (Figure 3.31A). The HIV-1 Nef-40H and TNF-α had a cooperative relationship to increase VCAM-1 expression above the levels of HIV-1 Nef-40H untreated HPMECs (*p*<0.01) however, the VCAM-1 mRNA expression level was not

significant when compared to the untransfected treated HPMECs (Figure 3.31A).The VCAM-1 expression level in HIV-1 Nef-40Y untreated cells was significantly higher (p<0.001) than the negative control (Figure 3.31B). Although VCAM-1 mRNA expression was observed in HIV-1 Nef-40Y expressing treated cells, it was of no statistical significance. HIV-1 Nef-MJ4 expressing cells did indeed increase the expression of VCAM-1 mRNA above the levels observed in untreated untransfected cells, however, it was of no statistical significance. The HIV-1 Nef-MJ4 variant and TNF-α had a synergistic relationship that significantly increased (p<0.0001) expression of VCAM-1 mRNA above the negative control cells, the TNF-α treated cells and the HIV-1 Nef-MJ4 expressing untreated cells (Figure 3.31C).

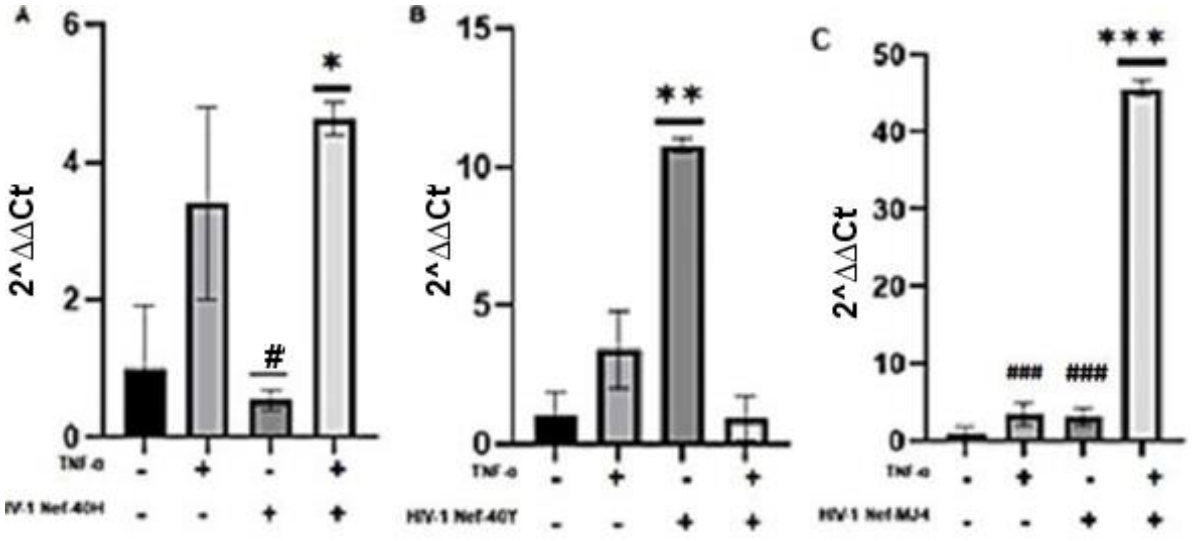

Figure 3.31: VCAM-1 mRNA Expression
The VCAM-1 mRNA expression levels after 24 hours post transfection in (A) HIV-1 Nef-40H, (B) HIV-1 Nef-40Y and (C) HIV-1 Nef-MJ4 expressing HPMECs. Statistical significance was established by comparing the cells against the untransfected untreated cells; *p<0.01; **p<0.001 and ***p<0.0005 compared with untransfected untreated HPMECs; $^{\#}p$<0.01 compared to untreated HIV-1 Nef-40H expressing HPMECs; $^{\#\#\#}p$<0.0001 compared with TNF-α treated and HIV-1 Nef-MJ4 expressing HPMECs. Error bars represent standard deviation from duplicate assays.

3.8.2. VCAM-1 protein expression profiling

One of the characteristics of endothelial dysfunction is the detachment of adhesion

molecules from the surface membrane of endothelial cells. To determine the concentration of soluble adhesion molecules, cell culture supernatant was harvested and analysed by an enzyme-linked immunosorbent assay (ELISA). The ELISA determined the amount of soluble VCAM-1 (sVCAM-1) present in the cell culture medium using immobilized human anti-sVCAM-1 antibodies. The cell culture medium from the untransfected TNF-α treated HPMEC and TNF-α treated cells were used as controls to determine the baseline of soluble adhesion molecules for the two groups of cells.

Measurement of the concentration of sVCAM-1 molecules in culture medium was done using a human sVCAM-1 ELISA kit. A standard curve was setup ranging from 0 ng/ml to 37.5 ng/ml. The experiment was performed in duplicates and the average optical density (450 nm) was used to calculate the concentration of sVCAM-1 present in the sample. Optical density values equal or lower than the blank value (0.46) was classified as having sVCAM-1 with a concentration of 0 ng/ml (Figure 3.32A). Optical densities between 0.46 and 0.504 translated to a concentration of 0.59 ng/ml. The sVCAM-1 concentration of 1,17 ng/ml was measured between an optical density of 0.505 to 0.571.

The untransfected TNF-α treated HPMECs (Figure 3.32, B2) had a higher optical density (OD) reading compared to untransfected untreated HPMECs (Figure 3.32, B1). The OD reading of sVCAM-1 in the supernatant from HIV-1 Nef-40H expressing untreated HPMECs increased in a time dependent manner from 0 to 48 hrs (Figure 3.32, B1), and from 6 to 24 hrs for the TNF-α treated HIV-1 Nef-40H cells (Figure 3.32, B2). The maximum OD reading for untreated HIV-1 Nef-40H cells was observed at 48 hours which translated to 0.59 ng/ml.

There was fluctuating pattern in the OD of the supernatant from the HIV-1 Nef-40Y expressing untreated cells (Figure 3.32, B1). The highest concentration of sVCAM-1 was observed at 3 hours at 0.59 ng/ml (Figure 3.32, B1, lane 3hr), which continued to fluctuate but remained above the OD of the negative control. The sVCAM-1 concentration from the untreated transfected cells were significantly higher (p<0.001) when compared to their respective negative controls. The multiple comparisons of the concentrations of sVCAM-1 in the supernatant of the HIV-1 Nef variants against each other were not significant for the untreated transfected cells.

The concentration of sVCAM-1 in the HIV-1 Nef-40Y supernatant treated with TNF-α reached a high of 1,17 ng/ml at 3 and 24 hours, with a lot of fluctuation in OD between these time points (Figure 3.32, B2, lanes 3 and 24). The concentration of sVCAM-1 from HIV-1 Nef-MJ4 supernatant from untreated cells increased from 0 ng/ml to its peak of 0.59 ng/ml at 3 hours (Figure 3.32, B1, lane 3). No sVCAM-1 was measured after 3 hours until 48 hours (Figure 3.32, B1, Nef-MJ4). Optical density readings of the supernatant from HIV-1 Nef-MJ4 TNF-α treated cells showed an increase above the negative control, reaching a peak concentration of 1,17 ng/ml at3 hours (Figure 3.32, B2, lane 3). No distinct pattern was observed at the peak, however, the concentration remained approximately equal to the control concentration of 0.59 ng/ml (Figure 3.32, B2, Nef-MJ4). The sVCAM-1 concentrations in the supernatant from the treated transfected cells were not statistically significant when compared to their negative controls. The multiple comparisons of the sVCAM-1 concentrations from the supernatant of HIV-1 Nef expressing treated cells were not of significance when compared to each other.

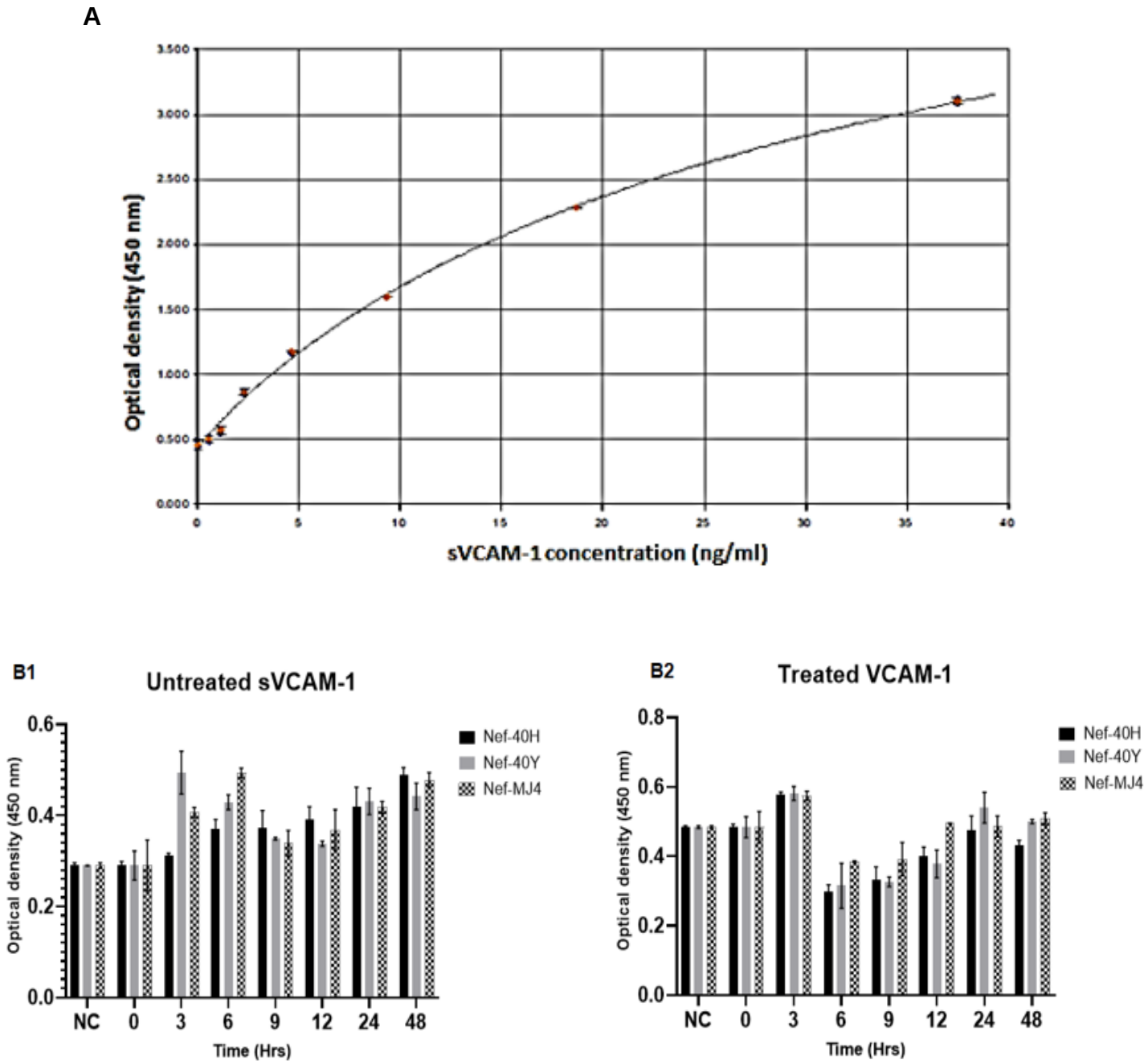

Figure 3.32: Optical density reading from sVCAM-1 ELISA

Standard curve of the sVCAM-1 ELISA kit had a R^2 value of 0.988 and the curve equation was $y = \frac{(0.421-5.44)}{(1+\frac{x}{32.5})^{0.933}} + 5.44$. (A). Measurements of the concentrations of sVCAM-1 in cell medium from the transfected untreated HPMECs (B1) and TNF-α treated HPMECs (B2). Error bars represents standard deviation obtained from duplicates assays.

The time dependent study was used to compare concentration of detached sVCAM-1 proteins from the HPMECs following 48hrs post transfection with Nef variants to identify the timepoint of optimal VCAM-1 detachment, in agreement with the expression of ICAM-1 and

VCAM-1 mRNA (Figure 3.31, B1 and B2), optimal sVCaM-1 detection was 24 hours after transfection. The concentration of sVCAM-1 from TNF-α untreated HPMECs was compared to levels found in TNF-α treated cells. It was established that TNF-α treated cells had significantly higher levels (p<0.001) of detached VCAM-1 molecules compared to the untreated cells (Figure 3.32). The HIV-1 40H variant had significantly higher concentration (p<0.01) of sVCAM-1 in untreated cells compared with the negative control (Figure 3.33A). The combination of TNF-α and HIV-1 Nef-40H had a significantly higher (p<0.001) concentration of sVCAM-1 compared to the negative control (Figure 3.33A). Although the combination of HIV-1 Nef-40H variant and TNF-α did increase the concentration of sVCAM-1, it was of no significance when compared to the concentration from HIV- 1 Nef-40H variant only and the untransfected treated cells. The concentration of sVCAM-1 from the supernatant of HIV-1 Nef-40Y variant was lower than the TNF-α treated untreated control but significantly higher (p<0.01) concentration than the negative control (Figure 3.33B). The combination of TNF-α and HIV-1 Nef-40Y had higher concentration (p<0.001) of sVCAM-1 above the negative control (Figure 3.33B). The TNF-α and HIV-1 Nef-40Y had higher concentration of sVCAM-1 than HIV-1 Nef-40Y variant alone and the TNF-α treated cells, it was of no significance when compared to the two aforementioned groups. The HIV-1 Nef-MJ4 variant had a significantly higher (p<0.001) concentration of sVCAM-1 compared the negative control (Figure 3.33C). The sVCAM-1 concentration in the supernatant from TNF-α and HIV-1 Nef-MJ4 variant had significantly higher (p<0.0001) sVCAM-1 concentration compared to the negative control (Figure 3.33C). No synergistic relationship was observed when multiple comparisons were done with HIV-1 Nef-MJ4 variant alone and the TNF-α treated cells.

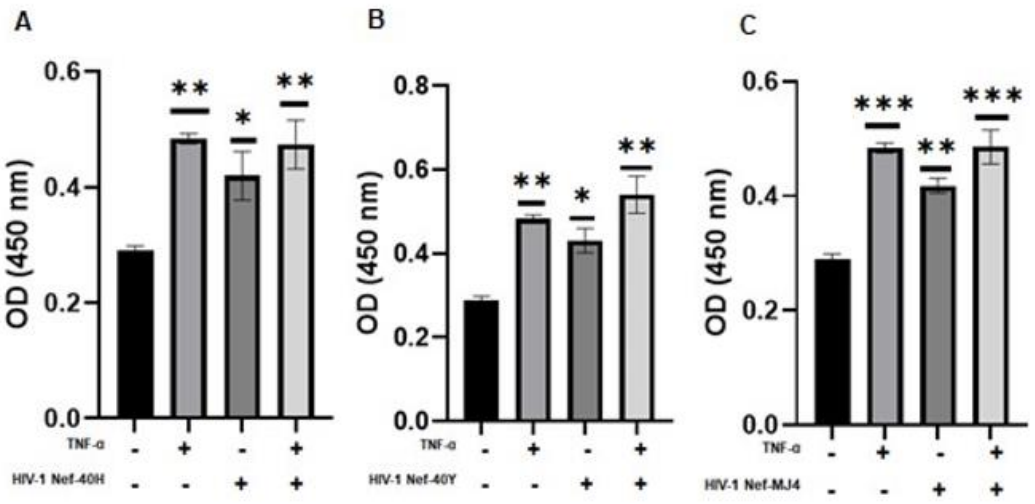

Figure 3.33: Optical density reading of sVCAM-1 concentration

The sVCAM-1 concentration after 24 hours post in (A) HIV-1 Nef-40H, (B) HIV-1 Nef-40Y and (C) HIV-1 Nef-MJ4 in culture medium. Statistical significance was established by comparing the OD reading from transfected cells supernatant to the negative control. *p<0.05, **p<0.005 and ***p<0.0005 compared with untransfected untreated HPMECs supernatant. Error bars represent standard deviation from duplicate assays.

Chapter 4: Discussion and conclusion

4.1. Discussion of results

The HIV-1 infection has been associated with an increased risk of cardiovascular disease. The increased rate of cardiovascular diseases in PLWH has been reported in both HIV-treated patients and ART-naïve patients infected with HIV-1. Endothelial dysfunction is one of the pathophysiological events in the development of atherosclerosis following CVDs. Multiple studies have reported HIV-1 Nef as a causative agent of CVDs in PLWH. HIV-1 Nef has high sequence variations which may lead to varying degrees of endothelial dysfunction. A study by Mezoh *et al.* (2022), identified the HIV-1 H40Y polymorphism to be associated with higher levels of plasma biomarkers of endothelial dysfunction in PLWH. The investigation of this polymorphism on endothelial dysfunction in *in vitro* was of interest to confirm its effects on endothelial dysfunction in a controlled environment. To achieve this, a sample of the HIV-1 *nef* gene from a patient infected with HIV-1 (*nef*-40H) was isolated using PCR. A reference subtype C HIV-1 *nef* gene was isolated used from the pMJ4 plasmid (*nef*-MJ4). The *nef* genes were subcloned into mammalian expression vectors. Attempts were made to construct stable expression plasmids using a pLKO.dCMV.TetO.3xFlag vector with the *nef* genes, however these plasmids were not successful in expressing HIV-1 Nef proteins. A second attempt was made to construct transient expression plasmids with a verified pcDNA vector. A successful cloned pcDNA 3.1(+)-Flag/Nef-40H was mutated to introduce the 40Y amino acid residue by site directed mutagenesis to produce the pcDNA 3.1(+)-Flag/Nef-40Y plasmid. During the *in vitro* analysis, the HIV-1 Nef proteins were expressed in human pulmonary microvascular endothelial cells under two different conditions, one with the treatment of TNF-α and one without the TNF-α. The TNF-α was used to increase the expression of the biomarkers of

endothelial dysfunction, ICAM-1, and VCAM-2. Real time quantitative PCR was used to measure mRNA expression of the biomarkers and ELISA was used to measure the concentration of the biomarkers in the culture medium. Although all HIV-1 Nef variants could induce the expression of ICAM-1 mRNA in HMPECs not treated with TNF-α, HIV-1 Nef-40H and Nef-MJ4 variants induced the expression of ICAM-1 mRNA at higher levels than HIV-1 Nef-40Y. The expression levels of ICAM-1 mRNA in HPMECs treated with TNF-α was lower than the control levels for all HIV-1 Nef variants, which suggested that the is no synergistic effect between HIV-1 Nef and TNF-α to increase the expression of ICAM-1 mRNA. In the context of VCAM-1 mRNA expression, all HIV-1 Nef variants did induce the expression of VCAM-1mRNA in HPMECs in the absence of TNF-α. However, HIV-1 Nef-40Y and Nef-MJ4 induced the expression of VCAM-1 mRNA at significantly higher levels than HIV-1 Nef-40H. In the presence of TNF-α, HMPECs transfected with HIV-1 Nef-40H and Nef-MJ4 expressed higher levels of VCAM-1 mRNA than HIV-1 Nef-40Y. A synergistic effect between TNF-α and HIV-1 Nef-40H and Nef-MJ4 was observed to enhance than expression of VCAM-1 mRNA to levels higher than the controls. This effect was not present with the HIV-1 Nef-40Y variant. These findings confirm the report from Mezoh *et al.* (2022) which showed that PLWH possessing the HIV-1 Nef 40H residue had higher plasma concentrations of biomarkers of endothelial activation than PLWH possessing the HIV-1 Nef 40Y residue. In addition a study by Almodovar et al (2012) showed that a series of polymorphisms in the *nef* gene including H40Y were associated with pulmonary hypertension. The sVCAM-1 concentration levels in the presence or absence of TNF-α were not significantly different when comparing the HIV-1 Nef variants against each other. However, the concentration levels were elevated when compared to their control groups.

Analysis of the PCR reactions to insert the restriction sites *Age*I and *Eco*RI produced

multiple unwanted bands of greater size than the gene of interest. This may have been to unspecific binding of the primers to the template DNA. PCR optimization could have been carried out to address the unspecific binding. Multiple steps could have been performed to optimize the protocol, including performing a gradient PCR to establish the optimal annealing temperature, reducing the number of cycles, or varying the concentrations of the buffers used (Roux, 2009). Even with the unwanted bands, the correct size bands were identified and excised from the agarose gel for downstream procedures. The digestion of the vector with the enzymes *Age*I and *Eco*RI worked well as clear differences could be observed between the undigested plasmid, single digested plasmids, and the double digested plasmid. However, results of the digest of the PCR products were not clear. This was because less than 10 base pairs were excised from the PCR product, and this was too small to visualize on the agarose gel. To address this problem, primers with a longer flanking sequence after the restriction sites could have been used to allow for efficient cleavage of the PCR products and better visualization on a higher resolution agarose gel (Zimmermann, *et al*., 1998). Poor digestion of the PCR products can lead to poor ligation of the PCR products to the vector. This was evident when performing colony PCR on the E.coli colonies transformed with the ligated products. The PCR products produced were greater in size than expected size of HIV-1 *nef* genes. This was further confirmed by restriction digest analysis, which produced fragments of greater size than expected. Confirming the ligation could have been carried out before transforming the E.coli cells to avoid wasting cells and reagents. Ligation mixture PCR could have been performed using the ligation mixture as the template DNA for the PCR reaction (Chandra & Wikel, 2005). Running an agarose gel with the ligation mixture and an empty plasmid could have shown if the ligation reaction was successful as the ligation mixture would have a band greater in size than the one found in the empty vector lane (Han *et al*., 2010). Sequencing of the

plasmids produced sequences that did not match known sequences of HIV-1 nef genes. This confirmed that the cloning of the gene of interest had failed and required the repeating of cloning. A reason for the incorrect sequences could be the result of using incorrect sequencing primers as the pLKO vector was a gift and the identity of the vector was not confirmed. To rule out the sequencing primers, the PCR primers could have been used to sequence the plasmids as they were specific to the gene of interest (Gochhait *et al*., 2007). The cloning failures were highlighted by the failure to produce recombinant HIV-1 Nef proteins after transfection. A anti-Nef antibody positive control ruled out the Western blotting protocol as the reason for the negative results. However, a positive control for the anti-Flag antibody should have been used to demonstrate that the anti-Flag antibody was working properly (Wu, *et al*., 2007). The unsuccessful cloning of HIV-1 nef genes into the pLKO plasmid demonstrated the importance of identifying and confirming all sequences, designing effective primers and improving the efficiency of the cloning experiments.

Primers to amplify the HIV-1 *nef* genes were designed to introduce a N-terminal Flag tag and restriction sites, *Bam*HI and *Eco*RI, so as to minimise nonspecific binding of the primers to the template DNA. The PCR was optimized to decrease formation of non-specific PCR products, thus improving ligation of the desired PCR products to the pGEM-T Easy vector. The use of the cloning vector allowed for screening of successfully ligated products and improved the efficiency of the restriction enzymes as more flanking base pairs were available after the restriction sites (Celie *et al*., 2016). Although restriction digestion was improved, restriction digest of the pcDNA vector with the restriction enzyme, *Eco*RI, produced partially digested products. To improve digestion, the amount of restriction enzymes added to the reaction and/or the duration of incubation time could have been increased (Zimmermann, *et al*., 1998). Ligation of the digested products to the pcDNA

vector was successful and more efficient compared to cloning into the pLKO vector. This is the result of using precise PCR primers and the cloning vector pGEM-T Easy vector. Mutating the Nef-40H expressing plasmid to produce the Nef-40Y expressing plasmid was achieved using a commercially available site-directed mutagenesis kit. Using a kit is more efficient than using traditional PCR methods (Shenoy and Visweswariah, 2003). Screening of the mutation could have been improved by excising the gene of interest first before performing the restriction digestion with the *Fat*I restriction enzyme. Sequencing of the constructs was done using the PCR primers as they were specific to the gene of interest, thus, unsuccessful sequencing would show that the gene of interest was not present in the plasmid. Successful expression of the recombinant Nef proteins was confirmed by Western blot analysis using the anti-Flag antibody. The anti-Nef antibody could have also been used to demonstrate that the commercially available monoclonal anti-Nef antibody raised against HIV-1 Nef proteins were ineffective at recognizing the subtype C HIV-1 Nef proteins. Profiling of the expression of the adhesion molecules by RT-qPCR did not produce a time dependent linear increase as observed with the expression of the recombinant Nef proteins. Analysis of the expression of the adhesion molecules mRNA could have been improved by analyzing levels after 24 hours. The data was more conclusive and consistent post 24 hours. This was confirmed by a study by Kanda *et al* (1998) which demonstrated that expression of adhesion molecules in endothelial cells peaked at 18-24 hours post stimulation and plateaued after 24 hours. The quantification of soluble VCAM-1 proteins by ELISA gave low values. This was due to the sample dilution instruction provided by the kit's manufacturer. Revising the dilution ratios would have increased the concentration of sVCAM-1 in each sample, thus giving more distinctive readings.

HIV-1 Nef is reported to facilitate its transfer from HIV-infected cells to bystander cells with

devastating effects. This has also been reported in patients infected with HIV-1 on ART who have reduced virion production, but early gene expression of HIV-1 Nef is not affected in the same manner (Appay *et al*., 2002). HIV-1 Nef is reported to cause cell death in endothelial cells. A study by Acheampong *et al* (2005) demonstrated that extracellular and endogenously expressed HIV-1 Nef induced apoptosis in primary human brain microvascular endothelial cells via the activation of caspases. Apoptosis was reported in lung microvascular endothelial cells transfected with HIV-1 Nef. HIV-1 Nef was observed to upregulate the expression of the endothelial-monocyte-activating polypeptide II (EMAP II), which facilitates the progression of pulmonary emphysema through mechanisms involved in endothelial cell death (Chelvanambi *et al*., 2019). In our study, HIV-1 Nef variants were transiently expressed endogenously in HPMECs. This experimental design was adopted following a study by Fan *et al*., 2010, in which the authors demonstrated that the HIV-1 Nef protein expression was primarily located in the cytoplasm and partially in the membrane, which is consistent with natural Nef protein localization. This, therefore, implies that the transfer of HIV-1 Nef or direct expression of HIV-1 Nef by the endothelial cells would have similar effects (Joseph *et al*., 2003; Fan *et al*., 2010). However, in our study, we assume that there was no cell death as HIV-1 Nef expression increased in a time-dependent manner. These findings may disagree with reported results due to the maintenance and transfection methods employed in this study; however other factors such as cell types, HIV-1 Nef variances, HIV-1 Nef concentrations, and treatment times may be the cause of this discrepancy regarding the toxicity effect of HIV-1 Nef (Jiang *et al*., 2010). In other publications, serum starvation procedures or limited growth factors were used before or during the treatment with HIV-1 Nef, which could help induce endothelial apoptosis (Jiang *et al*., 2010; Chelvanambi *et al*., 2019). The complete growth medium with or without TNF-α did not cause any cell death in HMPECs as demonstrated in the cell

maintenance experiment conducted, showing that treated HPMECs grew similarly to untreated HPMECs. However, human endothelial cells can be susceptible to TNF-α, thus resulting in the suppression of RNA and protein synthesis (Karsan *et al*., 1996).

It has already been established that HIV-1 infection is associated with an increased risk of CVDs in PLWH (Deeks *et al.*, 2013). HIV-1 infection results in chronic immune activation, inducing the increased expression of cell surface antigens and production of cytokines; thus, contributing to the high occurrence of CVDs (Sipsas and Sfikakis, 2004). HIV-1 proteins alone have been reported to be the same. HIV-1 Nef proteins have been reported to induce the release of inflammatory proteins interleukin-1 (IL-1), IL-6, and TNF- α in monocyte/macrophages (Olivetta *et al*., 2003) and induce the expression of ICAM-1 in endothelial cells (Fan *et al*., 2010). It was observed that the HIV-1 Nef protein- induced transcription of ICAM-1 in endothelial cells, required the activation of extracellular signal-regulated kinases (Fan *et al*., 2010). Recombinant exogenous HIV Nef proteins have been reported to activate nuclear transcription factors NF-κB and AP-1 in a dose- and time-dependent manner (Varin *et al.*, 2003). In this study, the expression of adhesion molecules was measured by RT-PCR. In the absence of TNF-α, HIV-1 Nef variants transfected into HPMECs could induce the expression of ICAM-1 and VCAM-1 mRNA significantly higher than in the control group HPMECs. This was supported by the findings in a study by Fan *et al* (2010), which demonstrated that HIV-1 Nef could induce the expression of adhesion molecules independently. This confirmed the study by Duffy *et al*. (2009) that reported that HIV Nef independently downregulated eNOS expression in porcine pulmonary artery endothelial cells and human pulmonary artery endothelial cells (HPAECs), causing endothelial dysfunction. In our study, the wild-type HIV-1 Nef (Nef-40H) and reference strain (Nef-MJ4) variants induced the ICAM-1 mRNA expression significantly higher than

the mutated HIV-1 Nef (Nef-40Y) variant. This confirmed the findings by Mezoh *et al*., (2022) that reported the HIV-1 40H polymorphism was associated with higher levels of ICAM-1 in ART-naïve South African individuals. In the context of VCAM-1 mRNA expression, HIV-1 Nef-MJ4 and Nef-40Y variants had significantly higher levels when compared to the HIV-1 Nef-40H variant.

The pre-treatment of endothelial cells with TNF-α enhances the expression of adhesion molecules from their basal levels, a characteristic feature of inflammation and endothelial cell activation (Lee *et al*., 2011; Bengalli *et al*., 2019). The treatment of endothelial cells with HIV-1 proteins and TNF-α is reported to increase the risk of endothelial dysfunction. A study by Jiang *et al*., (2010) demonstrated that HIV-1 Gp120 and TNF-α significantly enhance eNOS downregulation at mRNA and protein levels better than HIV-1 Gp120 alone in porcine coronary arteries and human coronary artery endothelial cells (HCAECs). In addition, a study by Matzen *et al*., (2004) demonstrated that human microvascular vein endothelial cells (HMVECs) treated with both HIV-1 Tat and TNF-α significantly increased the adhesion of leukocytes and peripheral blood mononuclear cells (PBMC) *in vitro* compared to HMVECs in the presence of HIV-1 Tat alone. These studies suggest that HIV-1 proteins and TNF-α may have synergistic effects to induce endothelial dysfunction. In our study, the expression of ICAM-1 mRNA in HIV-1 Nef expressing HPMECs in the presence of TNF-α was lower than the levels in the control group. This disagreed with the know characteristics of HIV-1 proteins in the presence of TNF-α. However, this could explain the findings in a study by Matzen and colleagues, in which it was observed that HIV-1 Nef expressing endothelial cells in the presence of TNF-α did not bind leukocytes better than HIV-1 Nef absent endothelial cells treated with TNF-α *in vitro* (Matzen *et al.,* 2004). The binding of leukocytes is facilitated by ICAM-1 and the leukocyte function

antigen-1 (LFA-1) (Chong *et al*., 2021), thus a decrease in ICAM-1 would result in poor binding of leukocytes by the endothelial cells. This could suggest that *in vitro*, stimulation of endothelial cells with both HIV-1 Nef and TNF-α does not increase the expression of ICAM-1. However, a clinical study conducted by Mezoh *et al*., (2022) involving HIV- infected ART-naïve South African individuals compared to HIV-uninfected healthy subjects, showed the population infected with HIV-1 to have significantly higher plasma levels of TNF-α and ICAM-1 than the uninfected population (Mezoh *et al*., 2022). Thereason for the discrepancy between *in vitro* and clinical studies may not be known but it demonstrates that HIV-1 Nef and TNF-α potentially play a role in increased expression of ICAM-1, however, the mechanism by which this may occur is still unclear.

In the context of VCAM-1, our study observed an increased expression of VCAM-1 mRNA in HIV-1 Nef expressing HPMECs in the presence of TNF-α compared to the control group. The HIV-1 Nef-40H and Nef-MJ4 variants demonstrated a synergistic effect to upregulate the expression of VCAM-1 mRNA, which was not seen with the HIV-1 Nef-40Y variant. This, therefore, suggests that the HIV-1 Nef H40Y polymorphism affects VCAM-1 mRNA expression *in vitro*, which the Nef-40H mutation potentially enhances VCAM-1 expression. The synergistic effect of HIV-1 Nef and TNF-α on VCAM-1 mRNA expression could explain the findings in a study by Matzen and colleagues who reported higher recruitment of peripheral blood mononuclear cells by HIV-1 Nef expressing endothelial cells in the presence of TNF- α compared to HIV-1 Nef expressing endothelial cells in the absence of TNF-α (Matzen *et al*., 2004). This results from VCAM-1 binding to the very late antigen (VLA-4) on peripheral blood mononuclear cells (Xie *et al*., 2011).

The increased levels of circulating forms of cellular adhesion molecules in patients infected with HIV-1 have gained interest as prognostic markers of endothelial dysfunction. These soluble adhesion molecules have been measured in numerous clinical studies, providing a

new and easy method for assessing the risk of CVDs among PLWH (Sipsas and Sfikakis, 2004; Graham *et al*., 2013; Lembas *et al*., 2022). In *in vitro* studies, differential mRNA expression studies generally tend to assume the levels of mRNA expression positively correlate with protein expression and have biological meaning. However, mRNA-protein correlation studies have demonstrated a poor correlation between mRNA and protein expression levels (Koussounadis *et al*., 2015). This would be later confirmed in our study. Considering that there was no significant difference when evaluating the expression of ICAM-1 mRNA in HPMECs cultured either in the presence or absence of TNF-α during the RT-qPCR analysis, the protein study was only performed on the soluble VCAM-1 protein. Additionally, sVCAM-1 and not sICAM-1 is reported to be a better marker of endothelial injury in patients with a history of coronary artery disease (Semaan *et al*., 2000). A study conducted by Mezoh *et al*. (2022) showed a significant difference in plasma levels of sVCAM-1 in subjects with HIV-1 compared to uninfected subjects (p<0.0005) than with sICAM-1 plasma levels (p<0.05). This implies that VCAM-1 could potentially be the most preferred biomarker for the early detection of cardiovascular diseases in PLWH.

In our study, the concentration of sVCAM-1 in the culture medium was measured by enzyme-linked immunosorbent assay (ELISA). In either the absence or presence of TNF-α, the levels of sVCAM-1 were significantly higher in the HIV-1 Nef variants compared to the control groups. However, no variant significantly performed better than the other. Additionally, no synergistic effect was witnessed between the HIV-1 Nef variants and TNF-α to increase the concentration of sVCAM-1. This observation, however, disagreed with the RT-qPCR data. The discrepancy between these results may exist for several reasons, including the type of cells used. A study by Videm and Albrigtsen (2008) reported that low concentrations of sVCAM-1 were released from human microvascular endothelial cells upon stimulation in *in vitro* studies, thus making sVCAM-1 an ineffective marker of

endothelial activation in these cells. This suggests the usage of a different cell line, such as human umbilical vein endothelial cells (HUVECs), may be better suited for *in vitro* sVCAM-1 expression profile studies (Ling *et al*., 2012).

4.2. Conclusion

In this study, RT-PCR analysis found that HIV-1 Nef-40H induces higher levels of ICAM-1 and VCAM-1 mRNA expression compared to Nef-40Y. Similar outcomes were found using the HIV-1 Nef-MJ4 reference strain. The HIV-1 Nef-40H and Nef- MJ4 variants had a synergistic relationship to significantly increase the expression of VCAM-1 mRNA, which was not observed in HIV-1 Nef-40Y variant. Although HIV-1 Nef-40H and Nef-40Y produced similar levels of sVCAM-1, significant mRNA expression of adhesion molecules in endothelial cells transfected with HIV-1 Nef- 40H could result in higher levels of expressed adhesion molecules over time. These findings suggest that PLWH that have the HIV-1 Nef- 40H variant could have a higher risk of CVDs compared to people living with HIV with the 40Y variant.

The confirmation of HIV-1 Nef role in the development of endothelial dysfunction and subsequent CVDs, allows for the targeting of HIV-1 Nef in therapeutic strategies specific to South African HIV-1 strains. This could contribute to effective reduction of non-AIDS related deaths among patients infected with the HIV-1 subtype C strains.

4.3. Study limitations and strengths and future studies

Several limitations were identified in this study. One of such limitations includes the fact that the functional activity of HIV-1 Nef was not confirmed in this study, therefore, it is not known if the expressed HIV-1 Nef proteins were biologically active. The HIV-1 Nef protein is known to downregulate CD4 and HLA genes, thus, an activity assay based on this property could be performed to confirm that the expressed HIV-1 Nef protein is biologically active (Mann *et al*., 2013). The stable expression of a protein is preferential over transient expression to have the continuous effect of a protein, however, attempts to construct a plasmid that would facilitate stable expression of HIV-1 Nef were unsuccessful. Failure in

cloning could have been due to no PCR optimization. Moreover, the pLKO plasmid used in this study was a gift and the plasmid identity was not confirmed prior to its use. Another limitation to this study is the low number of biological repeats that were performed. An increase in the number of repeats would provide more accurate data. Moreover, a technical repeat was not carried out. This study could possibly have also been limited using Human Pulmonary Microvascular Endothelial cells as not all types of endothelial cells react the same way during endothelial activation (Ling *et al*., 2012).

The strength of this study is that it is adaptable to several changes including studying multiple mutations and the use of different endothelial cell lines. This lends itself to being cost-effective and reproducible. The experimental design can be used to study polymorphisms in other HIV-1 proteins such as HIV-1 Tat, which have also been associated with endothelial activation and dysfunction in individuals infected with HIV-1. This is one of very few studies conducted that has looked at the effect of HIV-1 Nef on endothelial function, and the only study to look at endothelial activation brought on by exposure to HIV-1 subtype C Nef variants.

Further studies could be done on other identified HIV-1 Nef polymorphisms using the same experimental design. Studying the secondary and tertiary structures of the Nef protein will help determine if the mutations result in a conformational change of the protein's structure, which might equally explain changes in function. The HIV-1 Nef protein could equally be studied in the context of elite controllers or slow progressors' ability to cause endothelial dysfunction, as it would help identify elite controls and slow progressors who are at greater risk of developing CVDs. This could help identify domains of the HIV-1 Nef protein associated with increased risk of CVD, given that elite controllers and slow progressors have multiple polymorphisms and deletions in their HIV-1 *nef* sequences.

Chapter 5: References

Abbas, W. and Herbein, G. (2013) 'T-Cell Signaling in HIV-1 Infection', *The Open Virology Journal*, 7: 57-71.

Abraham, L. and Fackler, O.T. (2012) 'HIV-1 Nef: a multifaceted modulator of T cell receptor signaling', *Cell Communication and Signaling*, 10(39): 1-11.

Acheampong, E.A., Parveen, Z., Muthoga, L.W., Kalayeh, M., Mukhtar, M. and Pomerantz, R.J. (2005) 'Human Immunodeficiency Virus Type 1 Nef Potently Induces Apoptosis in Primary Human Brain Microvascular Endothelial Cells via the Activation of Caspases', *Journal of Virology*, 79(7): 4257-4269.

Achuthan, V., Perreira, J.M., Ahn, J.J., Brass, A.L. and Engelman, A.N. (2019) 'Capsid-CPSF6 interaction: Master regulator of nuclear HIV-1 positioning and integration', *Journal of Life Science (Westlake Village)*, 1(1): 39-45.

Achuthan, V., Perreira, J.M., Sowd, G.A., Puray-Chavez, M., McDougall, W.M., Paulucci-Holthauzen, A., Wu, X., Fadel, H.J., Poeschla, E.M., Multani, A.S. and Hughes, S.H. (2018) 'Capsid-CPSF6 interaction licenses nuclear HIV-1 trafficking to sites of viral DNA integration', *Cell host & microbe*, 24(3): 392-404.

Ait-Ammar, A., Kula, A., Darcis, G., Verdikt, R., Wit, S.D., Gautier, V., Mallon, P.W.G., Marcello, A., Rohr, O. and Lint, C.V. (2020) 'Current Status of Latency Reversing Agents Facing the Heterogeneity of HIV-1 Cellular and Tissue Reservoirs', *Frontiers in Microbiology*, 10(3060): 10-23.

Alkhatib, G. (2009) 'The biology of CCR5 and CXCR4', *Current Opinion in HIV and AIDS*, 4(2): 96-103.

Almodovar, S., Knight, R., Allshouse, A.A., Roemer, S., Lozupone, C., McDonald, D., Widmann, J., Voelkel, N.F., Shelton, R.J., Suarez, E.B. and Hammer, K.W. (2012) 'Human Immunodeficiency Virus nef signature sequences are associated with pulmonary

hypertension', *AIDS research and human retroviruses*, 28(6): 607-618.

Anand, A.R., Rachel, G. and Parthasarathy, D. (2018) 'HIV proteins and endothelial dysfunction: Implications in cardiovascular disease', *Frontiers in Cardiovascular medicine*, 5(185): 1-10.

Andrews, S.M. and Rowland-Jones, S. (2017) 'Recent advantages in understanding HIV evolution', *F1000 Research* , 6(597): 1-7.

Andrew, A. and Strebel, K. (2014) 'HIV-1 accessory proteins: Vpu and Vif', *Methods in Molecular Biology*, 1087: 135-158.

Appay, V., Hansasuta, P., Sutton, J., Schrier, R.D., Wong, J.K., Furtado, M., Havlir, D.V., Wolinsky, S.M., McMichael, A.J., Richman, D.D. and Rowland-Jones, S.L. (2002) 'Persistent HIV-1-specific cellular responses despite prolonged therapeutic viral suppression', *AIDS*, 16(2): 161-170.

Araínga, M., Edagwa, B., Mosley, R.L., Poluektova, L.Y., Gorantla, S. and Gendelman, H.E. (2017) 'A mature macrophage is a principal HIV-1 cellular reservoirin humanized mice after treatment with long acting antiretroviral therapy', *Retrovirology*, 14(1): 1-13.

Arildsen, H., Sorensen, K.E., Ingerslev, J.M., Ostergaard, L.J. and Laursen, A.L. (2013) 'Endothelial dysfunction, increased inflammation, and activated coagulation in HIV-infected patients improved after initiation of highly active antiretroviral therapy', *HIV Medicine*, 14(1): 1-9.

Arts, E.J. and Hazuda, D.J. (2012) 'HIV-1 antiretroviral drug therapy', *Cold Spring Harbor perspectives in medicine*, 2(4): 1-24.

Asamitsu, K. and Okamoto, T. (2017) 'The Tat/P-TEFb protein-protein interaction determining transcriptional activation of HIV', *Current Pharmaceutical Design,* 23(28): 4091-4097.

Ashorn, P., McQuade, T.J., Thaisrivongs, S., Tomasselli, A.G., Tarpley, W.G. and Moss, B.

(1990) 'An inhibitor of the protease blocks maturation of human and simian immunodeficiency viruses and spread of infection', *Proceedings of the National Academy of Sciences of the United States of America*, 87(19): 7472-7476.

Aylinde, D., Maudet, C., Transy, C. and Margottin-Goguet, F. (2010) 'Limelight on two HIV/SIV accessory proteins in macrophage infection: Is VPx overshadowing Vpr?', *Retrovirology*, 7(35): 1-12.

Baker, J.V. and Duprez, D. (2010) 'Biomarkers and HIV-Associated Cardiovascular Disease', *Current Opinion in HIV/AIDS*, 5(6): 511-516.

Barnes, P. & Karin, M., 1997. Nuclear Factor-κB — A Pivotal Transcription Factor in Chronic Inflammatory Diseases. *The New England Journal of Medicine,* 336(15), pp. 1066-1071.

Basmciogullari, S. and Pizzato, M. (2014) 'The activity of Nef on HIV-1infectivity', *Frontiers in Microbiology*, 5(232): 1-12.

Bbosa, N., Kaleebu, P. and Ssemwanga, D. (2019) 'HIV subtype diversity worldwide', *Current Opinion in HIV and AIDS*, 14(3): 153-160.

Bengalli, R., Zerboni, A., Marchetti, S., Longhin, E., Priola, M., Camatini, M. and Manteccaa, P. (2019) 'In vitro pulmonary and vascular effects induced by different diesel exhaust particles', *Toxicology Letters*, 306: 13-24.

Berger, E.E., Murphy, P.M. and Farber, J.M. (1999) 'Chemokine receptors as HIV-1 coreceptor: Roles in viral entry, tropism and disease', *Annual Reviewof Immunolgy*, 17: 657-700.

Berzow, D. *et al*., 2021. Human immunodeficiency virus–2 (HIV-2): a summary of the present standard of care and treatment options for individuals living with HIV-2 in Western Europe. *Clinical infectious diseases,* 72(3), pp. 503-509.

Biswas, I. and Khan, G.A. (2020) 'Endothelial dysfunction in cardiovascular diseases',

Basic and Clinical Understanding of Microcirculation, 10.

Blackard, J.T. (2012) 'HIV compartmentalization: a review on a clinically important phenomenon', *urrent HIV research*, 10(2): 133-142.

Blanco-Rodriguez, G., Gazi, A., Monel, B., Frabetti, S., Scoca, V. and Mueller, F. (2020) 'Remodeling of the Core Leads HIV-1 Preintegration Complex into the Nucleus of Human Lymphoocytes', *Journal of Virology,* 94(11): 1-20.

Blissenbach, M., Grewe, B., Hoffmann, B., Brandt, S. and Uberla, K. (2010) 'Nuclear RNA export and packaging functions of HIV-1 Rev revisited', *Journal of Viriology*, 84: 6598-6604.

Bramilla, A., Turchetto, L., Bovolenta, C., Veglia, F., Santagostino, E., Gringeri, A., Clementi, M., Poli, G., Bagnarelli, P. and Vicenzi, E. (1999) 'Defective nef alleles in a cohort of hemophiliacs with progressing and nonprogressing HIV-1 infection', *Virology*, 259: 349-368.

Brevetti, G., Schiano, V. and Chiariello, M. (2008) 'Endothelial dysfunction: a key to the pathophysiology and natural history of peripheral arterial disease?', *Atherosclerosis*, 197: 1-11.

Bryant, M. and Ratner, L. (1990) 'Myristoylation-dependent replication and assembly of human immunodeficiency virus 1', *Proceedings of the National Academy of Sciences of the United States of America*, 2: 523-527.

Buonarguro, L. (2007) 'Human immunodeficiency virus type 1 subtype distrubtion in the worldwide epidemic: pathogenic and therapeutic implications', *Journal of Virology*, 81(19): 10209-10219.

Burdick, R.C., Li, C., Munshi, M., Rawson, J.M.O., Nagashima, K., Hu, W.-S. and Pathak, V.K. (2020) 'HIV-1 uncoats in the nucleus near sites of integration', *Proceedings of the National Academy of Sciences*, 117(10): 5486-5493.

Bushman, F.D., Fujiwara, T. and Craigie, R. (1990) 'Retroviral DNA integration directed by

HIV integration protein in vitro', *Science*, 249(4976): 1555-1558.

Calfee, C.S., Gallagher, D., Abbott, J., Thompson, B.T., Matthay, M.A. and Network, t.N.A. (2012) 'Plasma angiopoietin-2 in clinical acute lung injury: Prognostic and pathogenetic significance', *Critical care medicine*, 40(6): 1731.

Campbell, E.M. and Hope, T.J. (2015) 'HIV-1 Capsid: The multifaceted key player in HIV-1 infection', *Nature Reviews Microbiology*, 13(8): 471- 483.

Campbell, T.D., Khan, M., Huang, M.B., Bond, V.C. and Powell, M.B. (2008) ' HIV-1 Nef protein is secreted into vesicles that can fuse with target cells and virions', *Ethnicity & disease*, 18(202): S2.

Capon, D.J. and Ward, R.H. (1991) 'The CD4-gp120 interaction and AIDS pathogenesis', *Annual Review of Immunology*, 9: 649-678.

Celie, P.H.N., Parret, A.H.A. and Perrakis, A. (2016) 'Recombinant cloning strategies for protein expression', *Current Opinion in Structural Biology*, 38: 145-154.

Cerutti, C. and Ridley, A.J. (2017) 'Endothelial cell-cell adhesion and signalling', *Experimental Cell Research*, 358: 31-38.

Chandra, P. & Wikel, S., 2005. Analyzing ligation mixtures using a PCR based method. *Biological procedures online,* Volume 7, pp. 93-100.

Chaillon, A., Gianella, S., Dellicour, S., Rawlings, S.A., Schlub, T.E., Oliveira, M.F.D., Ignacio, C., Porrachia, M., Vrancken, B. and Smith, D.M. (2020) 'HIV persists throughout deep tissues with repopulation from multiple anatomical sources', *The Journal of clinical investigation*, 130(4): 1699-1712.

Chatzizisis, Y.S., Coskun, A.U., Jonas, M., Edelman, E.R., Feldman, C.L. and Stone, P.H. (2007) 'Role of Endothelial Shear Stress in the Natural History of Coronary Atherosclerosis and Vascular Remodelling: Molecular, Cellular, and Vascular Behaviour', *Journal of the American College of Cardiology*, 49(25): 2379-2393.

Checkley, M.A., Luttge, B.G. and Freed, E.O. (2011) 'HIV-1 envelope glycoprotein biosynthesis, trafficking and incorporation', *Journal of Molecular Biology*, 410(4):582-608.

Chen, B. (2019) 'Molecular mechanism of HIV-1entry', *Trends in Microbiology*, 27(10): 878-892.

Chong, D.L.W., Rebeyrol, C., José, R.J., Williams, A.E., Brown, J.S., Scotton, C.J. and Porter, J.C. (2021) 'ICAM-1 and ICAM-2 Are Differentially Expressed and Up- Regulated on Inflamed Pulmonary Epithelium, but Neither ICAM-2 nor LFA-1: ICAM-1 Are Required for Neutrophil Migration Into the Airways In Vivo', *Frontiers in Immunology*, 12: 1-14.

Cohen, M.S., Gay, C.L., Busch, M.P. and Hecht, F.M. (2010) 'The Detection of Acute HIV Infection', *The Journal of Infectioous Diseases,* 202: 1-8.

Collaboration, A.T.C. (2010) 'Causes of death in HIV-1—infected patients treated with antiretroviral therapy, 1996–2006: collaborative analysis of 13 HIV cohort studies', *Clinical Infectious Diseases*, 50(10): 1387-1396.

Couturier, J., Suliburk, J.W., Brown, J.M., Luke, D.J., Agarwal, N., Yu, X., Nguyen, C., Iyer, D., Kozinetz, C.A., Overbeek, P.A. and Metzker, M.L. (2015) 'Human adipose tissue as a reservoir for memory CD4 T cells and HIV', *AIDS (London, England)*, 29(6): 667.

Craigie, R. and Bushaman, F.D. (2012) 'HIV DNA integration', *Cold Springs Harbor Perspectivies in Medicine*, 2: 1-18.

Cribbs, S.K., Lennox, J., Caliendo, A.M., Brown, L.A. and Guidot, D.M. (2015) 'Healthy HIV-1-infected individuals on highly active antiretroviral therapy harbor HIV- 1 in their alveolar macrophages', *AIDS research and human retroviruses*, 31(1): 64- 70.

Crowell, T.A., Gebo, K.A., Blankson, J.N., Korthuis, P.T., Yehia, B.R., Rutstein, R.M., Moore, R.D., Sharp, V., Nijhawan, A.E., Mathews, W.C. and Hanau, L.H. (2015) 'Hospitalization rates and reasons among HIV elite controllers and persons with medically controlled HIV infection', *The Journal of infectious diseases*, 211(11): 1692-1702.

Cybulsky, M.I., Iiyama, K., Li, H., Zhu, S., Chen, M., Iiyama, M. and al, e. (2001) 'A major role for VCAM-1, but not ICAM-1, in early atherosclerosis', *Journal of Clinical Investigation*, 107: 1255-1262.

Dallas-Yang, Q., Jiang, G. and Sladek, F.M. (1998) 'Digestion of terminal restriction endonuclease recognition sites on PCR products', *BioTechniques*, 24: 582-584.

Damgaard, C.K., Andersen, S.E., Knudsen, B., Gorodkin, J. and Kjems, J. (2004) 'RNA interactions in the 5′ region of the HIV-1 genome', *Journal of Molecular Biology*, 336: 369-379.

Danforth, K., Granich, R., Wiedeman, D., Baxi, S. and Padian, N. (2017) 'Global Mortality and Morbidity of HIV/AIDS', in Holmes, K.K., Bertozz, S., Bloom, B.R. and Jha, P. (ed.) *Major Infectious Diseases: Disease Control Prioritiies*, 3rd edition, Washington DC: The International Bank for Reconstruction and Development/ The World Bamk.

Darlix, J.-L., Godet, J., Ivanyi-Nagy, R., Fossé, P., Mauffret, O. and Mély, Y. (2011) 'Flexible Nature and Specific Functions of the HIV-1 Nucleocapsid Protein', *Journal of Molecular Biology*, 410(4): 565-581.

Data Collection on Adverse Events of Anti-HIV drugs (D: A: D) Study Group, (2010) ' Factors associated with specific causes of death amongst HIV-positive individuals in the D: A: D Study', *Aids*, 24(10): 1537-1548.

Das, A.T., Harwig, A. and Berkhout, B. (2011) 'The HIV-1 Tat protein has a versatile role in activating viral transcription.', *Journal of virology*, 85(18): 9506-9516.

Deeks, S.G., Tracy, R. and Douek, D.C. (2013) 'Systemic Effects of Inflammation on Health during Chronic HIV Infection', *Immunity*, 39(4): 633-645.

Derdeyn, C.A., Decker, J.M., Bibollet-Ruche, F., Mokili, J.L., Muldoon, M., Denham, S.A., Heil, M.L., Kasolo, F., Musonda, R., Hahn, B.H. and Shaw, G.M. (200) 'Envelope-constrained neutralization-sensitive HIV-1 after heterosexual transmission', *Science*, 303:

2019-2022.

Douglas, J.L., Viswanathan, K., McCarroll, M.N., Gustin, J.K., Fruh, K. and Moses, A.V. (2009) 'Vpu directs the degradation of the HIV restriction factor BST-2/tetherin via beta-TrCP dependent mechanism', *Journal of Virology*, 83: 7931-7947.

Dow, D.E. and Bartlett, J.A. (2014) 'Dolutegravir, the Second-Generation of Integrase Strand Transfer Inhibitors (INSTIs) for the Treatment of HIV', *Infectious Diseases and Therapy*, 3(2): 83-102.

Dries, L.W.J.v.d., Gruters, R.A., Borden, S.B.C.H.-v.d., Kruip, M.J.H.A., Maat, M.P.M.d., Gorp, E.v. and Ende, M.E.v.d. (2015) 'von Willerbrand Factor is elevated in HIV patients with a history of thrombosis', *Frontiers in Microbiology*, 6(180): 1-8.

Dube, M., Bego, M.G., Paquay, C. and Cohen, E.C. (2010) 'Modulation of HIV-1 host interaction: role of the Vpu accessory protein', *Retrovirology*, 7(114): 1-19.

Dubois, N., Khoo, K.K., Ghossein, S., Seissler, T., Wolff, P., McKinstry, W.J., Mak, J., Paillart, J.C., Marquet, R. and Bernacchi, S. (2018) ' The C-terminal p6 domain of the HIV-1 Pr55Gag precursor is required for specific binding to the genomic RNA', *RNA biology*, 15(7): 923-936.

Duffy, P., Wang, X., Lin, P.H., Yao, Q. and Chen, C. (2009) 'IV Nef protein causes endothelial dysfunction in porcine pulmonary arteries and human pulmonary arteries endothelial cells', *Journal of Surgical Research*, 156(2): 257-264.

Duong-Ly, K. & Gabelli, S., 2014. Explanatory chapter: troubleshooting recombinant protein expression: general. In: *Methods in enzymology.* s.l.:Academic Press, pp. 209-229.

Marcus, J. *et al*., 2020. Comparison of overall and comorbidity-free life expectancy between insured adults with and without HIV infection, 2000-2016. *JAMA network open,* 3(6), pp. e207954-e207954.

Dwyer-Lindgren, L., Cork, M.A., Sligar, A., Steuben, K.M., Wilson, K.F., Provost, N.R.,

Mayala, B.K., VanderHeide, J.D., Collison, M.L., Hall, J.B. and Biehl, M.H., (2019) 'Mapping HIV prevalence in sub-Saharan Africa between 2000 and 2017', *Nature*, 570(7760): 189-193.

Ebner, B.F., Chueng, T. and Martinez, C.A. (2020) 'Epigenetics, HIV, and Cardiovascular Disease Risk', *Current Problems in Cardiology*, 100615: 1-9.

El-Sadr, W.M., Lundgren, J.D., Neaton, J.D., Gordin, F., Abrams, D., Arduino, R.C., Babiker, A., Burman, W., Clumeck, N., Cohen, C.J., Cohn, D., Cooper, D., Darbyshire, J., Emery, S., Fätkenheuer, G., Gazzard, B., Grund, B., Hoy, J., Klingman, K., Losso, M. *et al*. (2006) 'CD4+ count-guided antiretroviral treatment interruption of antiretroviral treatmen', *New England Journal of Medicine*, 355: 2283- 2296.

Engelman, A.N. and Singh, P.K. (2018) 'Cellular and molecular mechanisms of HIV- 1 integration targeting', *Cellular and Molecular Life Sciences*, 75: 2491-2507.

Erlandson, K.M. and Karris, M.Y. (2019) 'HIV and aging: reconsidering the approach to management of comorbidities', *Infectious Disease Clinics*, 33(3): 769-786.

Esbjörnsson, J., Månsson, F., Kvist, A., Isberg, P.E., Nowroozalizadeh, S., Biague, A.J., Silva, Z.J.d., Jansson, M., Fenyö, E.M., Norrgren, H. and Medstrand, P. (2012) 'Inhibition of HIV-1 disease progression by contemporaneous HIV-2 infection', *New England Journal of Medicine*, 367(3): 224-232.

Esquiaqui, J.M., Kharytonchyk, S., Drucker, D. and Telesnitsky, A. (2020) 'HIV-1 spliced RNAs display transcription start site bias', *RNA*, vol. 26, no. 6, pp. 708-714.

Fackler, O.T. and Baur, A.S. (2002) 'Live and let die: Nef functions beyond HIV replication', *Immunity*, 16(4): 493-497.

Fackler, O.T., Morris, A., Tibroni, N., Giese, S.I., Glass, B., Schwartz, O. and Hans-Krausslich (2006) 'Functional characterization of HIV-1 mutants in the context of viral infection', *Virology*, 351(2006): 322-339.

Fagiani, E. and Christofori, G. (2013) 'Angiopoietins in angiogenesis', *Cancer Letters*, 28(1): 18-26.

Fan, Y., Liu, C., Qin, X., Wang, Y., Han, Y. and Zhou, Y. (2010) 'The Role of ERK1/2 Signaling Pathway in Nef Protein Upregulation of the Expression of the Intercellular Adhesion Molecule 1 in Endothelial Cells', *Angiology*, 61(7): 669-678.

Fanales-Belasio, E., Raimondo, M., Suligoi, B. and Butto, S. (2010) 'HIV virology and pathogenetic mechanisms of infection: A brief overview', *Annali dellÍstituto Superiore di Sanita*, 46(1): 5-14.

Fang, X., Wang, J., O'Carroll, I.P., Mitchell, M., Zuo, X., Wang, Y., Yu, P., Liu, Y., Rausch, J.W., Dyba, M.A. and Kjems, J. (2013) 'An unusual topological structure of the HIV-1 Rev response element', *Cell*, 155(3): 594-605.

Fauci, A.S., Pantaleo, G., Stanley, S. and Weissman, D. (1996) 'Immunopathogenic mechanisms of HIV infection', *Annals of Internal Medicine*, 124(7): 654-663.

Feinstein, M.J., Bahiru, E., Achenbach, C., Longenecker, C.T., Hsue, P., So-Armah, K., Freiberg, M.S. and Lloyd-Jones, D.M. (2016) 'Patterns of cardiovascular mortality for HIV-infected adults in the United States: 1999 to 2013', *The American journal of cardiology*, 117(2): 214-220.

Feng, Y., Broder, C.C., Kennedy, P.E. and Berger, E.A. (1996) 'HIV-1 entry cofactor: functional cDNA cloning of a seven-transmembrane, G protein-coupled receptor', *Science*, 272(5263): 872-877.

Fernandes, J.D., Booth, D.S. and Frankel, A.D. (2016) 'A structurally plastic ribonucleoprotein complex mediates post-transcriptional gene regulation in HIV-1', *Wiley Interdisciplinary Reviews: RNA*, 7(4): 470-486.

Fiebig, E.W., Wright, D.J., Rawal, B.D., Garrett, P.E., Schumacher, R.T., Peddada, L., Heldebrant, C., Smith, R., Conrad, A., Kleinman, S.H. and Busch, M.P. (2003) 'Dynamics of

HIV viremia and antibody seroconversion in plasma donors: implications for diagnosis and staging of primary HIV infection', *AIDS*, 17: 1871- 1879.

Fiedler, U. and Augustin, H.G. (2006) 'Angiopoietins: a link between angiogenesis and inflammation', *TRENDS in Immunology*, 27(12): 552-558.

Fiedler, U., Krissl, T., Koidl, S., Weiss, C., Koblizek, T., Deutsch, U., Martiny-Baron, G., Marmé, D. and Augustin, H.G. (2003) 'Angiopoietin-1 and angiopoietin-2 share the same binding domains in the Tie-2 receptor involving the first Ig-like loop and the epidermal growth factor-like repeats', *Journal of biological chemistry*, 278(3): 1721- 1727.

Fiorentini, S., Marini, E., Caracciolo, S. and Caruso, A. (2006) 'Functions of the HIV- 1 matrix protein p17', *Microbiologica-Quarterly Journal of Microbiological Sciences*, 29(1): 1-10.

Ford, E.S., Puronen, C.E. and Sereti, I. (2009) 'Immunopathogenesis of asympotic chronic HIV infection: the calm before the storm', *Current Opinions in HIV and AIDS*, 4: 206-214.

Foster, J.L., Molina, R.P., Luo, T., Arora, V.K., Huang, Y., Ho, D.D. and Garcia, J.V. (2001) 'Genetic and functional diversity of human immunodeficiency virus type 1 subtype B Nef primary isolates', *Journal of virology*, 75(4): 1672-1680.

Fourie, C., Rooyen, J.V., Pieters, M., Conradie, K., Hoekstra, T. and Schutte, A. (2011) 'Is HIV-1 infection associated with endothelial dysfunction in a population of African ancestry in South Africa?', *Cardiovascular Journal of Africa*, 22(3): 134-141.

Francisci, D., Giannini, S., Baldelli, F., Leone, M., Belfiori, B., Guglielmini, G., Malincarne, L. and Gresele, P. (2009) 'HIV type 1 infection, and not short-term HAART, induces endothelial dysfunction', *AIDS*, 23(5): 589-596.

Frankel, A.D. and Young, J.A. (1998) 'HIV-1: fifteen proteins and an RNA', *Annual Review of Biochemistry*, 67: 1-25.

Freed, E.O. (2001) 'HIV-1 Replication', *Somatic Cell and Molecular Genetics*, 26: 1- 21.

Freed, E.O. (2015) 'HIV-1 assembly, release and maturation', *Nature Reviews Microbiology*, 13: 484-496.

Freiberg, M.S., Chang, C.C., Kuller, L.H., Skanderson, M., Lowy, E., Kraemer, K.L., Butt, A.A., Goetz, M.B., Leaf, D., Oursler, K.A. and Rimland, D. (2013) ' HIV infection and the risk of acute myocardial infarction', *JAMA internal medicine*, 173(8): 614- 622.

Gallay, P., Swingler, S., Song, J., Bushman, F. and Trono, D. (1995) 'HIV nuclear import is governed by the phosphotyrosine-mediated binding of matrix to the core domain of integrase', *Cell*, 83(4): 569-576.

Geffin, R., Wolf, D., Müller, R., Hill, M.D., Stellwag, E., Freitag, M., Sass, G., Scott, G.B. and Baur, A.S. (2000) 'Functional and structural defects in HIV type 1 nef genes derived from pediatric long-term survivors', *AIDS*, 16(17): 1855-1868.

Geyer, M., Fackler, O.T. and Peterlin, B.M. (2001) 'Structure-function relationships in HIV-1 Nef ', *EMBO Reports*, 2(7): 580-585.

Gilchrest, B.A., Nemore, R.E. and Maciag, T. (1980) 'Growth of human keratinocytes on fibronectin — Coated plates', *Cell Biology International Reports*, 4(11): 1009- 1016.

Go, E.P., Ding, H., Zhang, S., Ringe, R.P., Nicely, N., Hua, D., Steinbock, R.T., Golabek, M., Alin, J., Alam, S.M., Cupo, A., Haynes, B.F., Kappes, J.C., Moore, J.P., Sodroski, J.G. and Desaire, H. (2017) 'Glycosylation Benchmark Profile for HIV-1 Envelope Glycoprotein Production Based on Eleven Env Trimers', *Journal of Virology*, 91(9): 1-19.

Gochhait, S., Malhotra, D., Rai, E. & R.N.K. Bamezai, R., 2007. Automated Fluoroscence Sequencing and Troubleshooting.. In: *In Advanced techniques in soil microbiology.* Heidelberg ed. Berlin: Springer, pp. 35-51.

Gona, P.N., Gona, C.M., Ballout, S., Rao, S.R., Kimokoti, R., Mapoma, C.C. and Mokdad, A.H. (2020) 'Burden andd changes in HIV/AIDS morbidity and mortality in Southern Africa Development Community Countries, 1990-2017', *BMC Public Health*

, 20(867): 1-14.

Gonzalez, M.E. (2017) 'The HIV-1 Vpr protein: A multifaceted target for therapeutic intervention', *International Journal of Molecular Science*, 18(1): 1-21.

Gorshkova, I.I., Rausch, J.W., Grice, S.F.L. and Crouch, R.J. (2001) 'HIV-1 reverse transcriptase interaction with model RNA-DNA duplexes', *Analytical Biochemistry*, 291(2): 198-206.

Göttlinger, H.G., Sodroski, J.G. and Haseltine, W.A. (1989) 'Role of capsid precursor processing and myristoylation in morphogenesis and infectivity of human immunodeficiency virus type 1', *Processdings of the National Academy of Sciences of the United States of America*, 15: 5781-5785.

Gragnano, F., Golia, E., Natale, F., Bianchi, R., Pariggiano, I., Crisci, M., Diana, V., Fimiani, F., Limongelli, G., Russo, M., Cirillo, P. and Calabro, P. (2017) 'von Willerbrand Factor and cardiovascular disease: from a biochemical marker to an attractive therapeutic target', *Current Vascular Pharmocology*,15(5): 404-415.

Graham, S.M., Mwilu, R. and Liles, W.C. (2013) 'Clinical utility of biomarkers of endothelial activation and coagulation for prognosis in HIV infection', *Virulence*, 4(6): 564-571.

Graham, S.M., Rajwans, N., Jaoko, W., Estambale, B.B.A., McClelland, S.R., Overbaugh, J. and Liles, C.W. (2013) 'Endothelial activation biomarkers increase after HIV-1 acquistion: plasma vascular cell adhesion molecule-1 predicts disease progression', *AIDS*, 27(11): 1803-1813.

Greenea, W.C., Debyser, Z., Ikeda, Y., Freed, E.O., Stephens, E., Yonemoto, W., Buckheit, R.W., Este, J.A. and Cihlar, T. (2008) 'Novel targets for HIV therapy', *Antiviral Research*, 80: 251-265.

Strategies for Management of Antiretroviral Therapy (SMART) Study Group,. (.S. (2006) 'CD4+ count–guided interruption of antiretroviral treatment', *New England Journal of*

Medicine, 355(22): 2283-2296.

Grunfeld, C., Pang, M.I.Y.I.N., Doerrler, W., Shigenaga, J.K., Jensen, P. and Feingold, K.R. (1992) 'Lipids, lipoproteins, triglyceride clearance, and cytokines in human immunodeficiency virus infection and the acquired immunodeficiency syndrome', *The Journal of Clinical Endocrinology & Metabolism*, 74(5): 1045-1052.

Guaraldi, G., Orlando, G., Zona, 1.S., Menozzi, M., Carli, F., Garlassi, E., Berti, A., Rossi, E., Roverato, A. and Palella, F. (2011) 'Premature Age-Related Comorbidities Among HIV-Infected Persons Compared with the General Population', *Clinical Infectious Diseases*, 53(11): 1120-1126.

Guenzel, C.A., Herate, C. and Benichou, S. (2014) 'HIV-1 Vpr: A still enigmatic multitasker', *Frontiers in Microbiology*, 5: 1-13.

Gulnik, S., Erickson, J.W. and Xie, D. (2000) 'HIV protease: enzyme function and drug resistance', *Vitamins and Hormones*, 58: 213-256.

Guo, F., Hsieh, E., Lv, W., Han, Y., Xie, J., Li, Y., Song, X. and Li, T. (2017) 'Cardiovascular disease risk among Chinese antiretroviral-naïve adults with advanced HIV disease', *BMC Infectious Diseases*, 17(1): 1-10.

Gurtler, L., Aepfelbacher, M., Bauerfeind, U., Blumel, J., Burger, R. and Gartner, B. (2016) 'Human immunodeficiency virus', *Transfusion Medicine and Hemotherapy*, 43: 203-223.

Han, J., Latulippe, F., Rai, S. & Yim, E., 2010. Troubleshooting for the Proposed Construction of pBAD24-ompA. *Journal of Experimental Microbiology and Immunology,* Volume 14, pp. 146-152.

Hanna, D.B., Ramaswamy, C., Kaplan, R.C., Kizer, J.R., Anastos, K., Daskalakis, D., Zimmerman, R. and Braunstein, S.L. (2016) 'Trends in cardiovascular disease mortality among persons with HIV in New York City, 2001–2012', *Clinical Infectious Diseases*, 63(8): 1122-1129.

Haqqani, A.A. and Tilton, J.C. (2013) 'Entry inhibitors and their use in the treatment of HIV-1 infection', *Antiviral Research*, 98(2): 158-170.

Harris, R.S. and Liddament, M.T. (2004) 'Retroviral restriction by APOBEC proteins', *Nature Reviews Immunology*, 4: 868-877.

Hemelaar, J. (2012) 'The origin and diversity of the HIV-1 pandemic', *Trends in Molecular Medicine*, 18(3): 182-192.

Hemelaar, J., Elangovan, R., Yun, J., Dickson-Tetteh, L., Fleminger, I., Kirtley, S., Williams, B., Gouws-Williams, E., Ghys, P.D., Alash'le, G.A. and Agwale, S. (2019) 'Global and regional molecular epidemiology of HIV-1, 1990–2015: a systematic review, global survey, and trend analysis', *The Lancet infectious diseases*, 19(2): 143-155.

Hiscott, J., Kwon, H. and Génin, P. (2001) 'Hostile takeovers: viral appropriation of the NF-kB pathway', *The Journal of clinical investigation*, 107(2): 143-151.

Hladik, F. and McElrath, J.M. (2008) 'Setting the stage: host invasion by HIV', *Nature Reviews Immunology*, 8: 447-458.

Honeycutt, J.B., Thayer, W.O., Baker, C.E., Ribeiro, R.M., Lada, S.M., Cao, Y., Cleary, R.A., Hudgens, M.G., Richman, D.D. and Garcia, J.V. (2017) 'HIV persistence in tissue macrophages of humanized myeloid-only mice during antiretroviral therapy', *Nature medicine*, 23(5): 638-643.

Hruz, P.W. (2011) ' Molecular mechanisms for insulin resistance in treated HIV- infection', *Best practice & research Clinical endocrinology & metabolism*, 25(3): 459- 468.

Hsue, P.Y., Hunt, P.W., Schnell, A., Kalapus, C., Hoh, R., Ganz, P., Martin, J.N. and Deeks, S.G. (2009) 'Role of viral replication, antiretroviral therapy, and immunodeficiency in HIV-associated atherosclerosis', *AIDS (London, England)*, 23(9): 1059-1067.

Hu, W.-S. and Hughes, S.H. (2012) 'HIV-1 reverse transcription', *Cold Springs Harbor Perspectives in Medicine*, 2: 1-22.

Hunt, P.W., Lee, S.A. and Siedner, M.J. (2016) 'Immunologic biomarkers, morbidity and mortality in treated HIV infection', *The Journal of Infectious Diseases*, 214: 44- 51.

Hwang, S.J., Ballantyne, C.M., Sharrett, A.R., Smith, L.C., Davis, C.E., Gotto, A.M.J. and Boerwinkle, E. (1997) 'Circulating adhesion molecules VCAM-1, ICAM-1, and E- selectin in carotid atherosclerosis and incident coronary heart disease cases: the Atherosclerosis Risk in Communities (ARIC) study', *Circuulation*, 96: 4219-4225.

Ishikawa, H., Tachikawa, H., Miura, Y. and Takahashi, N. (2006) 'TRIM11 binds to and destabilizes a key component of the activator-mediated cofactor complex (ARC105) through the ubiquitin-proteasome system', *FEBS Letters*, 20: 47824-4792.

Islam, F.M., Wu, J., Jansson, J. and Wilson, D.P. (2012) 'Relative risk of cardiovascular disease among people living with HIV: a systematic review and meta- analysis', *HIV Medicine*, 13(8): 453-468.

Jafarzade, B.S., Bolhassani, A., Sadat, S.M. and Yaghobi, R. (2017) 'Delivery of HIV-1 Nef Protein in Mammalian Cells Using Cell Penetrating Peptides as a Candidate Therapeutic Vaccine', *International Journal of Peptide Research and Therapeutics*, 23: 145-153.

Jeevani, T. (2011) 'Symptoms of AIDS related opportunistic infections and their effects on human body', *Journal of AIDS and Clinical Research*, 2(6): 132.

Jin, S.W., Alsahafi, N., Kuang, X.T., Swann, S.A., Toyoda, M., Göttlinger, H., Walker, B.D., Ueno, T., Finzi, A., Brumme, Z.L. and Brockman, M.A. (2019) 'Natural HIV-1 Nef polymorphisms impair SERINC5 downregulation activity', *Cell reports*, 29(6): 1449-1457.

Jin, Y.-J., Cai, C.Y., Zhang, X., Zhang, H.-T., Hirst, J.A. and Burakoff, S.J. (2005) 'HIV Nef-mediated CD4 downregulation is Adaptor Complex 2 dependent ', *Journal of Immunology,* 175: 3157-3164.

Johnston, M.I. and Fauci, A.S. (2008) 'An HIV vaccine—challenges and prospects', *New England Journal of Medicine*, 359(9): 888-890.

Joseph, A.M., Ladha, J.S., Mojamdar, M. and Mitra, D. (2003) 'Human immunodeficiency virus-1 Nef protein interacts with Tat and enhances HIV-1 gene expression', *FEBS Letters*, 548(1-3): 37-42.

Kanda, K., Hayman, G.T., Silverman, M.D. and Lelkes, P.I. (1998) 'Comparison of ICAM-1 and VCAM-1 Expression in Various Human Endothelial Cell Types and Smooth Muscle Cells', *Endothelium*, 6(1): 33-44.

Kandathil, A.J., Sugawara, S. and Balagopal, A. (2016) 'Are T cells the only HIV-1 reservoir?', *Retrovirology*, 13(1): 1-10.

Kariuki, S.M., Selhorst, P., Ariën, K.K. and Dorfman, J.R. (2017) 'The HIV-1 transmission bottleneck', *Retrovirology*, 14(22): 1-19.

Karn, J. and Stoltzfus, C.M. (2012) 'ranscriptional and posttranscriptional regulation of HIV-1 gene expression', *Cold Spring Harbor perspectives in medicine*, 2(2): 1-18.

Karsan, A., Yee, E. and Harlan, J.M. (1996) 'Endothelial Cell Death Induced by Tumor Necrosis Factor-α Is Inhibited by the Bcl-2 Family Member, A1*', *Cell Biology and Metabolism*, 271(44): 27201-27204.

Keele, B.F., Giorgi, E.E., Salazar-Gonzalez, J.F., Decker, J.M., Pham, K.T., Salazar, M.G., Sun, C., Grayson, T., Wang, S., Li, H. and Wei, X. (2008) ' Identification and characterization of transmitted and early founder virus envelopes in primary HIV-1 infection', *Proceedings of the National Academy of Sciences*, 105(21): 7552-7557.

Kempf, N., Postupalenko, V., Bora, S., Didier, P., Arntz, Y., Rocquigny, H.d. and Mély, Y. (2015) 'The HIV-1 Nucleocapsid Protein Recruits Negatively Charged Lipids to Ensure Its Optimal Binding to Lipid Membranes', *Journal of Virology*, 89(3): 1756- 1767.

Kestler, H.W., Ringler, D.J., Mori, k., Panicali, D.L., Sehgal, P.K. and Daniel, M.D. (1991) 'Importance of the nef gene for maintenance of high virus loads and for development of AIDS', *Cell*, 65: 651-662.

Kinlock, B.L., Wang, Y., Turner, T.M., Wang, C. and Liu, B. (2014) 'Transcytosis of HIV-1 through Vaginal Epithelial Cells Is Dependent on Trafficking to the Endocytic Recycling Pathway', *PLoS One*, 9(5): e96760.

Kirchhoff, F., Greenough, T.C., Brettler, D.B., Sullivan, J.L. and Desrosiers, R.C. (1995) 'Absence of Intact nef Sequences in a Long-Term Survivor with Nonprogressive HIV-1 Infection', *New England Journal of Medicine*, 332: 228-232.

Klasse, P.J. (2014) 'Neutralization of virus infectivity by antibodies: old problems in new perspectives', *Advances in biology*, 1-43.

Kline, E.R. and Sutliff, R.L. (2008) 'The Roles of HIV-1 Proteins and Antiretroviral Drug Therapy in HIV-1-Associated Endothelial Dysfunction', *Journal of Investigative Medicine*, 56(5): 752-769.

Kogan, M. and Rappaport, J. (2011) 'HIV-1 accessory protein Vpr: Relevance in the pathogenesis of HIV and potential for therapeutic intervention', *Retroviology*, 8(25): 1-20.

Kohlstaedt, L.A., Wang, J., Friedman, J.M., Rice, P.A. and Steitz, T.A. (1992) 'Crystal structure at 3.5 A resolution of HIV-1 reverse transcriptase complexed with an inhibitor', *Science*, 256(5065): 1783-1790.

Konnyu, B., Sadiq, S.K., Turanyl, T., Hirmondo, R., Muller, B., Krausslich, H.-G., Coveney, P.V. and Muller, V. (2013) 'Gag-Pol processing during HIV-1 virion maturation: A systems biology approach', *PLos Computational Biology*, 9(6): 1-15.

Korniy, N., Goyal, A., Hoffmann, M., Samatova, E., Peske, F., Pöhlmann, S. and Rodnina, M.V. (2019) 'Modulation of HIV-1 Gag/Gag-Pol frameshifting by tRNA abundance', *Nucleic Acids Research*, 47(10): 5210-5222.

Koussounadis, A., Langdon, S.P., Um, I.H., Harrison, D.J. and Smith, V.A. (2015) 'Relationship between differentially expressed mRNA and mRNA-protein correlations in a xenograft model system', *Scientific Reports*, 5(10775): 1-9.

Krishnan, L., Li, X., Naraharisetty, H.L., Hare, S., Cherepanov, P. and Engelman, A. (2010) 'Structure-based modeling of the functional HIV-1 intasome and its inhibition', *PNAS*, 107(36): 15910-15915.

Kuang, X.T., Li, X., Anmole, G., Mwimanzi, P., Shahid, A., Le, A.Q., Chong, L., Qian, H., Miura, T., Markle, T. and Baraki, B. (2014) 'Impaired Nef function is associated with early control of HIV-1 viremia', *Journal of Viirology*, 88(17): 10200-102013.

Kuritzkes, D.R. (2011) 'Drug resistance in HIV-1', *Current Opinions in Virology*, 1(6): 582-589.

Lackner, A.A., Lederman, M.M. and Rodriguez, B. (2012) 'HIV Pathogenesis: The Host', *Cold Spring Habor Perspectives in Medicine*, 2: 1-24.

Lam, G.Y., Huang, J. and Brumell, J.H. (2010) 'The many roles of NOX2 NADPH oxidase-derived ROS in immunity', *In Seminars in Immunopathology*, 32(4): 415-430.

Landi, A., Iannucci, V., Nuffel, A.V., Meuwissen, P. and Verhasselt, B. (2011) 'One protein torule them all: Modulation of cell surface receptors and molecules by HIV Nef', *Current HIV Research*, 9(7): 496-504.

Lau, K.A. and Wong, J.J.L. (2013) 'Current trends of HIV recombinantion worldwide', *Infectious Disease Reports*, 5(4): 15-21.

Lee, B.K., Lee, W.J. and Jung, Y.-S. (2017) 'Chrysin Attenuates VCAM-1 Expression and Monocyte Adhesion in Lipopolysaccharide-Stimulated Brain Endothelial Cells by Preventing NF-κB Signaling', *International Journal of Molecular Sciences*, 18(7): 1- 12.

Lee, S.-Y., Zaske, A.-M., Novellino, T., Danila, D., Ferrari, M., Conyers, J. and Decuzzi, P. (2011) 'Probing the mechanical properties of TNF-α stimulated endothelial cell with atomic force microscopy', *International Journal of Nanomedicine*,6: 179-195.

Lenassi, M., Cagney, G., Liao, M., Vaupotic, T., Bartholomeeusen, K., Cheng, Y., Krogan, N.J., Plemenitas, A. and Peterlin, B.M. (2010) 'HIV Nef is serceted in exosomes and

triggers apoptosis in bystander CD4+ T cells ', *Traffic*, 11: 110-123.

Liao, J.K. (2013) 'Linking endothelial dysfunction with endothelial cell activation', *The Journal of Clinical Investigation*, 123(2): 540-541.

Li, H., Dou, J., Ding, L. and Spearman, P. (2007) 'Myristoylation is required for human immunodeficiency virus type 1 Gag-Gag multimerization in mammalian cells', *Journal of virology*, 81(23): 12899-12910.

Lin, S., Nadeau, P.E. and Mergia, A. (2015) 'HIV inhibits endothelial reverse cholesterol transport through impacting subcellular Caveolin-1 trafficking', *Retroovirology*, 12(1): 62.

Liu, X. and Kumar, A. (2015) 'Differential signaling mechanism for HIV-1 Nef- mediated production of IL-6 and IL-8 in human astrocytes', *Scientific Reports*, 5(9867): 1-13.

Lo, J., Abbara, S., Shturman, L., Soni, A., Wei, J., Rocha-Filho, J.A., Nasir, K. and Grinspoon, S.K. (2010) 'Increased prevalence of subclinical coronary atherosclerosis detected by coronary computed tomography angiography in HIV-infected men', *AIDS (London, England)*, 24(2): 243.

Lukasz, A., Hellpap, J., Horn, R., Kielstein, J.T., David, S., Haller, H. and al., e. (2008) 'Circulating angiopoietin-1 and angiopoiettin-2 in critically ill patients: development and clinical application of two new immuunoassays', *Critical Care*, 12(4): 1-11.

Luo, X., Fan, Y., Park, I.W. and He, J.J. (2015) 'Exosomes are unlikely involved in intercellular Nef transfe', *PloS one*, 10(4): 1-25.

Lusic, M. and Siliciano, R.F. (2017) 'Nuclear landscape of HIV-1 infection and integration', *Nature Reviews Microbiology*, 15: 69-82.

Lv, Z., Chu, Y. and Wang, Y. (2015) 'HIV protease inhibitors: a review of molecular selectivity and toxicity', *HIV/AIDS (Auckland)*, 7: 95-104.

Mendoza, C. *et al*., 2020. Antiretroviral Therapy for HIV-2 Infection in Non-Endemic Regions. *AIDS Reviews,* 22(1), pp. 44-56.

Mann, J.K., Byakwaga, H., Kuang, X.T., Le, A.Q., Brumme, C.J., Mwimanzi, P., Omarjee, S., Martin, E., Lee, G.Q., Baraki, B., Danroth, R., McCloskey, R., Muzoora, C. and al, D.R.B.e. (2013) 'Ability of HIV-1 Nef to downregulate CD4 and HLA class Idiffers among viral subtypes', *Retrovirology*, 10(100): 1-16.

Manen, D.v., Wout, A.B.v. and Schuitemaker, H. (2012) 'Viral and host determinants of HIV-1 disease progession', in Volberding, P., Greene, W., Lange, J.M.A., Gallant, J.E. and Sewankambo, N. (ed.) *Sande's HIV/AIDS Medicine*, Saunders.

Mann, J.K., Byakwaga, H., Kuang, X.T., Le, A.Q., Brumme, C.J., Mwimanzi, P., Omarjee, S., Martin, E., Lee, G.Q., Baraki, B., Danroth, R., McCloskey, R., Muzoora, C. and al, D.R.B.e. (2013) 'Ability of HIV-1 Nef to downregulate CD4 and HLA class I differs among viral subtypes', *Retrovirology*, 10(100): 1-16.

Marecki, J.C., Cool, C.D., Parr, J.E., Beckey, V.E., Luciw, P.A., Tarantal, A.F., Carville, A., Shannon, R.P., Cota-Gomez, A., Tuder, R.M., Voelkel, N.F. and Flores, S.C. (2006) 'HIV-1 Nef Is Associated with Complex Pulmonary Vascular Lesions in SHIV-nef–infected Macaques', *American Journal of respiratory and Critical Care Medicine*, 174(4): 437-445.

Marecki, J., Cool, C., Voelkel, N., Luciw, P. and Flores, S. (2005) 'Evidence for Vascular Remodeling in the Lungs of Macaques infected with Simian Immunodeficiency Virus/HIV Nef Recombinant Virus', *Chest*, 128(6): 621S-622S.

Marlink, R.G., Allan, J.S., McLane, M.F., Essex, M., Anderson, K.C. and Groopman, J.E. (1986) 'Low sensitivity of ELISA testing in early HIV infection', *The New England Journal of Medicine*, 315(24): 1549.

Martínez-Ayala, P., Alanis-Sánchez, G.A., L.A.González-Hernández, Álvarez-Zavala, M., Cabrera-Silva, R.I., Andrade-Villanueva, J.F., Sánchez-Reyes, K., Ramos-Solano, M., Castañeda-Zaragoza, D.A., Cardona-Müller, D. and Totsuka-Sutto, S. (2020)

'Aortic stiffness and central hemodynamics in treatment-naïve HIV infection: a cross-sectional study', *BMC Cardiovascular Disorders*, 20(1): 1-8.

Mathebula, R.L., Maimela, E. and Ntuli, N.S. (2020) 'The prevalence of selected noncommunicable disease risk factors among HIV patients on antii-retoviral therapy in Bushbuckridge sub-district, Mpumalanga province', *BMC Public Health*, 20(247): 1-10.

Matzen, K., Dirkx, A.E.M., Egbrink, M.G.A.o., Speth, C., Götte, M., Ascherl, G., Grimm, T., Griffioen, A.W. and Stürzl, M. (2004) 'HIV-1 Tat increases the adhesion ofmonocytes and T-cells to the endothelium in vitro and in vivo: implications for AIDS- associated vasculopathy', *Virus Research*, 104: 145-155.

Mazzuca, P., Caruso, A. and Caccuri, F. (2016) 'HIV-1 infection, microenvironment and endothelial cell dysfunction', *The New Microbiologica*, 39(3): 163-173.

Meurs, M.v., Kümpers, P., Ligtenberg, J.J.M., Meertens, J.H.J.M., Molema, G. and Zijlstra, J.G. (2009) 'Bench-to-bedside review: Angiopoietin signalling in critical illness - a future target?', *Critical care*, 13(2): 1-12.

Mezoh, G., (2021) ‗Investigation into the Effect of HIV Viral Proteins on Endothelial Function in the HIV-Infected Population ‘, PhD thesis, University of the Witwatersrand, Johannesburg.

Mezoh, G., Lutchman, N., Prigge, K., Cave, E., Worsley, C., Mayne, E., Mabvakure, B., Lambson, B., Moore, P.L. and Crowther, N.J. (2018) 'Polymorphisms in HIV-1 nef and tat associated with endothelial dysfunction', Keystone Symposia Conference X8: HIV and Co-Infections: Pathogenesis, Inflammation and Persistence, British Columbia, Canada, 1-14.

Mezoh, G., Lutchman, N., Worsley, C., Gededzha, M., Mayne, E., Martinson, N., Moore, P.L. and Crowther, N.J. (2022) 'Biomarkers of Endothelial Activation in Black South African HIV-Positive Subjects are Associated with Both High Viral Load and Low CD4 Counts', *AIDS RESEARCH AND HUMAN RETROVIRUSES*, 38(2): 152- 161.

Migueles, S.A. and Connors, M. (2010) 'Long-term Nonprogressive Disease Among Untreated HIV-Infected Individuals', *JAMA*, 304(2): 194-201.

Milestone, D.S., O'Donnell, P.E., Stavrakis, G., Mortensen, R.M. and Davis, V.M. (2000) 'E-selectin expression and stimulation by inflammatory mediators are developmentally regulated during embryogenesis', *Laboratory Investigation*, 80: 943-954.

Miller, T.L., Borkowsky, W., DiMeglio, L.A., Dooley, L., Geffner, M.E., Hazra, R., McFarland, E.J., Mendez, A.J., Patel, K., Siberry, G.K. and Van Dyke, R.B., (2012) 'Metabolic abnormalities and viral replication are associated with biomarkers of vascular dysfunction in HIV-infected children', *HIV Medicine*, 13: 264-275.

Miller, T.L., Somarriba, G., Orav, E.J., Mendez, A.J., Neri, D., Schaefer, N., Forster, L., Goldberg, R., Scott, G.B. and Lipshultz, S.E. (2010) 'Biomarkers of vascular dysfunction in children infected with human immunodeficiency virus-1', *Journal of acquired immune deficiency syndromes*, 55(2): 182-188.

Mosepele, M., Mohammed, T., Mupfumi, L., Moyo, S., Bennett, K., Lockman, S., Hemphill, L.C. and Triant, V.A. (2018) 'HIV disease is associated with increased biomarkers of endothelial dysfunction despite viral suppression on long-term antiretroviral therapy in Botswana', *Cardiovascular Journal of Africa*, 29(3): 155-162.

Mouscadet, J.-F. and Tchertanov, L. (2009) 'Raltegravir: molecular basis of its mechanism of action', *European Journal of Medical Research,* 14(S3): 5-16.

Mu, H., Chai, H., Lin, P.H., Yao, Q. and Chen, C. (2007) 'Current update on HIV-associated vascular disease and endothelial dysfunction', *World journal of surgery*, 31(4): 632-643.

Muller, H.P. and Varmus, H.E. (1994) 'DNA bending creates favored sites for retroviral integration: an explanation for preferred insertion sites in nucleosomes', *The EMBO Journal*, 13(19): 4704-4714.

Muratori, C., Cavallin, L.E., Krätzel, K., Tinari, A., Milito, A.D., Fais, S., D'Aloja, P., Federico, M., Vullo, V., Fomina, A. and Mesri, E.A. (2009) 'Massive secretion by T cells is caused by HIV Nef in infected cells and by Nef transfer to bystander cells', *Cell host & microbe*, 6(3): 218-230.

Musumeci, D., Riccardi, C. and Montesarchio, D. (2015) 'G-Quadruplex forming oligonucleotides as anti-HIV agents', *Molecules*, 20(9): 17511-17532.

Mwimanzi, P., Markle, T.J., Martin, E., Ogata, Y., Kuang, X.T., Tokunaga, M., Mahiti, M., Pereyra, F., Miura, T., Walker, B.D., Brumme, Z.L., Brockman, M.A. and Ueno, T. (2013) 'Attenuation of multiple Nef functions in HIV-1 elite controllers', *Retrovirology*, 10(1): 1-12.

Ndung'u, T., Renjifo, B. and Essex, M. (2001) 'Construction and Analysis of an Infectious Human Immunodeficiency Virus Type 1 Subtype C Molecular Clone', *Journal of Virology*, 75(11): 4964-4972.

Nomaguchi, M., Fujita, M. and Adachi, A. (2008) 'Role of HIV-1 Vpu protein for virus spread and pathogenesis', *Microbes and Infection*, 10(9): 960-967.

Nsagha, D.S., Assob, J.C.N., Njuna, A.L., Tanue, E.A., Kibu, O.D., Ayima, C.W. and Ngowe, M.N. (2015) 'Risk factors of cardiovascular diseases in HIV/AIDS patients on HAART', *The open AIDS journal*, 6: 51.

Nwosu, Z.C., Ebert, M.P., Dooley, S. and Meyer, C. (2016) 'Caveolin-1 in theregulation of cells metabolism: a cencer perspective', *Molecular Cancer*, 15(1): 1-12.

Nyamweya, S. (2013) 'Comparing HIV-1 and HIV-2 infection: Lessons for viral immunopathogenesis', *Reviews in Medical Virology*, 23: 221-240.

Ohlmann, T., Mngardi, C. and MarceloLopez-Lastra (2014) 'Translation initiation of the HIV-1 mRNA', *Translation*, 2(2): 1-12.

Page, A.V. and Liles, W.C. (2013) 'Biomarkers of endothelial activation/dysfunction in infectious diseases', *Virulence*, 4(6): 507-516.

Palella Jr, F.J. and Phair, J.P., (2011) ‗Cardiovascular disease in HIV infection ‘. *Current opinion in HIV and AIDS*, 6(4): 266.

Pan, D., Xuan, B., Sun, Y., Huang, S., Xie, M., Bai, Y., Xu, W. and Qian, Z. (2016) 'An intein-mediated modulation of protein stability system and its application to study human cytomegalovirus essential gene function', *Scientific Reports*, 6(1): 1-11.

Pauwels, R. (2004) 'New non-nucleoside reverse transcriptase inhibitors (NNRTIs) in development for the treatment of HIV infections', *Current Opinion in Pharmacology*, 4(5): 437-446.

Paxton, W., Connor, R.I. and Landau, N.R. (1993) 'Incorporation of Vpr into human immunodeficiency virus type 1 virions: requirement for the p6 region of gag and mutational analysis', *Journal of Virology*, 67(12): 7229-7237.

Pebody, R. (2021) *Types of antiretroviral medications*, https://www.aidsmap.com/about-hiv/types-antiretroviral-medications [Accessed 25 November 2021].

Pedersen, K.K., Pedersen, M., Trøseid, M., Gaardbo, J.C., Lund, T.T., Thomsen, C., Gerstoft, J., Kvale, D. and Nielsen, S.D. (2013) 'Microbial translocation in HIV infection is associated with dyslipidemia, insulin resistance, and risk of myocardial infarction', *JAIDS Journal of Acquired Immune Deficiency Syndromes*, 64(5): 425- 433.

Pereyra, F., Lo, J., Triant, V.A., Wei, J., Buzon, M.J., Fitch, K.V., Hwang, J., Campbell, J.H., Burdo, T.H., Williams, K.C. and Abbara, S. (2012) 'Increased coronary atherosclerosis and immune activation in HIV-1 elite controllers', *IDS (London, England)*, 26(18): 2409.

Peyvandi, F., Garagiola, I. and Baronciani, L. (2011) 'Role of von Willebrand Factor in the haemostasis', *Blood Transfus,* 9(S2): 3-8.

Poon, A.F., Swenson, L.C., Dong, W.W., Deng, W., Pond, S.L.K., Brumme, Z.L., Mullins, J.I., Richman, D.D., Harrigan, P.R. and Frost, S.D. (2010) 'Phylogenetic Analysis of Population-Based and Deep Sequencing Data to Identify Coevolving Sites in the nef Gene

of HIV-1', *Molecular Biology and Evolution*, 27(4): 819-832.

Poorolajal, J. *et al*., 2016. Survival rate of AIDS disease and mortality in HIV-infected patients: a meta-analysis. *Public health,* Volume 139, pp. 3-12.

Preston, B.D., Poiesz, B.J. and Loeb, L.A. (1988) 'Fidelity of HIV-1 reverse transcriptase', *Science*,242(4882): 1168-1171.

Qian, K., Morris-Natschke, S.L. and Lee, K.-H. (2009) 'HIV Entry Inhibitors and Their Potential in HIV Therapy', *Medical Research Reviews*, 29(2): 369-393.

Qin, J.Y., Zhang, L., Clift, K.L., Hulur, I., Xiang, A.P., Ren, B.-Z. and Lahn, B.T.(2010) 'Systematic Comparison of Constitutive Promoters and the Doxycycline- Inducible Promoter', *PloS One*, 5(5): e10611.

Raitakaari, O.T. and Celermajer, D.S. (2000) 'Flow-mediated dilatation', *British Journal of Clinical Pharmacology*, 50: 397-404.

Ramji, D.P. and Davies, T.S. (2015) 'Cytokines in atherosclerosis: Key players in all stages of disease and promising therapeutic targets', *Cytokine & Growth Factor Reviews*, 26(6): 673-685.

Remme, M., Siapka, M., Sterck, O., Ncube, M., Watts, C. and Vassall, A. (2016) 'Financing the HIV response in sub-Saharan Africa from domestic sources: moving beyond a normative approach', *Social Science & Medicine*, 169: 66-76.

Rethy, L., Feinstein, M.J., Sinha, A., Achenbach, C. and Shah, S.J. (2020) 'Coronary microvascular dysfunction in HIV: a review', *Journal of the American Heart Association*, 9(1): 1-13.

Ridker, P.M., Hennekens, C.H., Roitman-Johnson, B., Stampfer, M.J. and Allen, J. (1998) 'Plasma concentration of soluble intercellular adhesion molecule 1 and risks of future myocardial infarction in apparently healthy men', *Lancet*, 351: 88-92.

Roebuck, K.A. and Saifuddin, M. (1999) 'Regulation of HIV-1 transcription', *Gene*

Expression the Journal of Liver Research, 8(2): 67-84.

Rosa, A., Chande, A., Ziglio, S., Sanctis, V.D., Bertorelli, R., Goh, S.L., McCauley, S.M., Nowosielska, A., Antonarakis, S.E., Luban, J. and Santoni, F.A. (2015) 'HIV-1 Nef promotes infection by excluding SERINC5 from virion incorporation', *Nature*, 526(7572): 212-217.

Ruben, S., Perkins, A., Purcell, R., Joung, K., Sia, R., Burghoff, R., Haseltine, W.A. and Rosen, C.A. (1989) 'Structural and functional characterization of human immunodeficiency virus tat protein', *Journal of Virology*, 63(1): 1-8.

Roux, K., 2009. Optimization and Troubleshooting in PCR. *Cold Spring Harbor Protocols,* Volume 4, pp. 1-7.

Ruelas, D.S. and Greene, W.C. (2013) 'n integrated overview of HIV-1 latency', *Cell*, 155(3): 519-529.

Russell, R.A., Moore, M.D., Hu, W.-S. and Pathak, V.K. (2009) 'APOBEC3G induces a hypermutation gradient: purifying selection at multiple steps during HIV-1 replication results in levels of G-to-A mutations that are high in DNA, intermediate in cellular viral RNA, and low in virion RNA', *Retrovirology*, 6(1): 1-15.

Schaefer, M.R., Wonderlich, E.R., Roeth, J.F., Leonard, J.A. and Collins, K.L. (2008) 'HIV-1 Nef targets MHC-1 and CD4 for degradation via a final common beta-COP- dependent pathway in T cells', *PLOS Pathogens*, 4(8): 1-18.

Schneck, N.A., Ivleva, V.B., Cai, C.X., Cooper, J.W. and Lei, Q.P. (2020) 'Characterization of the furin cleavage motif for HIV-1 trimeric envelope glycoprotein by intact LC-MS analysis', *Analyst*, 145(5): 1636-1640.

Schouten, J., Wit, F.W., Stolte, I.G., Kootstra, N.A., Valk, M.v.d., Geerlings, S.E., Prins, M., Reiss, P. and Group, f.t.A.C.S. (2014) 'Cross-sectional Comparison of the Prevalence of Age-Associated Comorbidities and Their Risk Factors Between HIV- Infected and Uninfected Individuals: The AGEhIV Cohort Study', *Clinical Infectious Diseases*, 59(12):

1787-1797.

Semaan, H.B., Gurbel, P.A., Anderson, J.L., Muhlestein, J.B., Carlquist, J.F., Horne, B.D. and Serebruany, V.L. (2000) 'Soluble VCAM-1 and E-Selectin, but Not ICAM-1 Discriminate Endothelial Injury in Patients with Documented Coronary Artery Disease', *Cardiology*, 93(1-2): 7-10.

Shah, A.S., Stelzle, D., Lee, K.K., Beck, E.J., Alam, S., Clifford, S., Longenecker, C.T., Strachan, F., Bagchi, S., Whiteley, W. and Rajagopalan, S. (2018) 'Global burden of atherosclerotic cardiovascular disease in people living with HIV: systematic review and meta-analysis', *Circulation*, 138(11): 1100-1112.

Shah, A.S., Stelzle, D., Lee, K.K., Beck, E.J., Alam, S., Clifford, S., Longenecker, C.T., Strachan, F., Bagchi, S., Whiteley, W. and Rajagopalan, S. (2018) 'Global burden of atherosclerotic cardiovascular disease in people living with HIV: systematic review and meta-analysis', *Circulation*, 138: 1100-1112.

Shaw, G.M. and Hunter, E. (2012) 'HIV Transmission', *Cold Spring Habour Perspective in Medicine*, 2: 1-24.

Shelton, M.N., Huang, M.B., Ali, S.A., Powell, M.D. and Bond, V.C. (2012) 'ecretion modification region-derived peptide disrupts HIV-1 Nef's interaction with mortalin andblocks virus and Nef exosome release', *Journal of virology*, 86(1): 406-419.

Shen, C., Ding, M., D. Ratner, R.C.M., Chen, Y. and Gupta, P. (2012) 'Evaluation of cervical mucosa in transmission bottleneck during acute HIV-1 infection using a cervical tissue-based organ culture', *PLoS ONE*, 7(3): 1-10.

Shenoy, A.R. and Visweswariah, S.S. (2003) 'Site-directed mutagenesis using a single mutagenic oligonucleotide and DpnI digestion of template DNA', *Analytical Biochemistry*, 319: 335-336.

Shiel, W.C. (2018) *Medical Definition of Cardiovascular disease*,

https://www.medicinenet.com/heart_disease_pictures_slideshow_visual_guide/article.htm [Accessed 14 September 2020].

Sierra-Aragón, S. and Walter, H. (2012) 'Targets for Inhibition of HIV Replication: Entry, Enzyme Action, Release and Maturation', *Intervirology*, 55: 84-97.

Singh, R.K., Lau, D., Noviello, C.M., Ghosh, P. and Guatelli, J.C. (2009) 'An MHC-I cytoplasmic domain/HIV-1 Nef fusion binds directly to the subunit of the AP-1 endosomal coat complex', *PLoS One*, 4: 6-15.

Sluis-Cremer, N., Arion, D. and Parniak, M.A. (2000) 'Molecular mechanisms of HIV-1 resistance to nucleoside reverse transcriptase inhibitors (NRTIs)', *Cellular and Molecular Life Sciences,* 57: 1408-1422.

So-Armah, K. and Freiberg, M. (2014) 'CVD risk in an aging HIV population – not just a question of biology', *Current Opinions in HIV/AIDS*, 9(4): 346-354.

Sowinski, S., Jolly, C., Berninghausen, O., Purbhoo, M.A., Chauveau, A., Köhler, K., Oddos, S., Eissmann, P., Brodsky, F.M., Hopkins, C., Önfelt, B., Sattentau, Q. and Davis, D.M. (2008) 'Membrane nanotubes physically connect T cells over long distances presenting a novel route for HIV-1 transmission', *Nature cell biology*, 10(2):211-219.

Spiel, A.O., Gilbert, J.C. and Jilma, M.D.B. (2008) 'Von Willebrand Factor in Cardiovascular Disease', *Circulation*, 117(11): 1449-59.

Spiliotis, M. (2012) 'Inverse fusion PCR cloning', *PLoS One*, 7(4): e35407.

Stacey, A.R., Norris, P.J., Qin, L., Haygreen, E.A., Taylor, E., Heitman, J., Lebedeva, M., DeCamp, A., Li, D., Grove, D., Self, S.G. and Borrow, P. (2009) ' Induction of a striking systemic cytokine cascade prior to peak viremia in acute human immunodeficiency virus type 1 infection, in contrast to more modest and delayed responses in acute hepatitis B and C virus infections', *Journal of virology*, 83(8): 3719-3733.

Stein, J.H., Brown, T.T., Ribaudo, H.J., Chen, Y., Yan, M., Lauer-Brodell, E.,

McComsey, G.A., Dubé, M.P., Murphy, R.L., Hodis, H.N. and J.S. Currier, J.S. (2013) 'Ultrasonographic measures of cardiovascular disease risk in antiretroviral treatment-naive individuals with HIV infection', *AIDS (London, England)*, 27(6): 929.

Stekler, J.D., Tapia, K., Maenza, J., Stevens, C.E., Ure, G.A., O'Neal, J.D., Lane, A., Mullins, J.I., Coombs, R.W., Holte, S. and Collier, A.C. (2018) 'No Time to Delay! Fiebig Stages and Referral in Acute HIV infection: Seattle Primary Infection Program Experience', *AIDS Research and Human Retroviruses*, 34(8): 657-667.

Steyers, C.M. and Miller Jr, F. (2014) 'Endothelial Dysfunction in Chronic Inflammatory Diseases', *International Journal of Molecular Sciences*, 15: 11324-11349.

Strebel, K. (2013) 'HIV accessory proteins versus host restriction factors', *Current Opinion in Virology*, 3: 692-699.

Strebel, K. (2014) 'HIV-1 Vpu—an ion channel in search of a job', *Biochimica et Biophysica Acta*, 1838: 1074-1081.

Subramanian, S., Tawakol, A., Burdo, T.H., Abbara, S., Wei, J., Vijayakumar, J., Corsini, E., Abdelbaky, A., Zanni, M.V., Hoffmann, U., Williams, K.C., Lo, J. and Grinspoon, S.K. (2012) 'Arterial inflammation in patients with HIV', *JAMA*, 308(4): 379–386.

Sundquist, W.I. and Kräusslich, H.-G. (2012) 'HIV-1 Assembly, Budding, and Maturation', *Cold Spring Harbor Perspectives in Medicine*, 2(7): 1-25.

Sundstrom, J.B., Ellis, J.E., Hair, G.A., Kirshenbaum, A.S., Metcalfe, D.D., Yi, H., Cardona, A.C., Lindsay, M.K. and Ansari, A.A. (2007) 'Human tissue mast cells are an inducible reservoir of persistent HIV infection', *Blood, The Journal of the American Society of Hematology*, 109(12): 5293-5300.

Swanstrom, R. and Coffin, J. (2012) 'HIV-1 Pathogenesis: The Virus', *Cold Spring Habor Perspectives in Medicine*, 2: 1-19.

Tawakol, A., Lo, J., Zanni, M.V., Marmarelis, E., Ihenachor, E.J., MacNabb, M., Wai, B.,

Hoffmann, U., Abbara, S. and Grinspoon, S. (2014) 'Increased Arterial Inflammation Relates to High-Risk Coronary Plaque Morphology in HIV-Infected Patients', *JAIDS Journal of Acquired Immune Deficiency Syndromes*, 66(2): 164-171.

Tjitro, R., Campbell, L.A., Basova, L., Johnson, J., Najera, J.A., Lindsey, A. and Marcondes, M.C.G. (2019) 'Modeling the function of TATA Box binding protein in transcriptional changes induced by HIV-1 Tat in innate immune cells and the effect of methamphetamine exposure', *Frontiers in Immunology*, 9: 3110-3130.

Toborek, M., Lee, Y.W., Pu, H., Malecki, A., Flora, G., Garrido, R., Hennig, B.,Bauer, H.C. and Nath, A. (2003) 'HIV-Tat protein induces oxidative and inflammatory pathways in brain endothelium', *Journal of Neurochemistry*, 84(1): 169-179.

Triant, V.A., Lee, H., Hadigan, C. and Grinspoon, S.K. (2007) 'Increased Acute Myocardial Infarction Rates and Cardiovascular Risk Factors among Patients with Human Immunodeficiency Virus Disease', *The Journal of Clinical Endocrinology & Metabolism*, 92(7): 2506-2512.

Turner, B.G. and Summers, M.F. (1998) 'Structural Biology', *Journal of Molecular Biology*, 285: 1-32. Ullrich, C.K., Groopman, J.E. and Ganju, R.K. (2000) 'HIV-1 gp120- and gp160-induced apoptosis in cultured endothelial cells is mediated by caspases', *Blood*, 96: 1438-1442.

UNAIDS (2019) *UNAIDS*, https://www.unaids.org/en/resources/fact-sheet [Accessed 30 March 2020].

Usami, Y., Wu, Y. and Gottlinger, H.G. (2015) 'SERINC3 and SERINC5 restrict HIV-1 infectivity and are counteracted by by Nef', *Nature*, 526(7572): 218-223.

Varin, A., Manna, S.K., Quivy, V., Decrion, A.-Z., Lint, C.V., Herbein, G. and Aggarwal, B.B. (2003) *The Journal of Biological Chemistry*, 278(4): 2219-2227.

Videm, V. and Albrigtsen, M. (2008) 'Soluble ICAM-1 and VCAM-1 as Markers of

Endothelial Activation', *Journal of Immunology*, 67: 523-531.

Visseaux, B., Damond, F., Matheron, S., Descamps, D. and Charpentier, C. (2016)'HIV-2 molecular epidemiology', *Infection, Genetics and Evolution*, 46: 233-240.

Volpe, M., Uglietti, A., Castagna, A., Mussini, C., Marchetti, G., Bellagamba, R., Bini, T., Mancusi, D. and Termini, R. (2017) 'Cardiovascular disease in women with HIV-1 infection', *International Journal of Cardiology*, 241: 50-56.

Walker, P.R., Ketunuti, M., Choge, I.A., Meyers, T., Gray, G., Holmes, E.C. and Morris, L. (2007) 'Polymorphisms in Nef associated with different clinical outcomes in HIV-1 subtype C-infected children', *AIDS Research and Human Retroviruses*, 23(2): 204-215.

Wang, B., Ge, Y.C., Palasanthiran, P., Xiang, S.H., Ziegler, J., Dwyer, D.E., Randle, C., Dowton, D., Cunningham, A. and Saksena, N.K. (1996) 'Gene Defects Clustered at the C-Terminus of the vpr Gene of HIV-1 in Long-Term Nonprogressing Mother and Child Pair: In VivoEvolution of vpr Quasispecies in Blood and Plasma', *Virology*, 223(1): 224-232.

Wang, T., Green, L.A., Gupta, S.K., Kim, C., Wang, L., Almodovar, S., Flores, S.C., Prudovsky, I.A., Jolicoeur, P., Liu, Z. and Clauss, M. (2014) 'Transfer of Intracellular HIV Nef to Endothelium Causes Endothelial Dysfunction', *PloS one*, 9(3): 1-11.

Wang, T., Yi, R., Green, L.A., Chelvanambi, S., Seimetz, M. and Clauss, M. (2015) 'Increased Cardiovascular Disease Risk in The HIV-Positive Population on ART: Potential Role of HIV-Nef and Tat', *Cardiovascular Pathology*, 24(5): 279-282.

Watts, J.M., Dang, K.K., Gorelick, R.J., Leonard, C.W., Jr, J.W.B., Swanstrom, R., Burch, C.L. and Weeks, K.M. (2009) 'Architecture and secondary structure of an entire HIV-1 RNA genome', *Nature*, 460(7256): 711-716.

Weston, R. and Marett, B. (2009) 'HIV infection: pathology and disease progression', *Clinical Pharmacist*, 1: 387-391.

WHO (2017) *Cardiovascular diseases*, https://www.who.int/news-room/fact-

sheets/detail/cardiovascular-diseases-(cvds) [Accessed 28 August 2020].

Wilen, C.B., Tilton, J.C. and Doms, R.W. (2012) 'HIV: Cell Binding and Entry', *Cold Spring Harbor Perspectives in Medicine*, 2(8): 1-13.

Wu, Y., Q. Li, Q. & Chen, X., 2007. Detecting protein–protein interactions by far western blotting. *Nature protocols,* 2(12), pp. 3278-3284.

Xia, W., Bringmann, P., McClary, J., P.Jones, P., Manzana, W., Zhua, Y., Wang, S., Liu, Y., Harvey, S., Madlansacay, M.R., McLean, K., P.Rosser, M., MacRobbie, J., L.Olsene, C. and R.Cobb, R. (2006) 'High levels of protein expression using different mammalian CMV promoters in several cell lines', *Protein Expression and Purification*, 45(1): 115-124.

Xia, Y., Chu, W., Qi, Q. and Xun, L. (2014) 'New insights into the QuikChangeTM process guide the use of Phusion DNA polymerase for site-directed mutageneesis', *Nucleic Acids Research*, 1: 1-9.

Xie, M., Dong, Y., He, L., Ren, H., Ji, Y. and Lv, S., (2011) ‗Expression of VLA-4 molecule in PBMC from patients with hemorrhagic fever with renal syndrome ‘. *Inflammation Research*, 60(7): 613-617.

Yu, X., Shang, H. and Jiang, Y. (2020) 'ICAM-1 in HIV infection and underlying mechanisms', *Cytokine,* 125: 1-9.

Zack, J.A., Arrigo, S.J., Weitsman, S.R., Go, A.S., Haislip, A. and Chen, I.S. (1990) 'HIV-1 entry into quiescent primary lymphocytes: molecular analysis reveals a labile, latent viral structure', *Cell*, 61(2): 213-222.

Zaikos, T.D., Terry, V.H., Kettinger, N.T.S., Lubow, J., Painter, M.M., Virgilio, M.C., Neevel, A., Taschuk, F., Onafuwa-Nuga, A., McNamara, L.A., IV, J.R., Bixby, D., Markowitz, N. and Collins, K.L. (2018) 'Hematopoietic stem and progenitor cells are a distinct HIV reservoir that contributes to persistent viremia in suppressed patients', *Cell reports*, 25(13): 3759-3773.

Zapp, M.L. and Green, M.R. (1989) 'Sequence-specific RNA binding by the HIV-1 Rev protein', *Nature*, 342(6250): 714-716.

Zhang, S., Kaplan, A.H. and Tropsha, A. (2009) 'HIV-1 Protease Function and Structure Studies with the Simplicial Neighborhood Analysis of Protein Packing (SNAPP) Method', *Proteins*, 73(3): 742-753.

Zhou, M.Y. and Gomez-Sanchez, C.E. (2000) 'Universal TA Cloning', *Current Issues in Molecular Biology*, 2(1): 1-7.

Zimmermann, K., Schögl, D. & Mannhalter, J., 1998. Digestion of terminal restriction endonuclease recognition sites on PCR products. *Biotechniques,* 24(4), pp. 582-584.

Zuo, J., Suen, J., Wong, A., Lewis, M., Ayub, A., Belzer, M., Church, J., Yang, O.O. and Krogstad, P. (2012) 'Functional Analysis of HIV Type 1 Nef Gene Variants from Adolescent and Adult Survivors of Perinatal Infection', *AIDS Research and Human Retroviruses*, 28(5): 486-492.

Appendices

Appendix A

A1: Ethics waiver granted by the Human Research Ethics Committee of the University of the Witwatersrand

UNIVERSITY OF THE WITWATERSRAND, JOHANNESBURG

HUMAN RESEARCH ETHICS COMMITTEE (MEDICAL)

Human Research Ethics Committee (Medical)

Research Office Secretariat:
Faculty of Health Sciences, Phillip Tobias Health Sciences Building, 3rd Floor, Office 301/2/4, 29 Princess of Wales Terrace, Parktown, 2193
Private Bag 3, Wits 2050
Office email: HREC-Medical.ResearchOffice@wits.ac.za
Website: www.wits.ac.za/research/about-our-research/ethics-and-research-integrity/

Ref: W-CBP-190802-01 02/08/2019

TO WHOM IT MAY CONCERN:

Waiver:	This certifies that the following research does not require clearance from the Human Research Ethics Committee (Medical)
Investigator:	Mr Tanani Sayimane et al (Student no. 578224)
Supervisor:	Ms Genevieve Mezoh
Department:	Chemical Pathology
Project title:	Impact of HIV-1 NEF Polymorphisms on endothelial function
Reason:	In vitro laboratory study using Human Pulmonary Microvascular Endothelial Cells (HPMEC). No human participants will be involved in the study.

Dr CB Penny

Chairperson: Human Research Ethics Committee (Medical)

A2: Biosafety clearance granted by the Institutional Biosafety Committee of the University of the Witwatersrand

UNIVERSITY OF THE
WITWATERSRAND
JOHANNESBURG

Research Office

INSTITUTIONAL BIOSAFETY COMMITTEE (IBC)
(R 14/16)

CLEARANCE CERTIFICATE **PROTOCOL NUMBER: 20190801**

BRIEF DESCRIPTION OF APPLICATION:

Functional in vitro analysis of the HIV-1 NEF H40Y mutation on endothelial function

APPLICANT: Mr T Sayimane

SUPERVISOR: Mrs G Mezoh

SCHOOL/DEPARTMENT : Chemical Pathology

DATE CONSIDERED: By Circulation 05 August 2019

EXPIRY DATE: 15 October 2024

DECISION OF COMMITTEE: Approved unconditionally

1. This clearance certificate expires on 15 October 2024 and may be renewed on application
2. An annual report must be provided on the anniversary date of this certificate, for as long as the project continues
3. Notification of any proposed modifications must be submitted on the attached form
4. Unreported changes to the application may invalidate the clearance given by the IBC

DATE: 15 October 2019

CHAIRPERSON: James F. S. Larkin 2019.10.17 11:52:19 +02'00'
(Professor J Larkin)

DECLARATION OF APPLICANT:

To be completed in duplicate and **one copy** returned to the Research Office, Phillip Tobias Building, Room 301, 3rd Floor, 29 Princess of Wales Terrace, Parktown, Faculty of Health Sciences, University

1. I have read, understood and accepted the approval conditions above
2. I agree to submit a yearly progress report to the Committee and to submit an interim report on the form provided, in the event of any significant unforeseen event, e.g. suspension of a drug trial, temporary closure or relocation of my laboratory etc
3. I note that the University Safety Officer, or his/her representative, may at any reasonable time inspect my laboratory or trial site to ensure compliance with current Health and Safety legislation. I undertake to offer my full co-operation in any such inspection
4. I have read, understood and will comply with the *recommended standard operating procedures for the handling of biohazardous materials* posted at http://web.wits.ac.za/Academic/Research/Biosafety.htm
5. I declare (delete as appropriate) that:
   a. I have all the approvals required by statute or regulation and by the funding agencies supporting this work, or
   b. that I will not begin work until such approvals are obtained

Signed: T Sayimane **Date:** 22/10/2019

PLEASE QUOTE THE PROTOCOL NUMBER IN ALL ENQUIRIES

A3: Plasmids maps

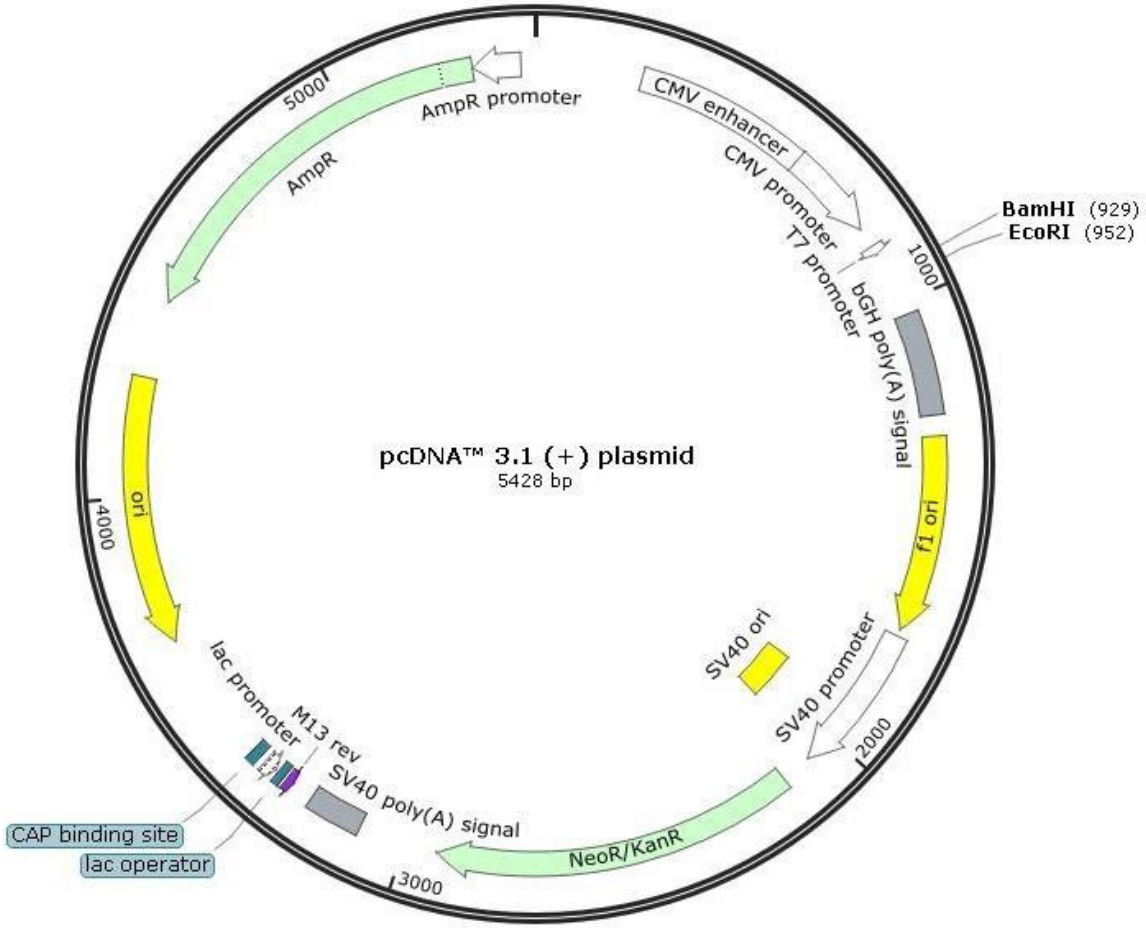

Figure A1: pcDNA 3.1 (+) plasmid
Cloning vector used for the construction of transient HIV-1 Nef expressing plasmids. The *nef* genes were inserted between restriction sites *Bam*HI and *Eco*RI.

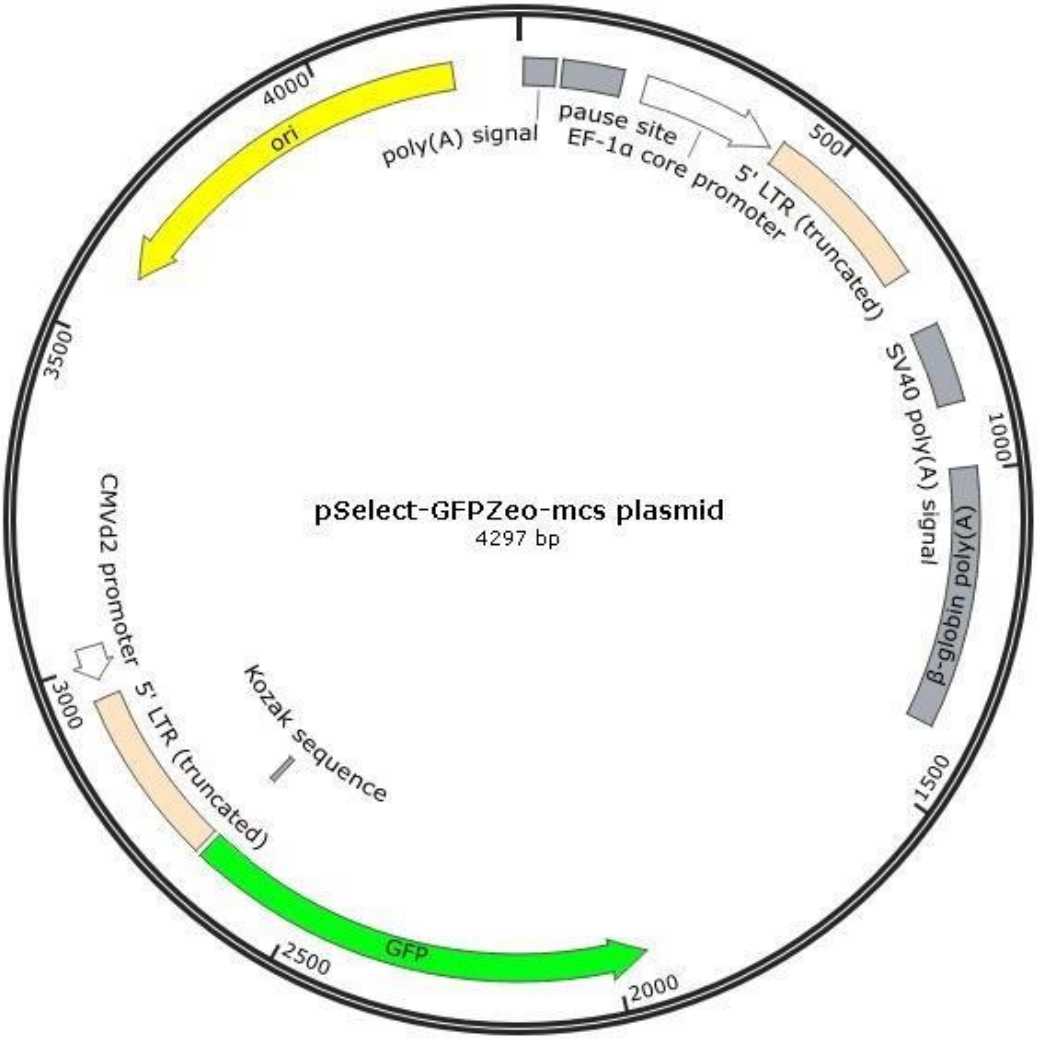

Figure A2: pSelect-GFPZeo-mcs plasmid
The pSelect-GFPZeo-mcs plasmid was used as a transfection positive control.

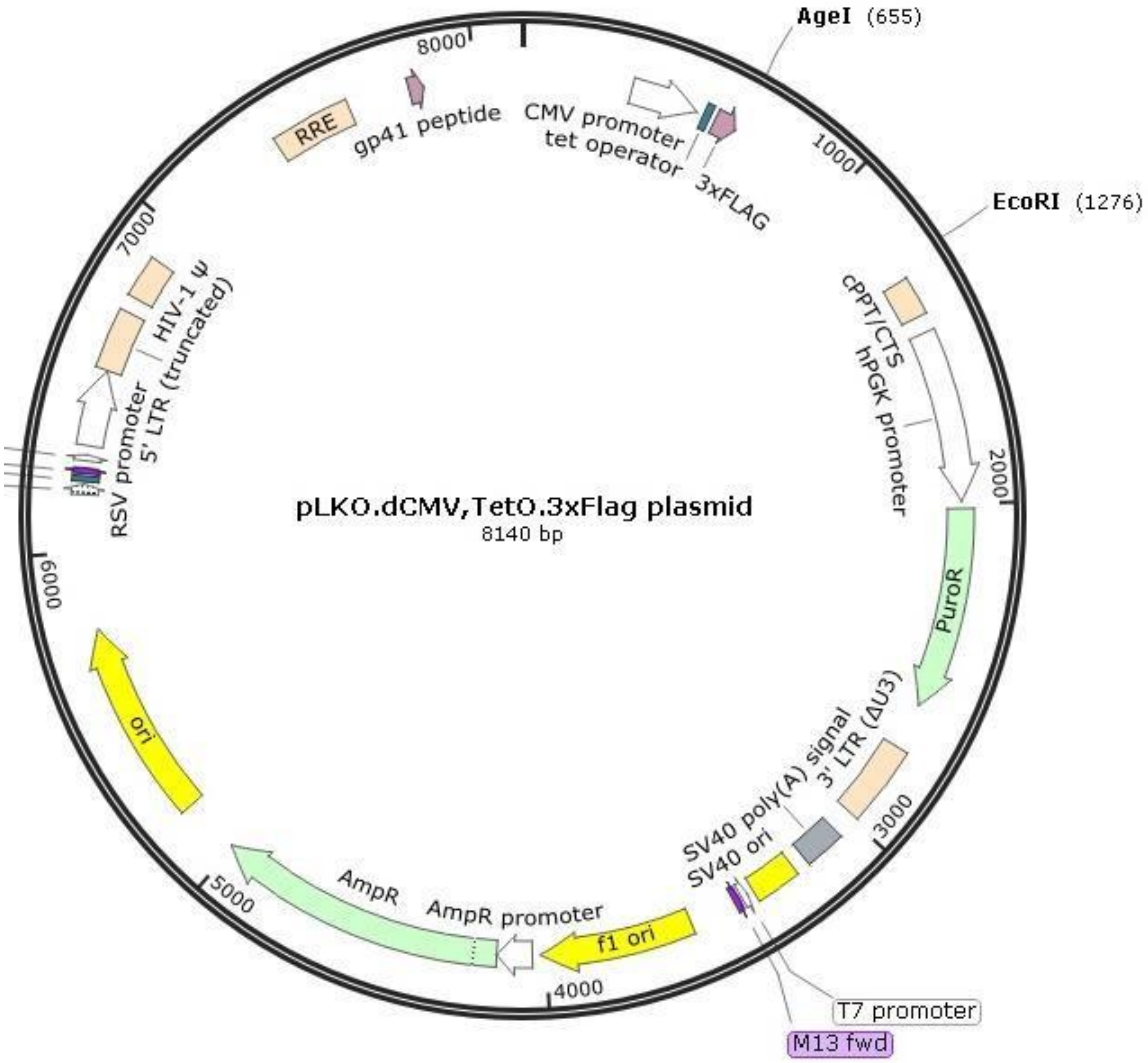

Figure A3: pLKO.dCMV,TetO.3xFlag plasmid
Cloning vector used for the construction of stable HIV-1 Nef expressing plasmids. The *nef* genes were inserted between restriction sites AgeI and EcoRI.